PARALLEL CONFERENCES ON ADVANCED MATERIALS

The 4TH International Workshop on Functional and Nanostructured Materials
1–6 September 2007, Gdansk and Hel Peninsula, Poland

The 8TH Conference on Intermolecular and Magnetic Interactions in Matter
2–5 September 2007, Gdansk, Poland

ORGANIZED BY

Department of Solid State Physics
Gdansk University of Technology, Poland

Academic Computer Centre TASK
Gdansk University of Technology, Poland

Department of Physics,
University of Athens, Greece

Szczecin University of Technology, Poland

Institute of Molecular Physics
Polish Academy of Sciences, Poznan, Poland

Lublin University of Technology, Poland

Poznan University of Technology, Poland

Polish Society for Crystal Growth

UNDER THE PATRONAGE OF

His Magnificence Rector
of the Gdansk University of Technology

Major of the City of Gdansk
Major of the City of Sopot
Major of the City of Gdynia

C O M M I T T E E S

Honorary Chairmen

Sir Sam Edwards (Cambridge, England),
J. T. Devreese (Antwerp, Belgium),
G. J. Papadopoulos, (Athens, Greece)

Scientific and program committee

J. Rybicki (Gdansk, Poland) – Chairman,
N. Guskos (Athens, Greece) – Co-Chairman,
J. M. Olchowik (Lublin, Poland) – Co-Chairman,
W. Sadowski (Gdansk, Poland) – Co-Chairman,
K. W. Wojciechowski (Poznan, Poland) – Co-Chairman

A. Alderson (Bolton, UK),
J. Badur (Gdansk, Poland),
A. DiCicco (Camerino, Italy),
Yu. Feldman (Jerusalem, Israel),
S. Glenis (Athens, Greece),
M. Grinberg (Gdansk, Poland),
I. Hatziagapiou (Athens, Greece),
W. G. Hoover (Livermore & UCD, CA, USA)
T. Kanaya (Kyoto, Japan),
S. F. Karmanenko (St. Petersburg, Russia),
H. Kleinert (Berlin, Germany),
T. Klimczuk (Los Alamos NL, USA),
T. Krzyżyński (Koszalin, Poland),
R. Lakes (Wisconsin, USA),
G. Levczenko (Donietsk, Ukraine),
B. Maruszewski (Poznan, Poland),
L. Murawski (Gdansk, Poland),
U. Narkiewicz (Szczecin, Poland),
A. G. Nasiopoulou (Athens, Greece),
T. Paszkiewicz (Rzeszow, Poland),
R. Reisfeld (Jerusalem, Israel),
W. Ryba-Romanowski (Wroclaw, Poland),
C. Rudowicz (Szczecin, Poland),
A. Sherman (Tartu, Estonia),
A. Tylikowski (Warsaw, Poland)

Industrial Advisory Board

A. Banaszkiewicz (ALSTOM Poland),
P. Gepner (INTEL Technology Poland),
A. Gołyga (Jabil Circuit Poland Sp. z o.o.),
R. Markowski (TECHNO-SERVICE S.A., Poland),
J. Mioduski (TECHNO-SERVICE S.A., Poland),
T. Kamińska (PSSE Poland),
A. I. Papadopoulos (Prefabricated Concrete Products, YPSONAS Ltd. Cyprus),
B. Pohl (H. Cegielski Rolling Stock Factory Ltd., Poland)

Local Organizing Committee

A. Witkowska – Chairwoman, M. Bobrowski – Secretary,

M. Białoskórski, M. Chmielewski, J. Dziedzic, W. Lizak,
M. Nakonieczny, L. Piotrowski, J. Rybicki, B. Strzelecka, L. Wicikowski

SPONSORS

Academic Computer Centre TASK
Gdansk University of Technology, Poland

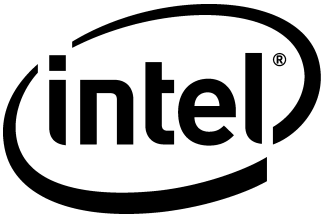

INTEL Technology Poland

Jabil Circuit Poland Sp. z o.o.

TECHNO-SERVICE S.A., Poland

PSSE, Gdansk Science and Technology Park,
Gdansk, Poland

Pomeranian Center of Advanced Technology,
Gdansk, Poland

International Center of Nanotechnology
and Advanced Functional Materials,
Gdansk, Poland

CONTENTS

Lectures

Oral communications

Posters

Last-minute abstracts

In memoriam Dr Marek Baran

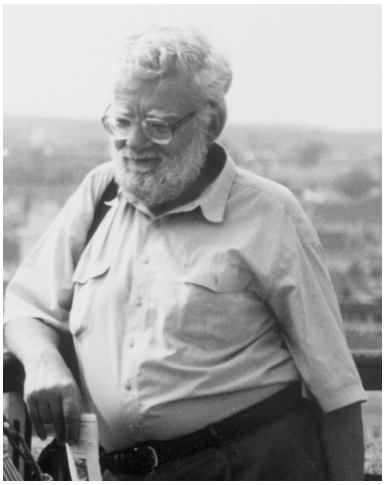

Dr Marek Baran, a long-standing employee of the Institute of Physics of the Polish Academy of Sciences, passed away on October 17, 2006, at his home in Warsaw.

He was an alumnus of the Warsaw University. In high school, he became interested in electronics and radio engineering. His commitment and skills were recognized by his professors and he was employed, while still a student, as an assistant at the Electronics Lab of the Institute of Experimental Physics. A few years after graduation, he joined the Magnetic Division of the Institute of Fundamental Technical Research of the Polish Academy of Sciences. Together with his division, he first moved to the Institute of Electron Technology and later, in 1970, to the Institute of Physics.

Dr Baran was a gifted experimentalist of great authority, recognized both in Poland and internationally for his contribution and expertise in magnetism and superconducting science. He was an expert on microwave spectroscopy techniques (electron paramagnetic resonance and ferromagnetic resonance), magnetometry (esp. Squid magnetometry) and other spectroscopic techniques, incl. nuclear resonance, muon spin rotation and Mössbauer measurements. Initially, he employed these techniques to study ferromagnetic materials but later he turned to research on high temperature superconductors, as one of the first in the Institute. This subsequently became the subject of his PhD thesis, viz. "Magnetic studies of the neutron radiation on properties of high temperature superconductors". In recent years he was focused on the magnetism of metalo-organic compounds and low-dimensional systems.

He authored or co-authored more than 300 publications across a variety of areas in magnetism and superconductivity. He was a great friend and colleague, always ready with help and advice. A source of inspiration and ideas for his younger colleagues, he taught them various experimental techniques in condensed matter physics. He was a wonderful person, a gentle human being, and a great scientist who will be sorely missed and always remembered.

LECTURES

Discrete Systems Free of the Peierls-Nabarro Potential

S. V. Dmitriev[1,2]

[1] *General Physics Department, Altai State Technical University, Lenin St. 46, Barnaul 656038, Russia*

[2] *Institute of Industrial Science, the University of Tokyo, Komaba, Meguro-ku, Tokyo 153-8505, Japan*

In the past few years, a variety of physical applications have stimulated enormous growth in the study of nonlinear discrete models and the differential-difference equations that describe them. These models have a two-fold role and importance. On the one hand, they serve as discretizations of the corresponding continuum field theories; on the other hand, they may also be important physical models in their own right, e.g. in the context of crystal lattices. Taking into account the discreteness of media at the molecular and atomic level is becoming increasingly important for nanotechnologies.

We offer a wide class of discrete nonlinear systems of remarkable properties: (i) they are translationally invariant (TI), i.e. their equilibrium static (stationary) solutions can be placed anywhere with respect to the lattice, due to the absence of the Peierls-Nabarro potential; (ii) static (stationary) versions of the discrete equations are exactly solvable.

We discuss the discrete equations reducible, in the continuum limit, to the Klein-Gordon field or to the nonlinear Schrödinger equation, with a number of applications in the physics of condensed matter and materials science.

Solitary waves in discrete systems free of the Peierls-Nabarro potential are not trapped by the lattice. As a result, they can propagate with a small velocity and be accelerated even by weak external fields, which is impossible in the usual discrete systems. Such lattices may be said to have better transport properties since solitons are highly mobile in TI lattices and they can carry mass, energy, momentum, electric charge, information, etc. Spectra of small-amplitude vibrations calculated for TI lattices hosting an equilibrium soliton always contain zero eigenvalues, corresponding to the translational invariance (the Goldstone mode).

The discretization method we offer uses the discretized first integral of the static (stationary) version of the corresponding continuum equation and is called the discretized first integral (DFI) approach [1–4]. We thus generalize the TI models constructed in the pioneering works [5].

References

1. Dmitriev S V, Kevrekidis P G, Yoshikawa N and Frantzeskakis D J 2006 *Phys. Rev. E* **74** 046609
2. Dmitriev S V, Kevrekidis P G, Yoshikawa N and Frantzeskakis D J 2007 *J. Phys. A: Math. Theor.* **40** 1727
3. Dmitriev S V, Kevrekidis P G, Khare A and Saxena A 2007 *J. Phys. A: Math. Theor.* **40** 6267
4. Dmitriev S V Kevrekidis P G, Sukhorukov A A, Yoshikawa N and Takeno S 2006 *Phys. Lett. A* **356** 324
5. Speight J M 1999 *Nonlinearity* **12** 1373; Kevrekidis P G 2003 *Physica D* **183** 68

Global Existence of Elastic Waves with Memory

B. Rubino

Sezione di Matematica per l'Ingegneria, University of L'Aquila,
P. le E. Pontieri, 2, 67100 L'Aquila, Italy

We treat the Cauchy problem for nonlinear systems of viscoelasticity with a memory term. We study the existence and the decay time of the solution to this nonlinear problem. The kernel of the memory term includes integrable singularity at zero and polynomial decay at infinity. We prove the existence of a global solution for space dimensions $n = 3$ and arbitrary quadratic nonlinearities.

Finite Element Analysis of a Deformation of an Auxetic Obstacle in a Channel During Fluid Flow

B. Maruszewski, T. Stręk

Institute of Applied Mechanics, Poznan University of Technology, Piotrowo 3, 60-965 Poznan, Poland

The paper deals with a finite element analysis of a fluid-structure interaction with an auxetic obstacle in a channel. Computer simulation results in shape deformations of auxetic obstacle in two-dimensional channel.

Auxetics are materials with the negative Poisson's ratio. When an auxetic material is stretched in one direction, it expands along the other one. This unusual behaviour of auxetic materials can be really observed and simulated using computational methods.

The geometry of the model consists of a horizontal flow channel with an obstacle (narrow vertical structure) placed inside it. The fluid flows from left to right and it acts with a force on the structure walls which result from the viscous drag and fluid pressure. The structure, being made of a deformable material, bends under the applied load. Consequently, the fluid flow also follows a new path.

The viscous fluid flow in the channel is described by the Navier-Stokes equation. Mechanical analysis of the deformation of the channel walls are done using structural mechanics plane stress model. Deformation of the obstacle in the channel is described by equation of motion of a solid continuum (the Navier equation) with the Rayleigh damping. So that only the Rayleigh damping has been used in terms to model viscous damping and specify two damping coefficients.

The problem has been solved with the help of COMSOL code (based on finite element method) and direct UMFPACK linear system solver. Flows with various values of inlet velocity ($u_0 = 0.05$, 0.1 and 1) and Poisson's ratio ($\nu = -0.99$, -0.7, -0.3 and $+0.3$) has been considered. Finite element analysis shows that the deformation of an isotropic obstacle in the channel during the flow grows up when Poisson's ratio or maximum inlet velocity increases.

Magnetoresistance Relating to the Integer Hall Effect

G. J. Papadopoulos

Department of Physics, Solid State Physics Section, University of Athens, Panepistimiopolis, GR 157 84, Zografos, Athens, Greece

The formalism, developed earlier, for the magnetoresistance exhibited by a material, in the form of a rectangular parallelepiped, subjected to a perpendicular magnetic field is shown to apply in the case whereby the carriers are constrained in a way as to form a two dimensional gas. Utilizing parameters relating to the geometry of the carrier gas together with other parameters involved in our formulae such as temperature, mobility, and carrier density we are able to obtain the quantized magnetoresistance pertaining to the von Klitzing quantized Hall effect emerging at low temperature. The analysis shows that derivation of the magnetoresistance, in question, results from combination of the diffusion coefficient in terms of the magnetic field and the free field carrier mobility. Indeed, by varying the zero field mobility one can see that for fixed low temperature and given carrier density the almost zero resistance regions, characteristic to the integer Hall effect, do not appear. Increase in the mobility leads to the quantized magnetoresistance, and depending on the mobility value certain of the narrow resistance elevations at values of the magnetic field associated with the various filling factors may or may not become manifest. The case whereby such resistance elevations hide out has been observed in experiments. However, depending on the mobility value an uninterrupted succession of resistance elevations does appear. Furthermore, the height of resistance elevations depends on the mobility.

References

1. G. J. Papadopoulos, J. Non-Cryst. Solids **352** (2006) 4206.
2. G. J. Papadopoulos, Rev. Adv. Mater. Sci. **14** (2007) 187–192.

Protein-like Behavior of a Single Multiblock Copolymer Chain in Selective Solvent

M. Banaszak

A. Mickiewicz University,
Umultowska 85, 61-614 Poznan, Poland

We present a lattice Monte Carlo study of a series of block copolymer chains in selective solvents of varying quality, first using diblock chains and then the corresponding multiblock chains. We report a variety of thermodynamic and structural properties such as energy, specific heat, end-to-end distance and radius of gyration for both the whole chain and the individual blocks. The simulations demonstrate that a multiblock copolymer in a selective solvent exhibits protein-like behavior, undergoing a two-step transition from a swollen state to a primary "pearl-necklace" state and then to a secondary superglobular state as the solvent quality decreases (i.e. upon cooling). As expected, we have also found that the multiblock chains' total mean-squared end-to-end distances decrease as the temperature is reduced.

Cubic Crystals with a Negative Poisson's Ratio

A. C. Brańka*, K. W. Wojciechowski

Institute of Molecular Physics, Polish Academy of Sciences,
Smoluchowskiego 17, 60-179 Poznan, Poland

Elastic properties constitute one of the most fundamental physical properties of any material. The knowledge of a body's behavior under stress or tension greatly facilitates the design and manufacture of materials with desirable physical properties. It is commonly observed that materials decrease their transverse dimensions under uniaxial load. However, the inverse phenomenon is also possible. Materials that expand in all directions when pulled in one direction are called auxetics [1–4]. Such deformations are described in terms of Poisson's ratio, $\nu = -\eta_T/\eta_L$, where η_T and η_L are strains in orthogonal (transverse and longitudinal) directions. An auxetic response involves a negative Poisson's ratio.

In general, physical properties of materials depend on directions; Poisson's ratio depends on the direction of the applied stretching. In anisotropic materials, ν can be positive in one direction and negative in another direction. Accordingly, anisotropic materials can display completely non-auxetic, completely auxetic or intermediate behavior [5, 6]. This new classification will be outlined in our presentation and briefly discussed for cubic crystals.

Materials with negative Poisson's ratio in all directions or completely auxetic materials are quite rare in nature. Also the design and manufacture of such materials remains a nontrivial task. This is mainly due to our insufficient knowledge of the mechanisms behind a negative Poisson's ratio. In particular, the connection between auxeticity and the form of interaction between constituent objects or particles is still not well understood and requires further clarification. As a step in this direction, we have investigated a solid composed of spherically-symmetric particles from the point of view of its elastic properties and mechanical stability via Molecular Dynamic simulation methods. It has been found that, for a particular form of inter-particle interactions and thermodynamic conditions, a negative Poisson's ratio can be achieved in any direction. The results obtained for a particular model system suggest a generic mechanism for designing (cubic) materials of negative Poisson's ratio.

Acknowledgments

This work has been supported by the Polish Ministry of Science and Higher Education, under grant no. N20207032/1512 (2007-2010).

References

1. Lakes R 1987 Science **235** 1038
2. Baughman R H, Shacklette J M, Zakhidov A A and Stafström S 1998 Nature **392** 362
3. Evans K E and Alderson A 2000 Adv. Mater. **12** 617.
4. papers and references in *Auxetixs and Related Systems*, 2005 phys. stat. sol. (b) **242** Wojciechowski K W, Alderson A, Brańka A, Alderson K L (Eds)
5. Ting T C T and Barnett M D 2005 J. Appl. Mech. **72** 929
6. Paszkiewicz T and Wolski S 2007 phys. stat. sol. (b) **244** 966

*Corresponding author: branka@ifmpan.poznan.pl

Magnetization Dynamics in the Landau-Lifshitz-Gilbert formulation: Modeling the FMR Experiment

M. R. Dudek[1*], N. Guskos[2†], B. Grabiec[1‡], M. Maryniak[3§]

[1] *University of Zielona Góra, Prof. Szafrana 4a, 65-516 Zielona Góra, Poland*

[2] *Solid State Section, Department of Physics, University of Athens, Panepistimiopolis, 15 784 Zografos, Athens, Greece*

[3] *Institute of Physics, Szczecin University of Technology, Al. Piastów 17, 70-310 Szczecin, Poland*

The ferromagnetic resonance (FMR) spectrum of carbon-coated magnetic nanoparticles in a non-magnetic elastic matrix has been investigated. Experimental absorption data have been compared with analogous data obtained with the stochastic Landau-Lifshitz equation for the magnetic moment of a ferromagnetic single-domain nanoparticle and stochastic equations describing rotational oscillations of the polymer region containing the magnetic nanoparticle. We demonstrate that if the polymer matrix anisotropies are blocking the rotational freedom of the easy axes direction of the magnetic nanoparticles, additional resonance peaks may appear in the FMR spectrum being the satellite peaks accompanying the main resonance peak. This is another mechanism of appearance of additional peaks in FMR spectra apart from the spin waves exchange mode in nanoparticles or inter-particle dipolar interactions. The compound Poisson process has been used to model this effect of the additional correlations introduced on the motion of a particle's magnetic moment.

*mdudek@proton.if.uz.zgora.pl
†ngouskos@phys.uoa.gr
‡bgrab@proton.if.uz.zgora.pl
§michalmaryniak@gmail.com

Stochastic Modelling of Nanostructures: an Engineering Perspective

F. Scarpa

University of Bristol, Queens Building, University Walk, Bristol, United Kingdom
f.scarpa@bris.ac.uk

Over the past five years there have been extensive research in the reduced mechanical modelling of multiwalled and singlewalled carbon nanotubes. Majority of the proposed modelling techniques are dominated by determinist approaches. However, significant uncertainties have been reported in the measured materials and geometric properties of carbon nanotubes. In this paper, perhaps for the first time, we propose a probabilistic mechanics approach to take account of these uncertainties at the nanoscale. It is considered that the mechanics of a nominally identical set of carbon nanotubes are governed by stochastic partial differential equations. Two approaches, namely a Stochastic Finite Element (SFE) based method and a stochastic beam model have been investigated. The probability density function of the natural frequencies of singlewalled carbon nanotubes is derived in closed-form for three different physically realistic cases. The analytical results are compared with high-fidelity stochastic finite element simulations and available experimental results. The studies taken in the paper indicate that stochastic approach can significantly enhance the applicability of the mechanistic modelling at the nanoscale.

Particle and Finite-Element Simulations for Materials

Wm. G. Hoover

Ruby Valley Research Institute,
Highway Contract 60, Box 598, Ruby Valley 89833, NV USA

Three different, but related, techniques for materials' simulation are described and illustrated with examples from the literature: (1) Molecular Dynamics, (2) Smooth-Particle Applied Mechanics, and (3) Finite-Element Continuum Mechanics. Molecular dynamics simulations emphasize the use of nonequilibrium boundary conditions (Nosé-Hoover thermostats and barostats from the 1980s, as well as Dellago's very recent use of ideal-gas regions to impose simultaneous temperature and pressure controls.) Molecular dynamics is based on repulsive and attractive interparticle forces. Smooth-particle methods provide a *macroscopic* simulation technique for fluid flows and high-strain-rate calculations. Smooth particles avoid the mesh-tangling that can occur in grid-based calculations. Both smooth particles and finite elements require continuum *constitutive equations* rather than *atomistic* interparticle forces. Applications will be presented so as to illustrate and compare the three methods. For a preview of the Smooth Particle method (SPAM), see my 2006 World Scientific book: *Smooth Particle Applied Mechanics – The State of the Art*. See also the comprehensive list of references on my webpage, http://williamhoover.info.

Elastic Properties of Selected Models in Two and Three Dimensions

K. W. Wojciechowski*

Institute of Molecular Physics, Polish Academy of Sciences,
Smoluchowskiego 17, 60-179 Poznan, Poland

It is well known that negative Poisson's ratio [1] is very unusual in real elastic media, despite that stability conditions are not in contradiction with such a behaviour. This means that common materials typicaly decrease their transverse dimensions when stretched. Materials which behave in the opposite way [2], i.e. which increase their transverse dimensions are called auxetics [3]. Recently, one observes increasing interest in such materials [4].

Studies of simple models help us to understand why auxetic behaviour is rather exceptional in highly symmetric elastic media. Such models may also reveal new mechanisms leading to auxetic behaviour in real systems.

A few models, both in two and three dimensions, showing highly symmetric structures will be described and discussed. It will be shown that, depending on the interactions, some of the models presented exhibit negative Poisson's ratio.

References

[1] Landau L D, Lifshits E M 1986 *Theory of elasticity*, Pergamon Press, London
[2] Lakes R 1987 *Science* **235** 1038
[3] Evans K E, Nkansah M A, Hutchinson I J, and Rogers S C 1991 *Nature* **353** 124
[4] See, e.g., Wojciechowski K W, Alderson A, Alderson K L, Maruszewski B, Scarpa F 2007 *Phys. Stat. Solidi B* **244** 813; see also papers and references in that issue.

*kww@man.poznan.pl

Auxetic Frameworks

A. Alderson

Centre for Materials Research and Innovation, The University of Bolton, Deane Road, Bolton, BL3 5AB, UK

Auxetic materials and structures are those which expand in width when pulled lengthwise, and contract in width when compressed. In other words, they exhibit negative Poisson's ratio behaviour [1]. They are of interest for their characteristic counter-intuitive response to an applied uniaxial mechanical load. They are also of interest because the auxetic property can lead to enhancements in a range of other physical properties [2]. Consequently, government funding agencies are now identifying auxetics as candidate materials for development in smart and advanced materials applications, and large research networks and consortia have developed to investigate this class of materials further.

The range of materials that have been discovered or produced in auxetic form is, perhaps, greater than one might expect when first encountering the concept of auxetic functionality. Auxetic metals, polymers, composites and ceramics are known [2] and, in the case of crystalline metals it has been reported that 69% of all cubic elemental metals exhibit auxetic behaviour [3], for example.

In the case of man-made auxetics, fabrication techniques vary depending on the type of auxetic material being developed. For example, in the case of auxetic laminate composites the auxetic effect is achieved using the same pre-preg materials and manufacturing methods as for conventional composites [4], whereas auxetic microporous polymers require an adaptation of traditional powder processing methods [5]. For auxetic foam, on the other hand, the auxetic embodiments require conversion from an existing conventional foam using an additional (post) processing stage [6].

The success of any fabrication method in producing auxetic behaviour lies in the ability of the fabrication route to produce an internal material structure which deforms in an appropriate manner. Such structures may be uniform, tessellating geometric motifs, such as those found in honeycombs and crystalline materials. Alternatively, the structure may have a degree of randomness or inhomogeneity as found, for example, in microporous polymers and foams.

A very good example of the necessary marriage between the geometry and deformation mechanism of the 'framework' which forms the appropriate structure responsible for the auxetic effect is provided by considering regular honeycombs deforming by hinging (alignment) of the honeycomb cell walls (ribs). The cells of a normal hexagonal (bees honeycomb) geometry extend in the direction of applied stretch but close up in the lateral direction when deformation is due to rib hinging. This, then, corresponds to a positive Poisson's ratio most usually associated with our everyday expectations of what happens to a material or structure when stretched, i.e. the material or structure becomes thinner in width. Conversely, if the honeycomb is fabricated in such a way that the tessellating motif now resembles that of an array of inverted or re-entrant hexagons (a repeating 'bow-tie' pattern), then rib alignment due to hinging actually causes the cells to open up in both principal directions when stretched along one axis. The combination of a tessellating re-entrant hexagon geometry with deformation via rib hinging, therefore, leads to auxetic functionality [7].

In principle, the structure from which the auxetic effect is derived is independent of scale. That is, auxetic behaviour can have its origins due to structural features at the nano, micro and macro lengthscales.

In this paper, I will discuss work performed at Bolton into a range of tessellating frameworks which can give rise to auxetic behaviour. In particular I will discuss

- the role of connectivity in novel honeycombs in achieving auxetic and non-auxetic response,
- scale-independency in auxetic rough particle assemblies,
- lessons from nature in achieving auxetic behaviour at the nanoscale, and
- potential applications of auxetic materials.

References

1. Evans K E, Nkansah M, Hutchison I J and Rogers S C 1991 *Nature* **353** 124
2. Evans K E and Alderson A 2000 *Advanced Materials* **12** (9) 617
3. Baughman R H, Shacklette J M, Zakhidov A A and Stafstrom S 1998 *Nature* **392** 362
4. Clarke J F, Duckett R A, Hine P J, Hutchinson I J and Ward I M 1994 *Composites* **25** (9) 863
5. Alderson K L and Evans K E 1992 *Polymer* **33** 4435
6. Lakes R 1987 *Science* **235** 1038
7. Evans K E, Alderson A and Christian F R 1995 *J. Chem. Soc. Faraday Trans.* **91** 2671

Solid-fluid Phase Transitions Under Extreme Pressures (Including Negative Ones)

A. Drozd-Rzoska[1], S. J. Rzoska[1], A. R. Imre[2]

[1] *Institute of Physics, Silesian University, Uniwersytecka 4, 40-007 Katowice, Poland*

[2] *KFKI Atomic Energy Institute, Budapest, Hungary*

During expansion, condensed matter (i.e. solids and liquids) can reach metastable states and stability limits, where systems can be stabilized by the appearance of a second phase [1]. These metastable states may often be characterized by their absolute negative pressure. In auxetic materials, fast volume expansion is inherent behavior; negative pressure states can be reached easily during uniaxial stretching [2]. The stability of a stretched solid for the solid-vapor phase transition has been presented before [3]; in this presentation we would like to discuss results offering a novel picture of the pressure dependence of the solid-liquid phase transition (melting) covering a very wide range of pressures, including a region below $p < 0$ [4].

References

1. A. R. Imre, H. J. Maris and P. R. Williams (Eds) 2002, Liquids Under Negative Pressure, Kluwer
2. K. W. Wojciechowski 1995 Mol. Phys. Rep. 10, 129
3. A.R. Imre 2006, Phys. Stat. Sol. b, 244, 893
4. S. J. Rzoska, A. Drozd-Rzoska, A. R Imre 2007 J. Noncryst. Solids, accepted

Ferrite-ferroelectric Layered Structures as Microwave Devices Tunable through Magnetic and Electric Fields

S. F. Karmanenko, A. A. Semenov, P. Yu. Belavskiy, B. A. Kalinikos

Electrotechnical University, St. Petersburg, 197376, Russia

Traditionally, ferrite materials have been used to create tunable MW devices. Tunability of ferrite devices is executed through variation of magnetic field in a very wide frequency range, which is relatively slow and associated with considerable consumption of power. Other materials that can be used in tunable MW devices are *ferroelectrics*, wherein frequency tuning is realized through variation of the applied electric field changing the material's dielectric permittivity, ϵ. Such "electric" tuning is possible in a narrow frequency range, but is relatively fast and not power consuming. A combination of ferrite and ferroelectric materials in a composite or layered structure will enable simultaneous "magnetic" and "electric" tuning of its microwave properties, combining the advantages of both tuning methods.

The theory of surface hybrid, electromagnetic-magnetostatic waves' propagation in free and metal-covered ferrite/dielectric structures has been developed in our earlier works. We have investigated theoretically and experimentally the dispersive characteristics of ferrite/ferroelectric layered structures including an air gap between their layers. The obtained dispersive equation is an effective approach to analyzing a spectrum of hybrid waves in order to define the layered structures' geometric and physical parameters and achieve good tunability with low microwave losses and external fields.

In this work, we present the results of a study of ferrite resonators patterned from yttrium iron garnet (YIG) heteroepitaxial film joined with ferroelectric layers of $Ba_xSr_{1-x}TiO_3$ (BST) ceramics. 14 μm thick YIG film was epitaxialy grown on a gallium gadolinium garnet (GGG) substrate of 0.5 mm thickness. The YIG/GGG resonator was rectangular in shape (about 1×2 mm). A Cu microstrip (0.5 mm wide) was formed on the back resonator side. The BST ferroelectric ceramic wafer of the $\approx 4 \times 3 \times 0.4$ mm dimensions was covered with a 4 μm thick copper layer on one side and with thin, "transparent" chromium film ($\approx$ 50 nm) on the other. The electric field could penetrate the Cr film without dissipation, while it was thick enough to apply bias voltage. We obtained a change of the resonance curve of the tested resonator structure due to the bias electrical field. A rather narrow resonance bandwidth (3.5 MHz) and a tuning region, Δf, estimated as three bandwidths were in evidence, where the quality factor remained essentially unchanged ($Q > 1000$).

Impurity-trapped Excitons: Experimental Evidence and the Theoretical Concept

M. Grinberg

Institute of Experimental Physics, University of Gdansk,
Wita Stwosza 57, 80-952 Gdansk

The paper summarizes the experimental evidence of anomalous luminescence in RE-doped dielectric materials. Special attention is paid to Eu^{2+}-doped XF_2 and X_2SiO_4, where X = Ba, Sr, Ca. Luminescence spectra, luminescence excitation spectra and time-resolved spectra obtained under ambient and high (hydrostatic) pressure at various temperatures are presented and discussed. The experimental data are evidence of temperature- and pressure-induced spectral transformation where anomalous luminescence is replaced by normal d-f emission in the Eu^{2+} center. A configurational model of an impurity-trapped exciton is presented, where a hole is trapped in an impurity (Eu^{3+}) and an electron is bound by the Coulomb long-range potential of such donor-type impurity. The model predicts strong electron-lattice coupling of the bound exciton and relaxation in the system's excited states, as well as the pressure effect of spectral transformation from anomalous to normal emission.

Mesoporous Silica Doped with Metalorganic Functionalizing Groups: Experimental and Theoretical Investigations

L. Laskowski[1,2], M. Makowska-Janusik[1], A. Kassiba[2], J. Świątek[1], A. Gibaud[2], A. Mehdi[3], J. Aluzun[3]

[1] *Institute of Physics, Jan Długosz University, Al. Armii Krajowej, 13/15, 42-200 Częstochowa, Poland*

[2] *Laboratoire de Physique de l'Etat Condense – UMR CNRS 6087, Université du Maine, Avenue O. Messiaen, 72085 Le Mans, France*

[3] *Laboratoire de Chimie Moléculaire et Organisation du Solide – UMR 5637 CNRS, Université Montpellier II-Place E. Bataillon, 34095 Montpellier Cedex 5, France*

Mesoporous organic-inorganic materials are a new class of functional systems widely investigated due to their potential electro- or magneto-optical properties. The most representative of silica-based periodic mesoporous materials are the MCM-41 silica solid and the SBA-15 family. Their one-dimensional channels are arranged in a regular hexagonal array similar to a honeycombed structure in MCM-41 and a cubic configuration in SBA-15. Whatever the architecture, encapsulation of organic molecules in the nanoporous channels may produce significant changes in the electronic, magnetic and optical properties of the guest molecules.

SBA-15-based materials functionalized by (1,4,8,11-tetraazacyclotetradecane) cyclam groups have been investigated. Incorporation of cyclam groups containing strongly chelated metal transition cations located in the walls or in the pores of mesoporous silica networks has been achieved experimentally. Spectroscopic investigations including UV-vis absorption, IR absorption and Raman scattering of the nickel-doped complexes were carried out and supported by computational simulations. Particularly, molecular modeling has proved to be a relevant tool to identify the structure and physical properties of active complexes, monitoring the macroscopic behavior of the functional materials. As an example, many reported experimental works have shown a decrease in the optical transparency and electro-optical properties of composite materials upon increasing the density of dopant molecules in the host matrix. This is due to inter-molecular interactions favored by agglomeration of active molecules in the system and the resulting inhomogeneous composites. the organo-metallic molecules of the considered mesoporous- based materials are implemented separately into the silica host matrix. The rigid gas model, a key approach for numerical simulations of the investigated materials' physical properties, was considered including the local field approach. Quantum chemical calculations of the structural and optical properties were performed using density functional theory (DFT) methods. The relevance of the mentioned theoretical simulation approaches with regard to the experimental results obtained mainly for cyclam groups chelating Ni^{3+} ions will be discussed.

Bimolecular Excited Species in Optical Emission from Organic Electroluminescent Devices

J. Kalinowski

Department of Molecular Physics, Gdansk University of Technology, Narutowicza 11/12, 80-952 Gdansk, Poland

1. Introduction

In the last two decades, significant research efforts have been focused on the photophysical properties of organic materials for photonic devices, including the development of organic electroluminescent devices, lying at the heart of display technology [1] and offering potential applications as novel sources of lighting that would be less expensive and more efficient than conventional incandescent and fluorescent sources of illumination [2]. Of particular interest are organic light-emitting diodes (LED's) based on emission from excimer and *exciplex* species, that is from bimolecular excited states revealing broad band luminescence spectra which allow to cover a significant part of the visible spectrum.

The focus of the present talk is on exciplex formation and single phosphorescent dopant blend-based emissive layers (EML) that produce high-performance organic LED's.

2. What is an organic LED?

In thin-film organic LED's, electrons are injected from a cathode and holes from an anode, and under an applied electric field the carriers approach each other in LED's emitters (EML's).

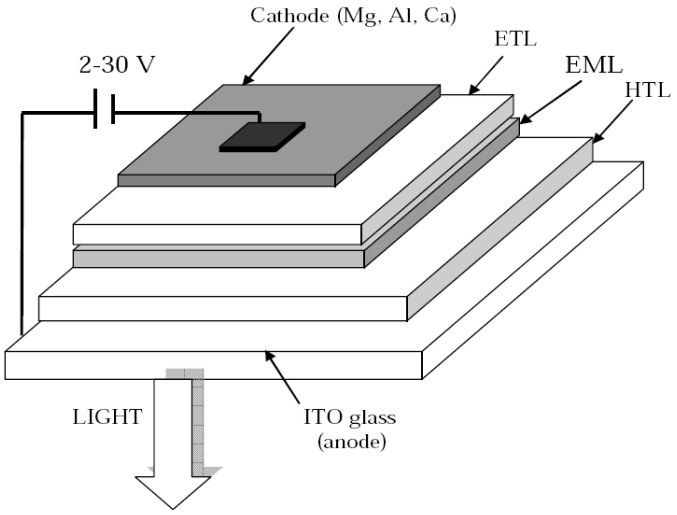

Figure 1: Fundamental setup of a double-layer organic LED: ETL – electron transport layer; EML (20–100 nm); HTL – hole transporting layer

3. Types of excited states

Excited states of molecular solids are traceable to properties of individual molecules. However, their interaction in the condensed phase imposes their collective response referred to as an exciton. If a nearby molecule becomes involved to form an excited state, e.g. due to exchange of energy or charge, a bimolecular excited state is created. As a consequence, new features occur in the emission spectrum or non-radiative decay of excitons is imposed, reducing the system's luminescence yield. Various excited states produced by electron-hole recombination of organic materials are depicted in Fig. 2.

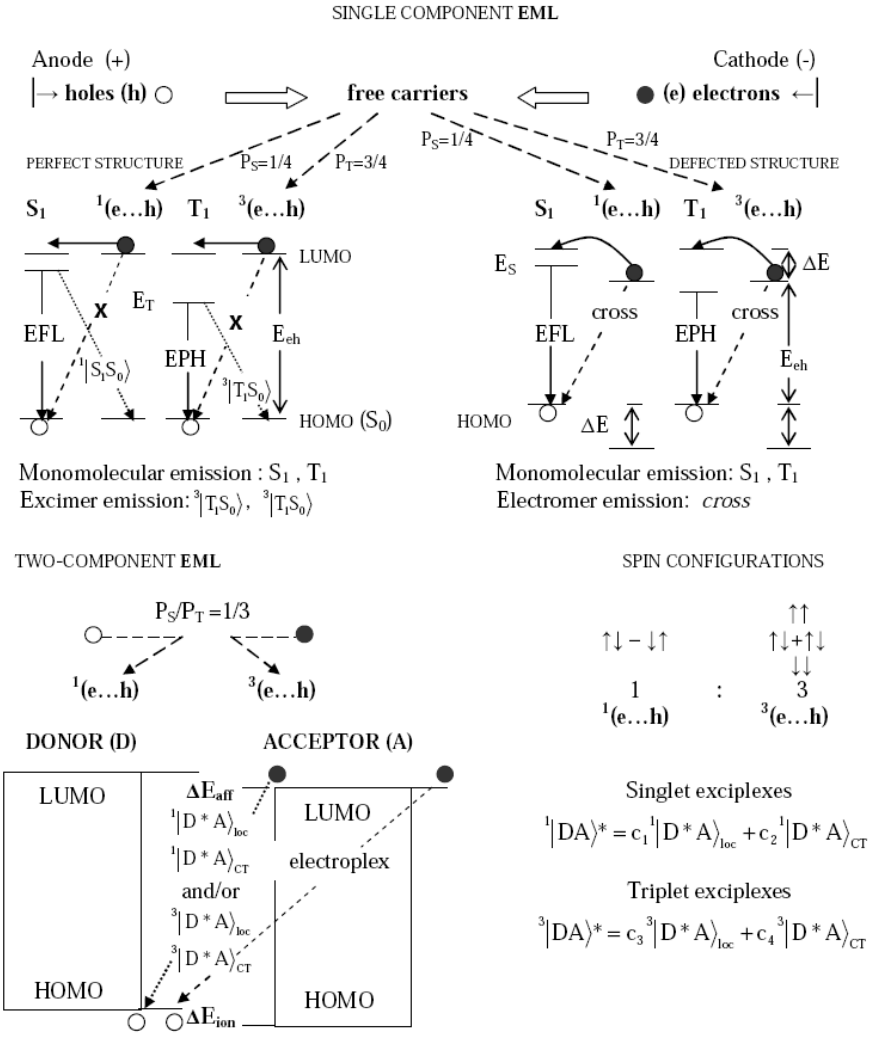

Figure 2: Formation of excited states by recombination

The range of materials nowadays available for organic LED's enables their emission spectra (and thus color) to span from near-UV, through visible, to the near-IR spectral region by selecting an appropriate organic compound for the emission layer. The type of excited states determines the spectral range, while their generation efficiency and decay pathways determine the emission yield of EML's.

4. Exciplex emitters

An exciplex is an excited complex of an electron donor (D) and an electron acceptor (A) molecules $|DA\rangle^*$ that is dissociative in the ground state [1] (cf. Fig. 2).

The dissociative property of the exciplex in its ground state imparts its broad featureless emission band, which is red-shifted from the parent molecules' emission spectra (Fig. 3, left).

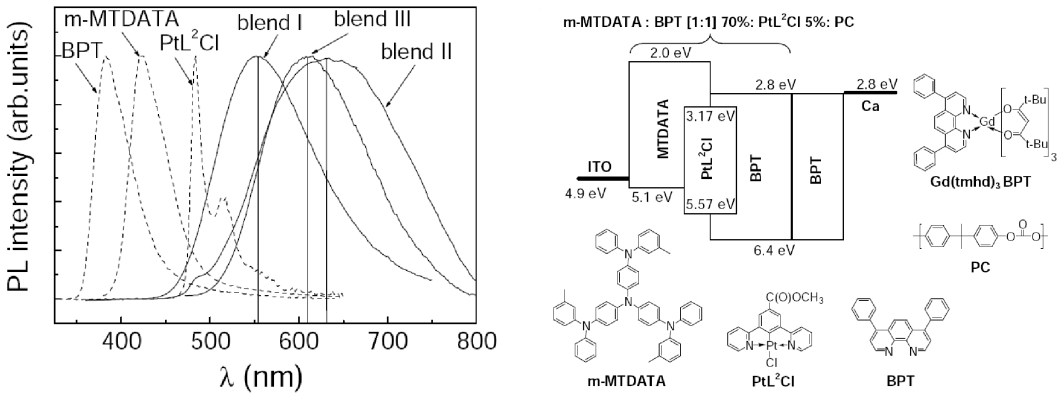

Figure 3: Left panel – normalized photoluminescence (PL) spectra from exciplex emissive blends compared with the PL spectra of their material components; right panel – the EXLED structure based on D (m-MTDATA) and A (BPT or Gd(tmhd)3) doped with phosphor (PtL^2Cl) blended with a PC binder

We have been able to fabricate highly efficient exciplex LEDs (EXLED's) using an organic phosphorescent sensitizer of high electronic affinity (PtL^2Cl) [3]. The obtained EXLED structure is shown in Fig. 3 (right). Its reddish-yellow light EML's of thickness 20–200 nm are blends of (I) – D (m- MTDATA): A (BPT) (1:1), (II) – (I):5wt% PtL^2Cl, and (III) – D (m-MTDATA):A (Gd(tmhd)$_3$BPT) with 25–30 wt% of PC. Due to the triplet character of the exciplexes ^{3} |DA⟩*, external quantum efficiency (QE) as high as ≈ 2.5% photons/electron (ph/e) has been achieved, exceeding by a factor of 2.5 that of singlet emissive exciplexes.

5. Excimer neat and blend emitter films

Excimers are single-component analogues of exciplexes. Recently, highly phosphorescent organic Pt complex flat molecules have been synthesized which allowed to greatly improve white (WL) LEDs [4] and near-infrared (NIR) organic LED's (see Fig. 3, right).

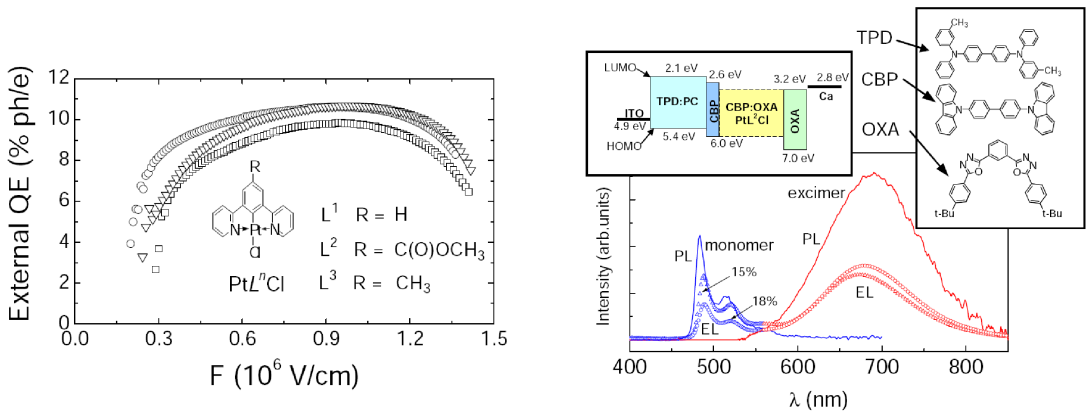

Figure 4: Left panel – external quantum efficiency (QE) vs. applied voltage for NIR organic LED's based on 60 nm- thick neat film made of PtL^nCl dopants [5]; right panel – normalized monomer and excimer electroluminescence (EL) spectra at two different PtL^2Cl concentrations of the WLED shown in the upper left corner inset. Monomer and excimer PL spectra are shown for comparison [4]. For the molecular structure of PtL^2Cl, see Fig. 3 (right)

Highly efficient WLED's have been fabricated using PtL^2Cl as a single dopant of a thin film blend emitter, mixing the monomer's bluish-green phosphorescence with the excimer's emission in red (Fig. 4, right). The external EL QEs 15±0.2% and 13±0.2% ph/e were respectively achieved at 40 and 1300 cd/m^2 brightness.

6. Summary and prospects

We have discussed electroluminescent emission from organic LED's involving molecular and bimolecular excited states. We have demonstrated the most efficient NIR- and WL-emitting organic LED's reported. These devices emit from single-phosphor neat or doped films forming their EML's. In order to achieve this, it was important to use organic materials revealing highly efficient monomolecular and excimeric phosphorescence and control both phosphor concentrations and the carrier/exciton confinement in the device. An alternative way to improve organic WLED's is to combine an electron donor with different electron acceptors allowing a number of broad exciplex spectra to overlap [6]. Recent experiments with blend films emitting from three different emissive states at the same time: (i) molecular excitons of the acceptor (^{3}A*), (ii) triplet excimers ^{3}(AA)* and (iii) triplet exciplex ^{3}(DA)* have led to efficient WLED's with a particularly high color rendering index of CRI = 90 [7].

6. References

1. Kalinowski, J., *Organic Light Emiting Diodes: Principles, Characteristics, and Processes*, Marcel Dekker, N. Y. (2005)
2. D'Andrade, B. W. and Forrest, S. R., White organic light-emiting devices for solid-state lighting, *Adv. Mater.* **16** (2004) 1585–1595
3. Virgili, D., Cocchi, M., Fattori, V., Sabatini, C., Kalinowski, J. and Williams, J. A. G., Highly efficient exciplex phosphorescence from organic light-emitting diodes *Chem. Phys. Lett.* **433** (2006) 145–149
4. Cocchi, M., Kalinowski, J., Virgili, D., Fattori, V., Develay, S. and Williams, J. A. G., Singledopant organic white electrophosphorescent diodes with very high efficiency and its reduced current density roll-off *Appl. Phys. Lett.* **90** (2007) 163508
5. Cocchi, M., Virgili, D., Fattori, V., Williams, J. A. G. and Kalinowski, J., Highly efficient nearinfrared organic excimer electrophosphorescent diodes. *Appl. Phys. Lett.* **90** (2007) 023506
6. Wang, D., Li, W. L., Su, Z. S., Li, T. L., Chu, B., Bi, D. F., Chen, L. L., Su, W. M. and He, H., Broad wavelength modulating and design of organic white diode based on lighting by using exciplex emission from mixed acceptors. *Appl. Phys. Lett.* **89** (2006) 233511
7. Kalinowski, J., Cocchi, M., Virgili, D., Fattori, V. and Williams, J. A. G., Mixing of excimer and exciplex emission: a new way to improve white light emitting organic electrophosphorescent diodes. *Adv. Mater.* in the press

Hybrid Core-shell Nanocomposites Based on Semiconducting or Metallic Nanocrystals Surrounded by Polyaniline

A. Kassiba[1*], L. Laskowski[1], W. Bednarski[1], A. Pud[2], M. Makowska-Janusik[3], N. Ogurtsov[2], N. Errien[1], M. Tabellout[1], A. Gibaud[1]

[1] *Laboratoire de Physique de l'Etat Condensé – UMR CNRS 6087, Avenue Olivier Messiane, 72085 Le Mans, France*

[2] *Institute of Organic Chemistry and Petrochemistry, National Academy of Sciences of Ukraine, Kharkovskoe Shosse 50, Kiev, 253160, Ukraine*

[3] *Institute of Physics, University J. Długosz in Częstochowa, 42-200 Częstochowa, Poland*

The interest in hybrid core-shell nanocomposites is motivated by the possibility to control the interface features between the nanoparticles and the polymer in order to fine-tune their electronic and optical properties. The involved phenomena depend on the charge transport mechanism or the interfacial polarization, the trapping or recombination of charges, as well as the Plasmon excitations when metallic nanoparticles are used. In addition to drawing from these architectures functionalities such as photoluminescence, electroluminescence or non-linear optical behavior, the challenge is to elucidate interactions at the interfaces by probing the dynamic of charge carriers following the nature of the nanoparticles and the electrical activity of the polymer which can be modulated by suitable acid doping. The presented work is devoted to nanocomposites based on doped or undoped polyaniline surrounding SiC, Au or Fe nanocrystals. Two main experimental techniques have been used to probe the charge carriers' (polarons', bipolarons') concentration and dynamics. By Raman, contributions from charge carriers such as polaron and bipolaron excitations are superimposed on the vibrational spectra from the material's bare constituents. The role of Plasmon enhancing surface detection by Raman can be characterized by comparing the behavior of SiC nanocrystals and that of Au or Fe clusters. It is possible to quantify the concentrations of polarons and characterize their dynamics in a wide temperature range through the EPR technique. Such comparative investigations and the key results of these nanocomposites will be discussed at the conference.

References

1. A. Kassiba, W. Bednarski, A. Pud, N. Errien, M. Makowska-Janusik, et al., Hybrid core-shell nanocomposites based on silicon carbide nanoparticles functionalized by conducting polyaniline: EPR investigations, J. Phys. Chem. C – under press (2007)
2. A. Pud, Yu. Noskov, A. Kassiba, K. Fatyeyeva, N. Ogurtsov, M. Makowska-Jausik, et al., New aspects of the low concentrated aniline polymerization in the solution and in SiC nanocrystals dispersion; J. Phys. Chem. B – under press (2007)

*Corresponding author Kassiba@univ-lemans.fr

Superconducting Properties and Crystal Structure of Noncentrosymmetric $Mg_{10}Ir_{19}B_{16}$

T. Klimczuk[1], F. Ronning[1], J. D. Thompson[1], H. Zandbergen[2], Q. Xu[2], R. J. Cava[3]

[1] *Condensed Matter and Thermal Physics, Los Alamos National Laboratory, Los Alamos, NM 87545, USA*

[2] *National Centre for HREM, Department of Nanoscience, Delft Institute of Technology, Al Delft, The Netherlands*

[3] *Department of Chemistry, Princeton University, Princeton, NJ 08540, USA*

The superconducting and normal state of $Mg_{10}Ir_{19}B_{16}$ has been investigated by magnetic susceptibility and specific heat measurements. $Mg_{10}Ir_{19}B_{16}$ in the normal state is the weak Pauli paramagnetic material. The estimated Sommerfeld coefficient and Debye temperature are 53 $mJ\,mol^{-1}K^{-2}$ and 280 K respectively. The value of specific heat jump at T_C was calculated to be 1.60 and electron phonon coupling coefficient $\lambda_{ep} = 0.66$. The thermal evolution of the specific heat below T_C ($T < 3.5$ K) suggests that $Mg_{10}Ir_{19}B_{16}$ is a weak coupling, BCS-type superconductor.

One- and Two-Dimensional Pb Structures on Vicinal Silicon

R. Zdyb

Institute of Physics, Maria Curie-Skłodowska University,
Pl. M. Curie Skłodowskiej 1, 20-031 Lublin, Poland

The crystallographic structure and morphology of Pb layers in their early stage of growth were investigated with Reflection High Energy Electron Diffraction (RHEED) and specific resistivity measurements techniques. Vicinal Si(335) of various surface morphologies, induced by the deposition and annealing of a submonolayer amount of Au, were used as substrates.

The obtained RHEED patterns have revealed that the growth of Pb on substrates with Au coverage of up to 0.3 monolayer (ML) is anisotropic. The preferred growth direction of Pb crystallites is parallel to the substrate step edges, or the [110] direction. In the case of substrates with more than 0.3 ML of Au, RHEED patterns have revealed isotropic growth of lead on wide (111) terraces of the substrate and anisotropic growth on high-index Miller planes.

Specific resistivity measurements have shown clear anisotropy when measured along and across the step edges. At 1 ML of Pb, the values of specific resistivity measured in both directions differed by several tens to several hundred percent, depending on the substrate morphology. Moreover, in the case of substrates with pre-deposited Au up to 0.3 ML, specific resistivity measured along the step edges has exceeded the percolation threshold at about 1 ML of Pb and confirmed the one-dimensional character of the growing Pb structures. On substrates with more than 0.3 ML of Au, a gradual switching to two-dimensional structures is clearly observable; the percolation threshold shifts towards lower values, as expected for two-dimensional structures.

Current-induced Magnetic Switching and Dynamics in Spin Valves

J. Barnaś[1,2], M. Gmitra[3], M. Misiorny[1], A. Fert[4]

[1] *Department of Physics, A. M. University, Poznan, Poland*

[2] *Institute of Molecular Physics, Polish Academy of Sciences, Poznan, Poland*

[3] *Department of Theoretical Physics and Astrophysics, P. J. Safarik University, Kosice, Slovak Republic*

[4] *Unite Mixte de Physique CNRS/THALES, Paleseau, France*

Transfer of spin from conduction electron systems to localized magnetic moments can generate transitions between the system's various magnetic equilibrium states. This phenomenon is referred to as *current-induced magnetic switching*. However, under certain conditions, the spin-transfer torque may cause a transition to precessional states of microwave frequencies, wherein energy is pumped from a voltage source to the magnetic system. Some of the models used to describe the spin transfer torque will be analyzed. *Current-induced switching* and dynamics in spin valves will also be presented and discussed in detail within a macro-spin model describing switching phenomena in metallic spin valves. Moreover, the close correlation with the normal and inverse giant magneto-resistance effect will be considered in view of the recently obtained experimental data. Particular attention will be paid to structures where microwave precessional states can be induced by current in the absence of an external magnetic field. Since *current-induced magnetic switching* is a general phenomenon, it may also occur in many spin-valves, e.g. magnetic tunnel junctions, spin valves including magnetic particles, quantum dots or molecules. Some of these spin valves will be considered in greater detail.

A Geometrically Frustrated Kagome Staircase Lattice with Chemical Disorder

R. Szymczak, M. Baran, J. Fink-Finowicki, B. Krzymańska,
P. Aleshkevych, H. Szymczak

Institute of Physics, Polish Academy of Sciences,
Al. Lotników 32/46, 02-668 Warsaw, Poland

The effect of nonmagnetic Mg^{2+} and magnetic Co^{2+} doping in Kagome staircase compounds was investigated using DC magnetic susceptibility. It has been demonstrated that the chemical disorder introduced by low-level doping had a weak effect on the exchange interactions in the Kagome system. The effect was weaker for Ni doping.

The crystal field was considerably weaker in $Ni_3V_2O_8$ than it was in $Co_3V_2O_8$ crystals. Co-doping increased the crystal field parameters of $Ni_3V_2O_8$ considerably and induced an easy axis along the c direction, in agreement with the experimental data. In contrast, doping with nonmagnetic Mg^{2+} ions considerably reduced the crystal field parameters of $Co_3V_2O_8$ crystals. It follows from the presented results that the a axis is an easy axis for pure and Mg-doped $Co_3V_2O_8$ crystals. The peculiar behavior of Co^{2+} ions is unquestionably related to the Jahn-Teller character of these ions.

Atomic Order of Magnetic Inclusion in Semiconductors

K. Ławniczak-Jabłońska[1*], I. N. Demchenko[1], A. Wolska[1], J. Sadowski[1,2], M. Klepka[1]

[1] *Institute of Physics PAS, Al. Lotników 32/46, 02-668 Warsaw, Poland*

[2] *MAX-Lab, Lund University, 221 00 Lund, Sweden*

The field of research referred to as spintronics concerns fabrication of materials with desirable magnetic properties at room temperature. Ga1-xMnxAs layers exhibit the paramagnetic to ferromagnetic phase transition for Mn content in excess of 0.5%. At the same time, MnAs clusters of sizable dimensions can be produced from a single-phase GaMnAs material through high-temperature post-growth annealing yielding multiphase materials. Since MnAs is a metallic ferromagnet with T_c of about 318 K, the GaAs:MnAs granular system is an interesting material, with small ferromagnetic nanoparticles immersed in the semiconductor host lattice providing built-in magnetic field at room temperature. This field affects the semiconductor band's structure leading to differentiation of semiconductor spin states. Therefore, is to growing a material with the two phases distributed homogeneously, simultaneously magnetic and semiconducting, is an attractive method of controlling spin polarization. Usually, Mn-doped GaAs is the first choice to obtain this kind of material, but the implantation of Mn+ into Si appears to be an equally promising way of producing magnetic inclusions. It has been shown that it is possible to achieve above room temperature ferromagnetism in such samples. The potential new spintronic devices based on the Si matrix would be easy to integrate with the existing technologies. However, despite their very interesting properties, there are still few reports on this subject.

Changes in the local structure around Mn atoms in (Ga,Mn)As layers after high-temperature annealing and in Si implanted with Mn^+ ions were determined through x-ray absorption spectroscopy and compared with their magnetic properties. Having considered several models of local atomic structure of Mn, we found the EXAFS spectra analysis to offer unambiguous evidence of a transition in the local structure around Mn atoms.

The Artemis and Athena programs, using the IFEFFIT data analysis package, were applied to process EXAFS data. The theoretical XANES spectra were calculated using the FEFF 8.2 code.

Acknowledgements

This work was partially supported with national grant of the Ministry of Science and High Education no. N202-052-32/1189 and by DESY and the European Community, under Contract RII3- CT-2004-506008 (IA-SFS).

*Corresponding author: jablo@ifpan.edu.pl

EXAFS Analysis of Diluted Mn in Bulk and Nanostructured Ge

R. Gunnella

Istituto di Fisica, Università di Camerino,
via Madonna delle Carceri, Camerino (MC), Italy

On the basis of our EXAFS studies, we have reached a homogeneous understanding of the barely known Mn_xGe_{1-x} system [2, 3]. A satisfactory picture was obtained by analyzing a wide set of samples grown under various nominal conditions either by implanting Mn^+ ions at 100 keV or by the co-evaporation (MBE) technique. We have shown ion implantation (as compared to MBE-grown samples in similar doses and substrate temperatures) to be remarkably successful in diluting Mn in Ge, already at the implantation temperature of 300°C, and at very high Mn doses ($4 \cdot 10^{16}$ at/cm^3) [4, 5]. Films grown by the MBE technique at similar Mn concentrations and substrate temperatures (> 70°C) were affected by the formation of Mn_5Ge_3 crystallites about 100 nm in size, ten times larger than those observed in the case of implanted samples.

Nevertheless, the single-phase DMS, i.e. the achievement of a material almost free of defects and spurious phases is yet to come, as we have observed the simple low-temperature growth to be insufficient to reduce the formation of defects. On the contrary, it appears to induce an amorphous Mn-rich phase, the crystallites' precursor, but probably also relevant occupation of interstitial sites [6, 7, 8]. The possibility of interstitial occupation is still controversial and invoked to some extent by theoreticians to explain the higher value of the nearest neighbor distance of Mn in Ge found experimentally (2.50 Å). A much lower value has been obtained from ab initio LDA+U calculations in substitutional occupation (2.42 Å) while a value more consistent with observations has been obtained for the tetrahedral interstitial site [9]. Such structural complexity hinders the establishment of clear-cut magnetic properties (Curie temperatures, magnetic moment) unaffected by ferromagnetic spurious signals and complicates comparison with ab initio calculations of the electronic properties.

References

1. Y. Ohno, D.K. Young, B. Beschoten, F. Matsukura, H. Ohno, Nature 402 (1999) 790
2. Y.D. Park, et al Science 295, 651 (2002)
3. S. Cho et al, Phys. Rev. B 66, 033303 (2002)
4. S. Picozzi, et al. Appl. Phys. Lett. 86, 062501 (2005)
5. L. Ottaviano et al, Appl. Phys. Lett. 88, 061907 (2006)
6. R. Gunnella, et al. Surface Science 577 (2005) 22 30
7. L. Ottaviano et al. J. Appl. Phys to be published
8. A. Verna et al, Phys. Rev. B 74, (2006)
9. A. Continenza, G. Profeta, and S. Picozzi, Phys. Rev. B 73, 035212 (2006)

Reorientation Effects and Magnetization Reversal in Synthetic Antiferromagnets

A. N. Bogdanov, U. K. Roessler

IFW Dresden, P. O. Box 270116, 01171 Dresden, Germany

Many recently synthesized nanostructured materials have magnetic constituents with antiferromagnetic coupling, e.g. ferromagnetic/antiferromagnetic bilayers, synthetic antiferromagnets, spin valves or toggle magnetic random access memory (MRAM) devices [1, 2]. In this report, a phenomenological macrospin model is derived in order to investigate magnetic states in antiferromagnetically coupled magnetic thin film elements. We analyze the possible magnetic configurations and study their evolution in the applied magnetic fields [3, 4, 5]. We present a detailed analysis of the magnetization processes in antiferromagnetically coupled multilayers and elucidate a number of effects recently observed in these nanostructures [4, 5].

References

1. T. M. Maffitt et al., *IBM J. Res. & Dev.* **50** (2006) 25
2. D. C. Worledge, *IBM J. Res. & Dev.* **50** (2006) 69
3. U. K. Roessler, A. N. Bogdanov, *Phys. Rev. B* **69** (2004) 094405
4. U. K. Roessler, A. N. Bogdanov, *J. Appl. Phys.* **101** (2007) 09D105
5. A. N. Bogdanov, U. K. Roessler, *Appl. Phys. Lett.* **89** (2006) 163109

Study of Magnetic Resonance of Magnetic Nanoparticles in a Polymer Matrix

N. Guskos[1,2*], J. Typek[2], M. Maryniak[2], E. A. Anagnostakis[1], A. Guskos[2]

[1] *Solid State Section, Department of Physics, University of Athens, Panepistimiopolis, 15 784 Zografos, Athens, Greece*

[2] *Institute of Physics, Szczecin University of Technology, Al. Piastów 17, 70-310 Szczecin, Poland*

From a physical point of view, polymers are very interesting materials as there are numerous intriguing physical processes at work in polymers in various temperature ranges, including those involved in the critical phenomena. The study of magnetic nanoparticles dispersed in low concentrations in polymers could facilitate further progress in two major areas: the investigation of matrix critical phenomena and the improvement of matrices' physical properties to improve their functionality. Aggregation and agglomeration of magnetic nanoparticles leads to the formation of nano- and microsize magnetic structures that can considerably modify the physical properties of a polymer matrix. Ferromagnetic resonance (FMR) spectroscopy is one of the main methods of studying the magnetic interactions and the role of critical (dynamical) processes in matrices. The FMR spectra depend strongly on the kinds of magnetic nanoparticles, their concentrations and temperature. A very low concentration of magnetic nanoparticles embedded in a non-magnetic matrix may significantly modify the points of its transition to the glass-state or its melting transition and the matrix could be studied more effectively by using the FMR technique.

Acknowledgements

This work was partially supported by the European Union/European Social Fund and from the Polish Government's Science Budget 2007–2008 under a research project.

*Corresponding author: ngouskos@phys.uoa.gr

Low Symmetry Centers in $LiNbO_3$ Doped with Yb and Er

S. M. Kaczmarek, T. Bodziony

Institute of Physics, Szczecin University of Technology,
Al. Piastów 17, 70-310 Szczecin, Poland

Electron paramagnetic resonance (EPR) and optical absorption spectroscopy studies of a $LiNbO_3$ single crystal doped with 1 wt% Yb^{3+} (sample #1) and 0.1 wt% Er (sample #5) are reported. Optical absorption measurements of the above-mentioned crystals suggest the presence of localized phonons.

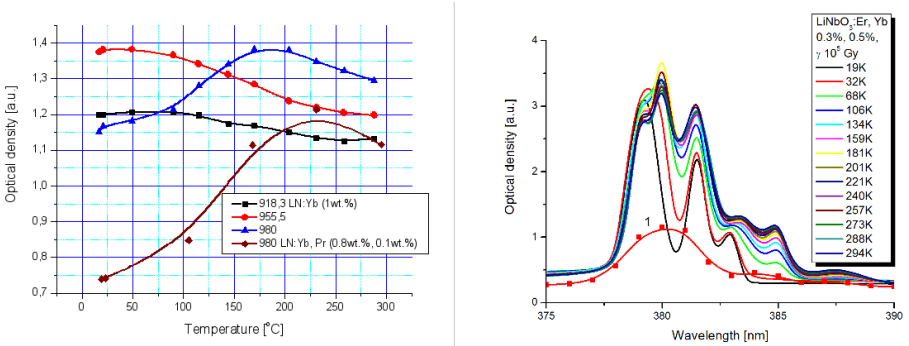

Figure 1: **a)** Temperature dependence of 918.3, 955.5 and 980 nm absorption peaks for LN:Yb (1 wt%) and LN:Yb, Pr (0.8 wt%, 0.1 wt%) single crystals, **b)** Low temperature absorption spectrum of LiNbO3: Er, Yb (0.3 wt%, 0.5 wt%). Curve 1 is an additional absorption spectrum of the crystal after irradiation with γ-quanta

Raman spectra of the following single crystals: (2) $LiNbO_3$: Nd, Yb (0.5 wt%, 0.7 wt%), (3) $LiNbO_3$: Nd, Mg (2 wt%, 6 wt%), and (4) $LiNbO_3$: Er (0.3 wt%) are discussed. Samples #2 – #4 reveal bands in the 50 - 220 cm^{-1} range providing indications similar to those of the optical studies.

In the case of sample #1, the localized phonons may be considered indirect evidence of local perturbations around Yb ions, possibly due to the formation of Yb–Yb ion pairs. The temperature behavior of the EPR lines' intensity and line width for sample #1 reveal antiferromagnetic coupling among Yb^{3+} ions in $LiNbO_3$: Yb^{3+}. Based on this presumption, EPR spectra are interpreted using a spin Hamiltonian for dissimilar Yb^{3+} ion pairs. This model yields overall agreement between the experimental line positions and the simulated results and explains the observed spectral features, which appear to be due to C_1 symmetry of Yb sites.

In the case of sample #5, the localized phonons may be considered indirect evidence of local perturbations around Er ions, possibly due to the formation of Er-Er ion pairs. The EPR lines originating from the ^{167}Er isotope of hyperfine structure and from the ^{even}Er isotopes causing the fine structure were identified. The angular dependence of the EPR lines allowed us to distinguish the presence of several non-equivalent centers. After deconvolution of the EPR line into several Lorentzian components, the Er^{3+} center with the lowest C_1 point group symmetry was resolved and values of the g tensor were estimated.

The obtained results confirmed the model of non-equivalent centers of rare-earth ions in lithium niobate having the lowest C_1 symmetry due to the presence of intrinsic defects in the near-neighborhood of RE^{3+}.

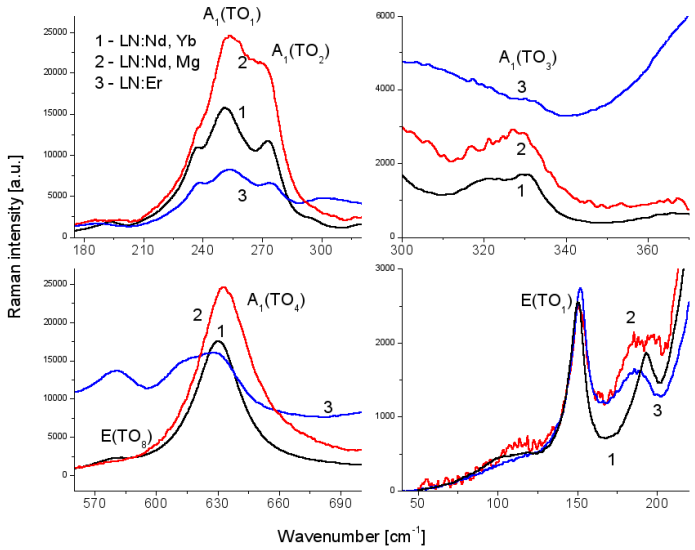

Figure 2: Raman spectra recorded for LN:Nd, Yb (1), LN:Nd, Mg (2) and LN:Er (3) single crystals

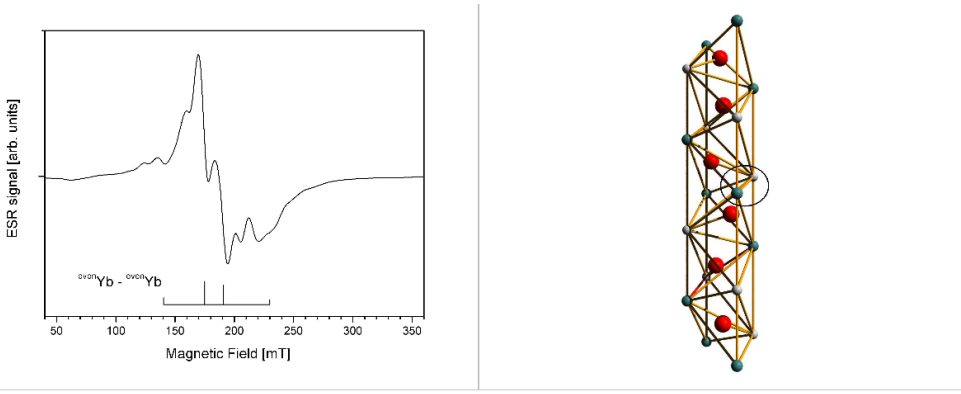

Figure 3: **a)** Sample of the EPR spectrum of $LiNbO_3$:Yb^{3+} (1 wt%) at 8 K measured in the ZX plane. Magnetic dipole-dipole splitting is indicated **b)** Schematic structure of the nearest neighbor ions around Yb^{3+} ions in the LN unit cell: Li^+ (light grey), Nb^{5+} (green), and O^{2-} (red); the most probable position of the Yb_{Li} – Yb_{Nb} ion pair is marked by a circle

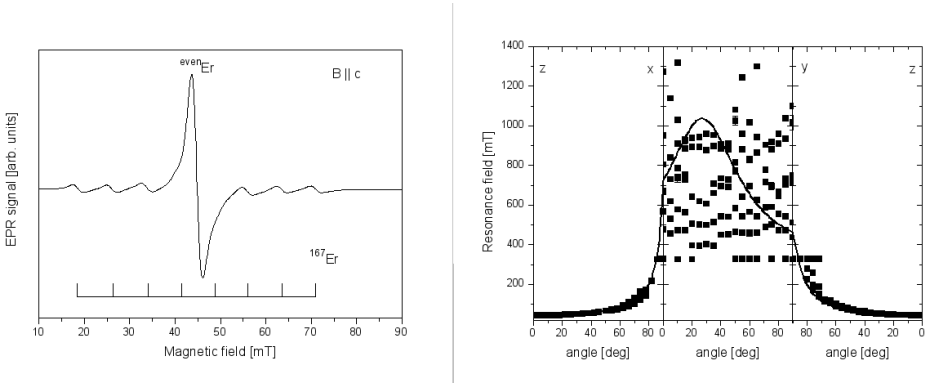

Figure 4: **a)** EPR spectrum of $LiNbO_3$: Er^{3+} crystal measured at $T = 8$ K. The magnetic field is oriented parallel to the c-axis ($B \| c, \theta = 0°$), **b)** Angular dependence of the EPR spectra of $LiNbO_3$: Er^{3+} crystal measured at 8 K in all three perpendicular planes: black squares mark positions of fitted Lorentzian lines and measured EPR lines from the spectrum (with errors); marked lines are calculated using the spin Hamiltonian (EPR-NMR program)

References

1. T. Bodziony, S. M. Kaczmarek, "A new low symmetry centres of Yb^{3+} impurities in lithium niobate single crystal", Optical Materials, 29 (2007) 1440-1446
2. T. Bodziony, S. M. Kaczmarek, J. Hanuza, "EPR and optical studies of $LiNbO_3$:Yb and $LiNbO_3$:Yb, Pr single crystals", J. All. & Comp., 10.1016/j.jallcom.2007.04.189
3. T. Bodziony, S. M. Kaczmarek, "EPR and optical study of coupled pairs in weakly doped $LiNbO_3$:Yb single crystal", Res. Chem. Intermediates, 6 (2007) in the print
4. T. Bodziony, S. M. Kaczmarek, C. Rudowicz, "EPR and optical study of magnetically coupled Yb^{3+} ion pairs in weakly doped $LiNbO_3$:Yb single crystal", J. Phys.: Cond. Master, under review
5. T. Bodziony, S. M. Kaczmarek, "EPR study of low symmetry Er centers in congruent lithium niobate", Phys. Stat. Sol. B, under review

Extended Free Radical Networks Derived from the Condensation of Cyanuric Chloride with p-Phenylenediamine

N. Guskos[1,2*], G. Żołnierkiewicz[2], A. Guskos[2], D. Petridis[3]

[1] *Solid State Section, Department of Physics, University of Athens, Panepistimiopolis, 15 784 Zografos, Athens, Greece*

[2] *Institute of Physics, Szczecin University of Technology, Al. Piastów 17, 70-310 Szczecin, Poland*

[3] *NCSR "Demokritos", Aghia Paraskevi, Attikis, Athens, Greece*

Covalent layered networks were derived by condensation of cyanuric chloride with bridging para- or meta- phenylenediamine. The local chemical environment of the layered solid can be modified by a redox reaction to produce new reconstructed derivatives. Thus, a blue product was obtained by treating an alcoholic dispersion of the layered solid with ferric nitrate or potassium persulfate, signaling the possible formation of an extended free radical. When iron nitrate was used as oxidant, the temperature-dependent magnetic resonance spectra were measured in the 290–90 K region. The magnetic resonance measurements showed the coexistence of two spectra originating from two different magnetic centers: a narrow line centered at $g = 2.0038(1)$, of line width $\Delta H = 6$ Gs (free radical), and a broader line centered in the lower resonance magnetic field (cluster) [1]. This suggested the presence of aggregated radicals. A new sample was prepared so that the broader line was more intense. The narrow line was centered as above, but its line width was greater ($\Delta H = 8.5(2)$ Gs) and the broader line was more intense with the resonance field's stronger shift towards the lower magnetic field. The temperature dependence of the magnetic resonance lines was highly variable in both cases. At higher temperatures, integrated intensities decreased with decreasing temperatures in both spectra. This behavior is similar to that of magnetic nanoparticles in nonmagnetic matrixes [2]. The resonance field of the broader line was shifted towards the lower magnetic field with $\Delta H_r/\Delta T = 1.5(1)$ Gs/K while the narrow line was shifted towards the higher magnetic field with $\Delta H_r/\Delta T = 0.020(1)$ Gs/K. The width of the broader line increased with decreasing temperature, while the narrow line remained almost constant. The broader line originated from a magnetic iron oxide, e.g. Fe_3O_4 [3], and could form internal magnetic field capable of interaction with free radicals. It could direct free radicals to form the magnetic ordering state.

References

1. Bourlinos A B, Giannelis E P, Sanakis Y, Bakandritsos A, Karakassides M, Gjoka M and Petridis D 2006 *Carbon* (44) 1906
2. Guskos N, Likodimos V, Glenis S, Typek J, Maryniak M, Roslaniec Z, Baran M, Szymczak R, Petridis D and Kwiatkowska M 2006 *J. Appl. Phys.* (99) 084307
3. Guskos N, Anagnostakis E A, Likodimos V, Typek J and Narkiewicz U 2005 *J. Appl. Phys.* (97) 0204304

*Corresponding author: ngouskos@phys.uoa.gr

Advanced Nanostructured Metallic Composites for Energy Storage

M. Jurczyk*, M. Nowak

Institute of Materials Science and Engineering, Poznan University of Technology, M. Skłodowska-Curie 5 Sq., 60-965 Poznan, Poland

A major problem of the future world with renewable energies and reduction of environmental pollution will be energy storage. Novel nanostructured materials may successfully solve this problem. Currently, the most important goal of research in hydrogen storage materials is to develop materials of high hydrogen storage capacity, fast hydrogenation/dehydrogenation kinetics and low cost [1]. For example, the hydrogen storage capacity of Mg and Mg_2Ni is rather high, respectively 7.6% and 3.6% of mass. However, their hydrogen absorption and desorption temperature is too high and their hydrogenation/dehydrogenation kinetics is insufficient for practical applications. Considerable effort has been made to remedy the disadvatages of microcrystalline hydride materials including alloying element additions, surface modifications and forming composites with catalytic components. At the same time, the research in hydrogen storage materials entered an exciting new phase with the advance of nanocrystalline alloys, which exhibit substantially enhanced absorption/desorption kinetics, even at room temperature [2].

In order to optimize the choice of inter-metallic compounds for a battery application, it is crucial to attain better understanding of the role of each constituent alloy on the electronic properties of the material. Nanocrystalline metal hydrides offer a breakthrough in the prospects for practical applications. Their excellent properties, significantly exceeding those of traditional hydrides, are a result of combined engineering of many factors, incl. alloy composition, surface properties, microstructure and grain size. The present authors and their co-workers have investigated the microstructure and properties of TiFe-, TiNi-, ZrV_2- and $LaNi_5$-type nanocrystalline alloys in order to reveal the influence of materials' microstructure on the electrochemical properties of hydrogen storage alloys [3].

In this work, we have studied experimentally the structure, electrochemical and electronic properties of nanostructured $LaNi_5$/M- and Mg_2Ni/M-type composites, where M=C, Ni, Cu or Pd. These materials were prepared by high-energy ball-milling (HEBM) of host phases with catalytic elements. The properties of hydrogen storage materials can be modified substantially by alloying to obtain the desired storage characteristics. For example, it has been found that substituting nickel with cobalt in $LaNi_{4-x}Mn_{0.75}Al_{0.25}Co_x$ alloy greatly improves the discharge capacity and cycle life of $LaNi_5$ materials. In nanocrystalline $LaNi_{3.75}Mn_{0.75}Al_{0.25}Co_{0.25}$ powder, discharge capacities up to 260 mA h g^{-1} have been obtained. The Mg_2Ni electrode, mechanically alloyed and annealed, displayed its maximum discharge capacity (100 mA h g^{-1}) at the 1st cycle, but degraded strongly during further cycling. In nanocrystalline $Mg_{1.5}Mn_{0.5}Ni$ alloy, discharge capacities up to 241 mA h g^{-1} were measured. At the same time, mechanically coated $LaNi_5$- and Mg_2Ni-based alloys with graphite, nickel, copper or palladium have effectively reduced the degradation rate of the studied electrode materials. Finally, the properties of nanocrystalline alloys and their nanocomposites were compared with those of microcrystalline samples. The substitution of Ni in the $LaNi_5$ alloy or Mg in the Mg_2Ni alloy with transition metals leads to significant modifications of the shape and width of the XPS valence band of both nanocrystalline and microcrystalline samples. Especially, the valence bands of the nanocrystalline alloys are considerably broader compared with those measured for the microcrystalline samples. The strong modifications of the electronic structure of the nanocrystalline $LaNi_5$- and Mg_2Ni-type alloys could significantly influence their hydrogenation properties, similarly to the behavior observed earlier for nanocrystalline FeTi-, TiNi- and ZrV_2-type alloys. The present paper will review our recent results.

*Corresponding author: fax: +48 61 665 3576, phone: +48 61 665 3508, e-mail address: jurczyk@sol.put.poznan.pl

Acknowledgements

The financial support of the Polish Ministry of Education and Science under the contract No 3 T10A 033 29 is gratefully acknowledged.

References

1. L. Schlapbach, A. Züttel, Nature (London) 414 (2001) 353
2. M. Jurczyk, Bull. Pol. Ac.: Tech., 52 (2004) 67
3. M. Jurczyk, M. Nowak, in: Nanostructured Materials in Electrochemistry (Ed. A. Eftekhari), chapter 9, Wiley-VCH (2007) – in print

Glass-forming Ability of Selected Metallic Systems

B. Idzikowski

Institute of Molecular Physics, Polish Academy of Sciences,
M. Smoluchowskiego 17, 60-179 Poznan, Poland

Topological criteria for amorphization of multi-component alloys are discussed. A model is proposed for metallic glass formation through destabilization of the host crystalline lattice by substitutional and/or interstitial solute elements. A solute element may partition between substitutional and interstitial sites and the model calculates relative site frequency as a function of the strain energy associated with each site. The strain energy, in turn, depends upon solute's and solvent's elastic properties and relative sizes, and upon temperature. The crystalline lattice is destabilized, which may lead to amorphization, when solute elements produce a critical internal strain required to change local coordination numbers [1].

For example, we have found fully amorphous structures in melt-spun alloys from the $DyMn_{6-x-y}Fe_{x+y}Ge_{6-x}Al_x$ ($x, y = 0, 1, \ldots, 6$) pseudo-ternary system [2]. During rapid solidification, the amorphous states compete with the nucleation of ternary inter-metallic compounds of different crystallographic structures. All amorphous samples exhibit multi-step crystallization behavior without a clear indication of glass transition below the first exothermic effect. Some of the amorphous alloys exhibit magnetic ordering above room temperature and complex magnetic transitions similar to the properties of crystalline 1-6-6 compounds. The occurrence of glassy states in Dy-$(Mn,Fe)_6$-$(Ge,Al)_6$ cannot be classified with the usual rules developed for the glass-formation ability in multinary amorphous metals. Repulsive interactions between certain alloy components play are important for the stability of these amorphous structures. This effect requires four or five alloy components within a basic amorphous structure. The results suggest that chemical interactions are important for a refined confusion principle in multinary metallic glass-formers.

Another type of amorphization and nanocrystallization processes during heat treatment has been observed in NANOPERM-type materials. With increasing temperature of treatment, amorphous $Fe_{41}Ni_{40}Zr_7B_{12}$ alloy undergoes nanocrystallization with its SRO (short range order) close to the fcc-crystal structure [3]. Magnetization of a sample annealed above 582°C for 1 hour becomes enormously sensitive to pressure (and thus volume) changes. Even a small increase in the annealing temperature, e.g. from 582°C to 595°C, leads to pronounced magneto-volumetric phenomena. The pressure-induced reduction of magnetization is by almost an order of magnitude. This behavior is comparable with the Invar characteristics of the crystalline $Fe_{67}Ni_{33}$ alloy. This reflects an abrupt increase in the range of the coherent (crystalline) regions, a qualitative change in their electron structure and a relevant evolution in the characteristic behavior of itinerant ferromagnets. In general, the temperature dependencies of magnetic parameters corresponding to nanosized grains deviate from those of bulk alloy of the same composition. Three mechanisms responsible for the observed effects are proposed: (i) influence of impurities in nanograins, (ii) contribution of grain surface or, most probably, (iii) changes in lattice parameters of $Cr_{23}C_6$-type grains. Different magnetic behavior may be observed for low, medium and high volumetric fractions of crystallites.

Both families of alloys exhibit unusual magnetic behavior in amorphous states as well as after relaxation of their glassy structure or after the first stage of crystallization. These problems are also discussed.

References

1. A.R. Yavari: "The changing faces of disorder" Nature Mater, 6 (2007) 181
2. P. Kerschl, U. K. Rößler, T. Gemming, and K.-H. Müller, Z. Śniadecki, B. Idzikowski: "Amorphous states of melt-spun alloys in the system Dy-$(Mn,Fe)_6$-$(Ge,Al)_6$" Appl. Phys. Lett. 90 (2007) 031903
3. B. Idzikowski, A. Szajek, J.-M. Greneche, J. Kovac: "Nanogranular $Fe_xNi_{23-x}B_6$ phase formation during devitrification of nickel-rich $Ni_{64}Fe_{16}Zr_7B_{12}Au_1$ amorphous alloy", Appl. Phys. Lett. 85 (2004) 1392

Some Recent Developments on Systems Exhibiting Negative Behaviour

J. N. Grima

Department of Chemistry University of Malta, Msida MSD 2080

Systems (materials or structures) which are described as exhibiting "negative behaviour" are those which have some property X where in most materials, X would be positive, but in negative materials, this property is negative. Examples of negative systems include materials and structures having a negative Poisson's ratio (auxetic) which exhibit the counter-intuitive behaviour of getting fatter when stretched and thinner when compressed, or systems which have a negative thermal expansion coefficient (NTE), i.e. systems which get smaller when heated and expand when cooled.

Such negative systems are generally found to have various enhanced characteristics with the result of having many potential practical applications. For example, auxetics exhibit improved indentation resistance, enhanced acoustic properties, etc. which make them ideal for use as protective materials whilst NTE materials are very useful in applications involving the manufacture of composite materials which can be tailor made to exhibit pre-desired thermal expansion properties.

Here we discuss some of the recent developments in this field by discussing mechanisms which can lead to negative properties. In particular we will look at how such anomalous behaviour can be manifested in various systems ranging form mechanical models to single crystalline materials (e.g. silicates and zeolites).

ORAL COMMUNICATIONS

Cross-scaled Simulation Methods of Investigating Nanomechanical Properties of Metals

J. Dziedzic[1], M. Bobrowski[1,2], M. Białoskórski[1,2], J. Rybicki[1,2,3]

[1] *Department of Solid State Physics, Faculty of Technical Physics and Applied Mathematics, Gdansk University of Technology, Narutowicza 11/12, 80-952 Gdansk, Poland*

[2] *TASK Computer Centre, Gdansk University of Technology, Narutowicza 11/12, 80-952 Gdansk, Poland*

[3] *Institute of Mechatronics, Nanotechnology and Vacuum Technique, Koszalin University of Technology, Racławicka 15–17, 75-620 Koszalin, Poland*

Our recent results in cross-scaled modeling of nanomechanical properties of metals at the atomic scale are presented. In particular, a new computer code enabling embedding tight-binding (TB) calculations into a molecular-dynamics (MD) framework is introduced.

Nanoindentation and nanoscratching of a cuboid-shaped copper slab with various crystallographic orientations ((100), (110), (111)) by an infinitely hard indenter have been simulated in pure MD and hybrid TB+MD approaches. The time-space evolution of plastically deformed regions predicted by both computational models have been compared carefully. The results are discussed in terms of stress field distributions and geometrical characteristics of local atomic neighborhoods. The normal and tangent forces experienced by the indenter have been analyzed for the considered workmaterial's orientations. The need to include quantum-based force fields in the vicinity of the indenter's tip in order to obtain realistic brittle behavior is discussed critically.

A Phase Diagram of Symmetric A–B Diblock Copolymer Solutions: a Lattice Monte Carlo Simulation Study

S. Wołoszczuk

Department of Macromolecular Physics, Faculty of Physics,
Adam Mickiewicz University, Poznan, Poland
tango@amu.edu.pl

A phase diagram for symmetric A–B diblock copolymer solutions of various concentrations was constructed using the Cooperative Motion Algorithm [1] (see [2] for the method's description). We started from pure melt (50% segments of type A and 50% of type B, concentration $\Phi = 1.0$) and replaced some diblock chains with a selective solvent of type A. The solvent's selectivity implies that its interactions with the A block were different from those of the B block. After the first modification, we obtained a solution consisting of 55% of A segments (copolymer A blocks and added solvent molecules) and 45% of B segments (copolymer B blocks), in $\Phi = 0.9$ concentration. Next, we performed a simulation with 60% of A segments (concentration $\Phi = 0.8$). In further steps, we changed the concentration as above in 0.1 decrements (5% increment of the A segment volume fraction), finally reaching 95% of A-segments, i.e. a concentration of $\Phi = 0.1$.

The simulation started at each concentration from a homogenous "athermal" state. Such a perfectly mixed system was quenched to a set of temperatures below and above the order-disorder transition (ODT) and another set of very low temperatures. We used quenching instead of slow cooling having found [3] that quenching should be considered a more favorable method to achieve equilibrium states in block copolymer simulations. This particularly concerns temperature ranges in which structural relaxations become very sluggish; similar problems appear in real systems [5].

We have obtained a set of thermodynamic and structural properties such as energy, specific heat, and mean- squared end-to-end distance calculated both for the whole chain as well separately for particular blocks, in order to identify the obtained self-assembled nanostructures and provide an outline of a phase diagram as a function of the chain's concentration, Φ. We have observed classical nanostructures such as lamellas, hexagonally and cubically packed cyliners, FCC-, BCC; and SC-packed micelles, as well as a very interesting non-classical double-continuous gyroid phase. We have also identified such microstructures as hexagonally and cubically perforated lamellas, and an intermediate lengthened micellar phase between the cylinder and the micelle region.

With reference to our earlier work on low-temperature ordering effects in triblock and diblock copolymer melts [3, 4], we have found that the observed phenomenon also appears, in a similar form, throughout the concentration range of copolymer solutions.

References

1. S. Woloszczuk, P. Knychala, M. Banaszak and M. Radosz, unpublished
2. T. Pakula, Simulation Methods for Polymers, ed. M. J. Kotelyanski, D. N. Thedorou (Marcel-Dekker, 2004), chap. 5
3. M. Banaszak, S. Wołoszczuk, S. Jurga, and T. Pakula, J. Chem. Phys., **119(21)**, 11451 (2003)
4. M. Banaszak, S. Wołoszczuk, S. Jurga, and T. Pakula, J. Chem. Phys., **121(23)**, 12044 (2004)
5. G. Floudas, T. Pakula, G. Velis, S. Sioula, and N. Hadjichristidis, J. Chem. Phys., **108**, 6498 (1998)

Growing Lyzosyme Crystals under Various Physicochemical Conditions

J. Siódmiak, A. Gadomski

University of Technology and Life Sciences in Bydgoszcz, Kaliskiego 7, 85-796 Bydgoszcz, Poland

A computer model of the growth of lyzosyme crystals under a variety of physicochemical conditions is proposed. The growth unit is constituted by the protein in its HP (hydrophobic-hydrophilic) cubic representation. The crystal's growth is driven by hydrophobic interactions between incoming growth units and the crystal's surface. The energies of HH, HP and PP interactions are taken from the well-known HP model and can be modified within the limits of the Miyazawa-Jernigan matrix, which describes interactions between amino acids in proteins. Suitably chosen energy values of HH, HP and PP interactions can mimic various physicochemical conditions of the system in which the crystal can grow. Some combinations of energy values lead to different crystal forms being obtained, which is an experimentally confirmed phenomenon.

Properties of Polymers in Confinement

P. Romiszowski, A. Sikorski

Department of Chemistry, University of Warsaw,
Pasteura 1, 02-093 Warszawa, Poland

We designed and developed a simple model of polymer chains. The chains consisted of identical united atoms (segments) and were restricted to a simple cubic lattice with excluded volume interactions only (an athermal system). The polymers were confined between two parallel impenetrable walls with one end of each chain grafted to the wall. A single linear polymer chain was located in such environment. The structural properties of the brush were determined from the Monte Carlo simulations. A Metropolis-like sampling algorithm with local changes of chain conformation was used. The short- and long-time dynamic properties of the model system were studied. The influence of the system's density and the length of chains on the probe polymer chain's mobility was studied and discussed. The mechanism of the chain's motion was also investigated.

References

1. Romiszowski P and Sikorski A 2006 *J. Non-Cryst. Solids* **352** (40–41) 4303
2. Romiszowski P and Sikorski A 2006 *J. Chem. Phys.* **125** (10) 104901

In-situ XAS Fuel Cell Measurements and EXAFS Analysis of a Nano-structured Pt Cathode Electrocatalyst

A. Witkowska[1,2], E. Principi[2], A. DiCicco[2,3], S. Dsoke[4], R. Marassi[4], L. Olivi[5], V. Rossi Albertini[6]

[1] *Department of Solid State Physics, Gdansk University of Technology, Narutowicza 11/12, 80-952 Gdansk, Poland*

[2] *CNISM, CNR-INFM SOFT, Department of Physics, University of Camerino, I-62032 Camerino (MC), Italy*

[3] *IMPMC-CNRS, Universitè P. et M. Curie, 140 rue de Lourmel, 75015 Paris, France*

[4] *Chemistry Department, University of Camerino, I-62032 Camerino (MC), Italy*

[5] *ELETTRA Sincrotrone Trieste S. C. p. A., 34012 Basovizza, Trieste, Italy*

[6] *ISM-CNR, via del Fosso del Cavaliere, 100, 00133 Roma, Italy*

Understanding the structure and dynamics of nanomaterials and their physico-chemical properties is currently regarded as a challenging research activity with crucial consequences for material design of various novel applications. Much effort is currently devoted to the study of Pt-based nano-metallic electrocatalysts in order to improve the performance of polymer electrolyte membrane fuel cells (PEMFC's) and reduce their cost.

The size, shape and morphology of the platinum group metals] and/or Pt-based metal alloy particles and the amount and type of species adsorbed on these particles are important physical quantities directly affecting the catalyst's performance. Therefore, a number of studies have been conducted to characterize the catalyst's structure. In this context, X-ray absorption spectroscopy (XAS), which yields unique information due to its high sensitivity to local atomic arrangements around selected catalytic metal sites, appears to be a particularly powerful tool [1]. XAS may be especially useful for obtaining information on poisoning and structural degradation and can be used under *in-situ* conditions: in fuel cell-relevant conditions, e.g. [2, 3], or even in real fuel cells, e.g. [4, 5]. In the latter case, due to the background absorption of cell components and to the low mass content of metal catalysts, reliable and high quality data may only be obtained using specially designed fuel cells and optimized experimental setup. Then, in order to obtain reliable structural information and avoid misinterpretation, XAFS analysis of metallic nanoparticles, supported or unsupported, should be accurate and sufficiently sophisticated.

In this contribution, we report some of the X-ray absorption fine structure (XAFS) results measured at the Pt L_3-edge for a pure platinum catalyst (20%Pt supported on Vulcan XC-72, Pt loading 1.0 mg/cm^2) obtained using a single fuel cell especially modified to perform low-noise *in-situ* XAS experiments in transmission and fluorescence modes, in a wide range of X-ray energies [6]. A structural analysis of the EXAFS spectra was performed using a GNXAS data-analysis method [7, 8]. The methodology applied to advance EXAFS multiple-scattering analysis accounts both for the catalytic nanoparticles' size distribution and sample inhomogeneities (investigated with scanning electron microscopy, SEM, transmission electron microscopy, TEM, and X-ray diffraction techniques) [9].

The obtained results demonstrate that detailed information about the structural changes induced by the working conditions (potential and temperature) or time (the ageing effect) in the nanocatalyst can be obtained through *in-situ* XAFS measurements and analysis.

Acknowledgements

We gratefully acknowledge the support of the Synchrotron Light Laboratory ELETTRA for the beam time at the XAFS 11.1 station.

This research has been carried out as part of the NUME Project "Development of composite proton membranes and of innovative electrode configurations for polymer electrolyte fuel cells" (MIUR, FISR 2003).

References

1. Russell A E and Rose A 2004 *Chem. Rev.* **104** 4613
2. Herron M E, Doyle S E, Pizzini S, Roberts K J, Robinson J, Hards G and Walsh F C 1992 *J. Electroanal. Chem.* **324** 243
3. Maniquet S, Mathew R J and Russell A E 2000 *J. Phys. Chem. B* **104** 1998
4. Viswanathan R, Hou G, Liu R, Bare S R, Modica F, Mickelson G, Segre C U, Leyarovska N and Smotkin E S 2002 *J. Phys. Chem.* **B 106** 3458
5. Wiltshire R J K, King C R, Rose A, Wells P P, Hogarth M P, Thompsett D, and Russell A E 2005 *Electrochim. Acta* **50** 5208
6. Principi E, DiCicco A, Witkowska A, Marassi R 2007 *J. Synchr. Rad.* **14** (3) 276
7. Filipponi A, DiCicco A and Natoli C R 1995 *Phys. Rev. B* **52** 15122
8. Filipponi A and DiCicco A 1995 *Phys. Rev. B* **52** 15135
9. Witkowska A, DiCicco A and Principi E 2007 *Phys. Rev. B* (in print)

Electrical resistivity of liquid metallic hydrogen

V. Shvets[1], Ya. Lepikh[2], S. Artemenko[1], O. Bukhanenko[1]

[1] *Department of High Mathematics, Odessa State Academy of Refrigeration, Dvorianska 1/3, 65082 Odessa, Ukraine*

[2] *Department of Experimental Physics, Odessa National University, Dvorianska 2, 65082 Odessa, Ukraine*

The electrical resistivity of metallic hydrogen has been calculated. To this end, the perturbation theory was employed in terms of electron-proton interaction for the reciprocal relaxation time characterizing electrical conductivity. The second- and third-order terms, as well as an approximate expression for the series sum, were calculated in detail. In doing so, a random-phase approximation with allowance for exchange interaction and correlations in the local-field approximation was used for an electron subsystem and the exact solution of the Percus-Yevick equation for the hard-sphere model was employed for the proton subsystem. In this case, at a given density and temperature, the only parameter of the theory was the hard-sphere diameter. In order to determine this parameter, the effective pair-wise inter-proton interaction was calculated. The hard-sphere diameter was determined from the dependence of the inter-proton interaction on the distance and the known temperature of the system. The dependence of the resistivity of metallic hydrogen on the density and temperature has been examined in a wide range of the latter quantities. In the entire range of densities and temperatures considered, resistivity proved to be close to its limiting value, for which the nearly-free-electron model is applicable.

References

1. Shvets V T 2007 *Physics of Disordered Metals*, Maiak, 500
2. Shvets V T 2007 *JETP* **104** (4) 655

Vanadates and Cobaltates with Kagomé-like Magnetic Structure: Crystal Growth and Properties

S. Barilo[1], A. Yakubovskii[2], V. Plakhty[3],
H. Szymczak[4], W. Flavell[5]

[1] *Institute of Solid State & Semiconductor Physics, 220072 Minsk, Belarus*

[2] *Russian Scientific Center "Kurchatov Institute", 123182 Moscow, Russia*

[3] *St. Petersburg Nuclear Physics Institute, 188350 Gatchina, St. Petersburg, Russia*

[4] *Institute of Physics, 02-668 Warsaw, Poland*

[5] *University of Manchester, Manchester M60 1QD, UK*

The transition metal ions on Kagomé-geometry present one of the most highly frustrated two-dimensional quantum spin systems with only nearest neighbor antiferromagnetic Heisenberg interactions. It was recently shown that properties of geometrically frustrated vanadates and cobaltates can be tuned by chemical engineering to allow the observation of either a spin gap formation or an unusual long range magnetic order and ferroelectricity in the frustrated Kagomé-like lattices. The relationship between the electronic and magnetic structure of these oxides and their unique properties remains quite poorly understood.

Here we report on the results of magnetization and NMR measurements performed on single crystals of poor and mixed vanadates $M_3V_2O_8$ (M = Ni, Co) and $Ln\mathrm{BaCo_4O_{7+\delta}}$ (Ln = Y, Tb, Dy, Ho, Yb). A novel approach to the flux growth technique was explored to limit number of nuclei and to grow high quality single crystals of both the compounds. Details of post growth treatment and characterization of the samples are also presented.

In the lattice of $M_3V_2O_8$ the planes that contain the edge sharing MO_6 octahedra are not flat as in the regular Kagomé-lattice but buckled. These Kagomé-staircase magnetic layers are separated by the non-magnetic VO_4 tetrahedra. As a consequence a noncollinear long range magnetic order and ferroelectricity develop in $Ni_3V_2O_8$ due to reduction of the geometric frustration. The NMR spectra of this compound reveal for the first time that two inequivalent positions of vanadium exist, which might be explained if an extra high anisotropy of Ni^{2+} orbitals will be involved into consideration. Additional neutron and synchrotron diffraction studies needed to monitor the local structural features resulting in coupling of incommensurate magnetic and ferroelectric ordering in the Kagomé staircase $Ni_3V_2O_8$ and its Co-counterparts.

We investigated systematically dc-magnetization of a recently-identified class of tetrahedrally coordinated mixed-valent cobalt oxides, $Ln\mathrm{BaCo_4O_{7+\delta}}$. This structure consists of planes of corner-sharing CoO_4 tetrahedra that form a Kagomé net when considering only the Co ions. These planes are connected in the third dimension by another CoO_4 tetrahedral layer of the triangle symmetry with a one-third density of those of the Kagomé plane. Magnetization measurements on single crystals of $Ln\mathrm{BaCo_4O_{7+\delta}}$ (Ln = Y, Tb, Dy, Ho) clearly show a spin-glass behaviour. Meanwhile, the crystal structure of this material is indicative of a 2D critical dimensionality, which should not allow a spin-glass state with Edwards-Anderson order parameter. Therefore, this family presents a good candidate for a chiral-glass state with ordered local chirality as predicted theoretically by Kawamura. A recent neutron diffraction study on a powder sample of $YbBaCo_4O_7$ shows a structural phase transition at 175 K from trigonal ($P31c$) to monoclinic (Cc) on cooling. This first order transition that buckles the Kagomé planes and allows a long-range antiferromagnetic order to set in at $T \approx 60$ K is accompanied by an anomaly in the crystal magnetization.

Zinc Oxide Hollow ZnO Micro- and Nano-structures: Synthesis, Morphology and Growth Mechanism

L. N. Demyanets, V. V. Artemov, L. E. Li

A. V. Shubnikov Institute of Crystallography of the Russian Academy of Sciences, 119333 Leninsky pr. 59, Moscow, Russia

Hollow structures of ZnO are of special interest as active functional elements for optical nanodevices, as potential micro-reactors or as micro-containers for synthesis and encapsulation of various compounds. We report the synthesis and characterization of ZnO microstructures of hexagonal or spherical shapes and fully or partly hollow interiors.

The microstructures of the first kind are hollow hexagonal prisms of a regular polyhedral shape, with aspect ratio AR < 1. The prisms are single-crystalline, with well-developed {10-10} and (0001) faces and a hollow hexagonal core. The cages are single-, two- or three-walled; the inner holes are 2–5 μm, the outer diameters are up to 8 μm. Such cages are formed in hydrothermal KF solutions at temperatures of 120–200°C.

The micro- and nanostructures of the second kind are partly hollow faceted nanowires and rods with two typical sizes; AR $\gg 5$ (0.5–1 μm in length, 50–100 nm in width and 5–10 μm in length, 0.7–1.5 μm in width). Such structures arise under hydrothermal treatment of Zn plates at 150–220°C in H_2O and MOH solutions. Thin nanotubes are characterized by a hexagonal inner hole, about 50 nm in diameter, and the wall width of 50–100 nm.

The hollow structures of the third kind are polycrystalline spheres with hexagonal holes. Such cages are formed under wet oxidation conditions as a result of oxidation of metallic zinc powder with H_2O_2 solutions at $T_i < 50$°C. These spherical hollow structures are polycrystalline and are built from textured self-assembling ZnO nanocrystals.

Morphology-dependent Behavior of Lasing Action in ZnO-based Disordered Active Media

L. E. Li, L. N. Demyanets

A. V. Shubnikov Institute of Crystallography of the Russian Academy of Sciences, 119333 Leninsky pr. 59, Moscow, Russia

The lasing characteristics of nano- and micro-sized ZnO objects have been studied on samples prepared by HT-pyrolysis and hydrothermal synthesis. Depending on the growth technique and conditions, ZnO nanocrystallites of various morphology and size have been obtained. Lasing behavior of the synthesized samples was found to depend strongly on the crystallites' shapes and sizes. Different mechanisms of feedback formation are responsible for such dependence. Two types of ZnO-based disordered active media are discussed in accordance with the mechanism of feedback formation.

For type I (classical random lasers), the feedback is provided by random closed loops, which are formed due to strong backscattering of light. Numerous individual grains participate in the formation of such loops. Excited media usually contain rounded or irregularly-shaped crystallites of small sizes (crystallites' diameter, D, of less than ≈ 100 nm and aspect ratio AR $\lesssim 2$). As a result, type I lasers are characterized by high emission losses, high lasing thresholds and unstable lasing spectrum parameters from pulse to pulse.

For type II (microlasers), the feedback is provided by natural high-Q microcavities. Well-faceted crystallites of specific shapes and sizes ($D \gtrsim 150$ nm, AR $\gtrsim 5$) serve as such cavities. Every 1D-crystallite works as a microlaser. Type II lasers are characterized by low losses, low thresholds and stable lasing spectra. Such materials seem to be the most promising for applications in microelectronic devices.

Acknowledgements

The work was partially supported by the RFBR, Grant 2116 06-02-17230.

Vapor Phase Composition and Mass Transfer Processes in Growing $Zn_xCd_{1-x}Te$ Solid Solution

G. Ilchuk*, V. Ukrainets, R. Petrus', V. Kusnezh

Department of Physics, National University "Lvivs'ka Politekhnika", 12 S. Bandera Street, Lviv, 79013, Ukraine

Chemical vapor transport (CVT) is a method of growing monocrystal and epitaxial layers of semiconductor compounds. Partial pressure temperature dependences were calculated for the vapor phase (VP) components of a $Zn_xCd_{1-x}Te$-NH_4X (X=Cl, Br, I) thermodynamic system in the 900–1400 K temperature range and the 10^3–10^5 Pa pressure range, for solid solution compositions $x_{CdTe} = 0.1$, 0.2, 0.3. We used a generalized mathematical model for our calculations, the key components of which can be represented in a physical and chemical scheme: possible molecular forms of the vapor phase (VP) → system of independent chemical reactions for VP → system of chemical equilibrium equations → conservation laws of matter quantity → Dalton's law → Raul's law. Such systems were realized in the CVT growing method for a $Zn_xCd_{1-x}Te$ solid solution in the closed volume, using chlorine, bromine and iodine ammonium as transport agents. On the basis of our theoretical analysis, we can see from the obtained partial pressure (p_i) temperature dependences ($p = f(T)$) that the HX; H_2; Te_2; N_2; CdX_2; ZnX_2 components have the highest values of p_i. The molecular form concentration ratio n_{CdX_2}/n_{ZnX_2} in the vapor phase determines the composition x_{ZnTe} of the grown solid solution. The concentration ratio depends on the composition of the source, the total pressure in system, the deposition zone temperature and the transport agent used.

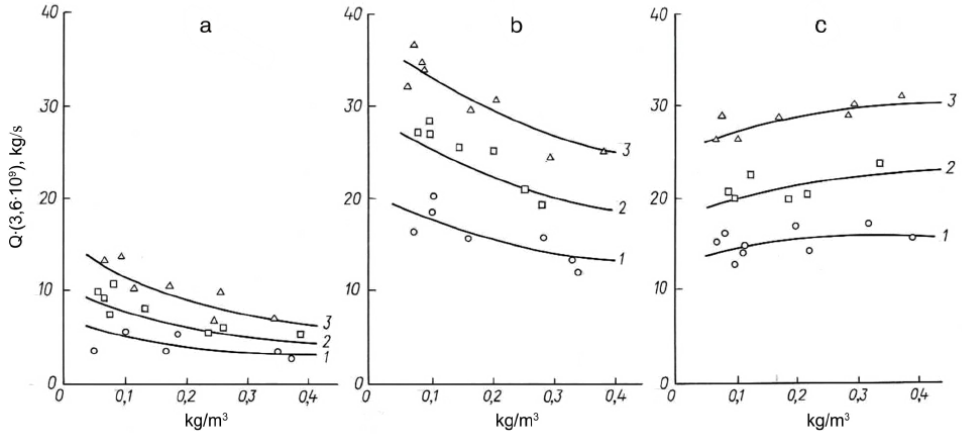

Figure 1: The $Zn_xCd_{1-x}Te$ solid solution ($x = 0.2$) mass transfer rate theoretical (—) and experimental (△, ○, □) dependences on transport agent's concentration in $Zn_xCd_{1-x}Te$-NH_4X systems (a – chlorine, b – bromine, c – iodine) for T_{dep}=1100 K and ΔT=30 K (1); 50 K (2); 90 K (3)

The mass transfer calculations for the $Zn_xCd_{1-x}Te$ solid solution's growth process with the presence of a temperature gradient were reduced to searching for heterogenic reaction characteristic flows, Q1 and Q2. Under conditions of our experiments for viscid flows and diffusion description, the Curtiss-Hirchfelder equation was used. Additional information was the corresponding molecular forms of partial pressure

*Corresponding author: gilchuk@polynet.lviv.ua

above the source surface. Theoretical and experimental investigation of the solid solution's mass transfer rate was conducted for deposition zone temperatures of T_{dep}=1100 and 1200 K in the temperature range of 30, 50, 70 K (see Fig. 1). It is apparently possible in $Zn_xCd_{1-x}Te$-NH_4X systems to control the content of zinc telluride (x_{ZnTe}) in the $Zn_xCd_{1-x}Te$ solid solutions by x increase in the source, by increasing the transport agent's concentration or by changing atomic number of the NH_4X transport halogen in the sequence (Cl → Br → I).

On the basis of our analysis, we have obtained a quantitative correlation for zinc telluride content control during the growth of $Zn_xCd_{1-x}Te$ solid solutions.

Percolation of Carbon Nanotube-Reinforced Nanocomposites: a Study Using the RG Theory

Sina Ghassemi, Akbar Afaghi Khatibi

School of Mechanical Engineering, University of Tehran, PO Box 11365-4563, Tehran, Iran

Electrically conductive polymer composites have broad applications as antistatic materials as well as in self-regulating heaters, overcurrent and overheating protection devices and electromagnetic radiation shielding. Conductive polymer composites can be obtained by compounding polymers with conductive fillers, such as carbon black, carbon fiber, metallic powder, graphite flake, etc. For example, with carbon black as filler, the percolation threshold is about 15–20% by weight. This amount of carbon black not only causes processing problems but reduces the mechanical properties as well, especially the composites' impact toughness. Moreover, the highly concentrated filler tends to slough and thus contaminate the environment.

Nano-scale manipulation of composites may yield a group of materials which are conductive but exhibit much better physical and mechanical properties than their existing counterparts. Electrically conductive polymer nanocomposite materials, as compared with conductive metal-filled systems, offer substantial weight savings, flexibility, durability, low-temperature processability and tailored reproducible conductivity. They can be used to produce conductive paints, coatings, caulks, sealants, adhesives, fibers, thin films, thick sheets and tubes, as well as electromagnetic interference shielding for large structural components, electrostatic painting, electrostatic discharge and optoelectronic device applications.

The conductive behavior of nanocomposites exhibits no linear relationship with the loading of carbon nanotubes. Below the critical amount, referred to as the percolation threshold, the change in conductivity is negligible and the nanocomposite's conductivity is almost equal to that of the polymer. Above the percolation threshold, a continuous network of conducting elements is established through the polymer matrix. At this stage, a significant increase in the nanocomposite's conductivity can be observed. However, with the filler's concentration increasing further, the rate of conductivity slows down and subsequently reaches a plateau value.

The reported levels of CNT loading for the percolation threshold vary widely, ranging from less than 1 to over 10 wt% [1]. In addition, a much more exact value has not been found through previous numerical studies. In this work, the renormalization group (RG) theory is used to evaluate the critical concentration of Carbon Nanotubes for continuous percolation of nanocomposites. RG provides a powerful method for modeling large heterogeneous systems [2]. Some of its successful applications can be found in studies of barrier properties of polymer-clay nanocomposites [3], micro-crack connectivity [4] and transport in porous media [5].

The basic hypothesis of the RG approach is the probability, P, that a cell becomes conductive is the same at all orders. Therefore, the next step in this modeling approach is the construction of a renormalization transformation, $P' = R(P)$, between the original probability, P, and the renormalized probability, P', when the order is changed [2]. In order to apply the RG theory to evaluate critical CNT concentration in conductive nanocomposites, an n-order cell was considered as a simple cube with its corners representing eight constitutive $(n-1)$-order elements. Each corner was marked by a solid dot when the corresponding $(n-1)$-order element was conductive.

Derivation of all conductive and topologically different configurations was concluded by considering a direction (e.g. top to bottom) as the ideal conductivity direction. All possible configurations of any order (from 0 to 8) were then considered and summed up. By solving the equation $P = P' = R(P)$, the percolation threshold was estimated as 0.1368 wt%,a carbon nanotube concentration in good agreement with experimental results [6].

References

1. Ounaies Z, C Park, KE Wise, EJ Siochi, JS Harrison, 2003 Comp. Sci. Tech. 63 1637
2. Wilson KG and J Kogut 1999 Phys. Rep. 12 75
3. Chunsheng Lu and YW Mai, 2005 PRL 95, 088303
4. Arcangelis LS, S Redner and A Coniglio 1985 Phys. Rev. B 31 R4725
5. Banavar JR, Cieplak M and DL Johnson 1988 Phys. Rev B 37 R7975
6. Kymakis E, Alexandou I, Amaratunga GAJ, 2002 Syn. Met 127 59

Synthesis and Physicochemical Properties of Noble Metals and Transition Metal Oxides Confined in Silica Mesoporous materials MCM-41

W. Gac[1], G. Giecko[1], S. Pasieczna-Patkowska[1], J. Ryczkowski[1], A. Machocki[1], T. Borowiecki[1], A. Deryło-Marczewska[2], G. Żukociński[2]

[1] *Departament of Chemical Technology, University of Maria Curie-Skłodowska, Pl. M. Curie-Skłodowskiej 3, 20-031 Lublin, Poland*

[2] *Department of Adsorption, University of Maria Curie-Skłodowska, Pl. M. Curie-Skłodowskiej 3, 20-031 Lublin, Poland*

Silica mesoporous materials are characterized by regular structure, large surface area, extending to 1000 m^2g^{-1}, and narrow pore size distribution in the range from 2 to 10 nm. Their properties can be easily modeled by the application of different preparation methods and thermal treatment conditions, as well as introduction of metals, metal oxides, different metal complexes or organic species. Silica mesoporous materials have aroused interest in various fields, including catalysis, sorption, material science and nanotechnology, as host structures for the preparation of new nanostructured materials such as metal nanowires or mesoporous carbon materials.

The aim of our study was to obtain silica mesoporous materials modified with silver or gold and transition metal oxides. Samples were obtained by various preparation routes, including direct hydrothermal, template ion exchange and impregnation methods. Pore dimensions were modified by application of various surfactant molecules. The samples' properties were investigated with a set of experimental techniques, including nitrogen sorption, X-ray diffraction, atomic force microscopy (AFM), UV-Vis, FT-IR/PAS spectroscopy and temperature-programmed methods. The samples were tested in the CO oxidation reaction.

The obtained materials were characterized by large surface area and ordered pore structure. The introduction of large amounts of modifiers by the hydrothermal method led to a reduction in the surface area and distortions of the regular structure. The samples obtained by the TIE method had inferior structural properties. The presence of modifiers was found to influence the mechanism of surfactant removal. We observed changes of the nature of oxide species and metal crystallites at the particular preparation stages and catalytic activity due to different pretreatment conditions.

Acknowledgements

This work was supported by the Polish Ministry of Education and Science as research project No. 3T09B11429.

The Influence of Substrate Nature and UV Irradiation on Electro-optical Properties of ZnO Thin Films

F. Iacomi[1*], C. Baban[1], N. Iftimie[2], D. Timpu[3], D. Luca[1]

[1] *Al. I. Cuza University, Faculty of Physics, 11 Carol I Blvd., 700506, Iași, Romania*

[2] *National Institute of Research & Development for Technical Physics, 47 Mangeron Boulevard, Iași, RO-700050, Romania*

[3] *"Petre Poni" Institute of Macromolecular Chemistry, Grigore Ghica Voda 41A, RO-700487, Iași, Romania*

Zinc oxide (ZnO) has a wide band-gap of ≈ 3.3 eV at room temperature and is an n-type semiconductor in its non-stoichiometric form. Due to its low electrical resistivity and high transmittance, it is a potential candidate material for use in optoelectronic devices [1–3].

In this paper, we report on the influence of substrate nature and UV irradiation on the structure and optical and electrical properties of ZnO thin films.

Zn films were prepared by thermal evaporation in vacuum from an Mo crucible heated at 970 K on various substrates (glass, quartz, SiO_2/(004)Si). An annealing process was performed at 623 K for 2 h in order to obtain ZnO thin films.

In order to improve their optical and electrical properties, the films were UV irradiated for 2h (150W mercury lamp, 3.18–3.65 eV).

Structural studies were performed by using a DRON 3 diffractometer (CuK_α radiation). The films' morphology and roughness of thin was investigated with a home-made Atomic Force Microscope.

The film's transmittance was measured using a UV-vis-NIR spectrometer. Their electrical properties were determined using a Keithley equipment.

The X-ray diffraction patterns of all ZnO thin films exhibit a hexagonal structure with preferred crystallite orientation along the c-axis parallel to the substrate surface.

The grain size (Sherrer relation), the preferred crystallite orientation and the surface roughness depended on the nature of the substrate and on the UV irradiation (Tab. 1).

Strong changes in surface morphology and roughness were in evidence after UV irradiation, suggesting the occurrence of a re-crystallization process.

The wavelength dependence of the studied ZnO thin films' transmittance spectra showed high transparency in the visible region. The substrate and UV irradiation influenced the transmittance value. The optical absorption coefficient was determined from transmittance spectra and found to obey the relation $\alpha h\nu = A(h\nu - E_{\rm op})^{1/2}$ for the allowed direct transition ($h\nu$ being photon energy; A – a constant and $E_{\rm op}$ – the band gap energy). The optical band gap values, as determined from the linear portion of the plots $(\alpha h\nu)^2$ versus $h\nu$ to $\alpha = 0$, are presented in Tab. 1. The band gap energy increased for the samples subjected to UV irradiation.

Table 1. XRD grain size, D, optical band gap energy, $E_{\rm op}$, electrical resistivity, ρ

Sample	D [nm]	$E_{\rm op}$ [eV]	$\rho \cdot 10^4$ [Ωm]
ZnO/glass	18.09	3.224	9.9
UV-ZnO/glass	18.05	3.224	8.0
ZnO/quartz	13.88	3.200	1400.00
UV-ZnO/quartz	16.01	3.264	249.6
ZnO/SiO_2/(004)Si	17.22		4.5
UV-ZnO/SiO_2/(004)Si	17.73		2.2

*Corresponding author: iacomi@uaic.ro

The electrical resistivity of the studied samples (Tab. 1) was also dependent on the crucible's temperature and the nature of substrate and treatment. The electrical resistivity was observed to decrease after UV irradiation. No correlation was found between resistivity and the X-ray (002) reflection peak intensity (representing the film's crystalline quality). The obtained results support the assumption that the resistivity is mainly determined by the boundary effect model.

References

1. W. J. Jeong, S. K. Kim, G. C. Park, Thin Solid Films, 506-507 180 (2006).
2. H. Gong, J. Q. Hu, J. H. Wang, C. H. Ong, F. R. Zhu, Sensors and Actuators B 115, 247 (2006).
3. D. G. Kang, G. S. Kim, S. W. Jeong, Y. Roh, S. H. Jeong, J. H. Boo, Thin Solid Films, 475 160

Formation of Nanocrystalline Yttrium Aluminum Garnet Highly Doped with Neodymium via the Sol-Gel Method

L. Lipińska[1], A. Rzepka[1], J. Cz. Dobrowolski[2], A. Pajączkowska[1]

[1] *Institute of Electronic Materials and Technology, 01-919 Warsaw, Poland*

[2] *Industrial Chemistry Research Institute, 01-793 Warsaw, Poland*

Yttrium aluminum garnet (YAG) doped with neodymium (Nd) is well known as a laser material. Single crystals of YAG obtained by the Czochralski method are doped by Nd up to 1,5%. YAG:Nd. At the same time, nanocrystalline powders have many potential applications, for example, as stable phosphors or materials for laser ceramics.

In this work, we present a study in the formation of nanocrystalline phases in a $Y_3Al_5O_{12}$ (YAG) – $Nd_3Al_5O_{12}$ (NAG) system. Solid solutions of $Y_{3(1-x)}Nd_{3x}Al_5O_{12}$ with Nd concentrations up to 27.5 at% were formed (although crystals were obtained with Nd concentrations up to 12 at%). The perovskite phase of the $Nd_{0.73}Y_{0.27}O_3$ formula, a two-phase system and, finally, perovskite $NdAlO_3$ were detected to form with increasing concentration of Nd. Garnet NAG did not appear. The obtained nanopowders exhibited crystalline structure confirmed with X-ray diffraction (XRD). The nanopowders' size and morphology were analyzed with scanning electron microscopy (SEM) and high-resolution scanning electron microscopy (HRSEM).

We have succeeded in preparing the phases of YAG and YAG substituted with Nd from aluminum nitrate, rare earth oxides and complexing, polymerizing compounds by the modified sol-gel method. The proposed route based on inorganic salts and metal oxides is simple and less time-consuming. All the reactants were carefully solved in acetic acid solutions and treated thermally after removing the solvent. The mechanism of YAG powder formation by the sol-gel method was examined. Synthesis of nanocrystals of the yttrium aluminum garnet structure is complex and proceeds in several stages during gelation and continued during the thermal treatment in the temperature range from 1000 to 10000°C. DTA, X-ray diffraction and FT-IR spectroscopy were applied in order to explain the formation of YAG nanopowders,.

The high heat effect, manifesting itself as a maximum in the DTA curve at 858°C, is connected with phase change during which nanocrystalline powder of yttrium aluminum garnet is formed. As a result of the phase change peaks characteristic for YAG monocrystals appear in the diffractograms. Electron microscope photographs confirm that the amorphous xerogel is transformed into small, well-shaped particles with narrow size distribution. The FTIR spectrum of the powder calcinated at 1000°C exhibits absorption bands only in the spectral range below 1000 cm^{-1}, characteristic for the Me–O stretching and bending vibrations. The mechanism of YAG nanocrystal formation from inorganic salts different from those accompanying the alcoholate pathway is discussed.

The applied simple polycomponent oxide method appears to be effective in producing large amounts of nanocrystalline powders.

Acknowledgements

This work has been supported by the Ministry of Education and Science under research project No. 3T11B00430.

Semiconductor Nanoheterointerface Eigenstate Photonic Modification

E. A. Anagnostakis

Solid State Physics Section, Department of Physics,
University of Athens, Athens, Greece
emmanagn@otenet.gr

Modification of technological semiconductor nanodevices' two-dimensional electron gas (2DEG) eigenstates by absorption of regulated successive photon doses is crucial for their optoelectronic functionality. We have studied it for the generic case of a conventional nanoheterodiode in terms of the 2DEG fundamental eigenenergy sub-level's correlation with the respective 2DEG areal density versus instantaneous cumulative photonic intake. Application of this treatment to the experimental photoresponse of a typical $Al_xGa_{1-x}As/GaAs$ modulation-doped heterodiode enables realistic tracing of the pertinent 2DEG eigenstate photonic modification. The scheme appears to be indirectly justified by the measured 2DEG mobility photonic evolution's compatibility with the one deduced for the nanoheterointerface fundamental wavefunction penetration length into the energetic barrier region adjacent to the 2DEG quantum well.

Parallel conferences on advanced materials
The 4th International Workshop on Functional and Nanostructured Materials
The 8th Conference on Intermolecular and Magnetic Interactions in Matter
1–6 September 2007, Gdansk, Poland

Changes of Main Optical Gaps by Crystal Field Linked with Lattice Deformations: Computer Evaluations for Zn_3P_2 and Cd_3P_2

G. P. Chuiko*, V. V. Martyniuk

Kherson National Technical University,
Department of General and Applied Physics, Laboratory of Solid State Theory,
Beryslavske Shosse, 24, 73008, Kherson, Ukraine

Introduction

Zinc phosphide is well-known as an inexpensive material with excellent direct optical gap ($E_g \approx 1.5$ eV) for high-efficiency solar elements [1, 2 and 3]. Cadmium phosphide is not only a promising material for lasers acting within a window of atmosphere transparency due to $E_g \approx 0.59$ eV [3]. It has also been recommended as a valuable quantum amplifier for fiber lines [4]. Thus, both crystals are suitable materials for optoelectronic applications.

These crystals have similar polymorphous transformations near 1118 K and 1010 K, respectively [5]. Such transformations have been determined as a positional ordering of metallic atoms in their sublattices having one quarter of vacant sites [6]. The space symmetry changes from cubic $Fm3m - O_h^5$ to tetragonal $P4_2/nmc - D_{4h}^{15}$. Of course, the transformations are accompanied by some tetragonal deformations of lattices, but they appear to be very small for both materials. However, they have a considerable impact on the parameters of the crystalline field [7] in addition to their direct input into Hamiltonians [8]. The factor mentioned above is often referred to as the Kildal parameter [9] and influences the band gaps near $\mathbf{k} = \mathbf{0}$.

The main object of this report is a computer evaluation of changes in actual optical gaps caused by direct and indirect influences of the tetragonal deformations arising during the mentioned phase transformations.

Theory and the input data

The Hamiltonians for the low-temperature tetragonal phases have been used in the form of [8], with obvious simplifications due to the presence of the symmetry centers in our crystals. The secular equation may be written down as:

$$\varepsilon^4 - (E_g - \delta - \Delta)\varepsilon^3 - \left(\left(\sin\Theta^2 + \frac{\cos\Theta^2}{\eta^4}\right)(Pk)^2 + E_g(\delta + \Delta) + \frac{2\Delta}{9}\left(\frac{1-\eta^2}{\eta^2}\right) - \frac{2\delta\Delta}{3}\right)\varepsilon^2 -$$

$$-\left(\left(\left(\delta + \frac{2\Delta}{3}\right)\sin\Theta^2 + \frac{2\cos\Theta^2\Delta}{3\eta^4}\right)(Pk)^2 + \frac{2E_g\Delta}{3}\left(\delta - \frac{\Delta}{3}\left(\frac{1-\eta^2}{\eta^2}\right)\right)\right)\varepsilon -$$

$$-\frac{\Delta}{3}\left(\delta - \frac{\Delta}{3}\left(\frac{1-\eta^2}{\eta^2}\right)\right)(Pk)^2\sin\Theta^2 = 0.$$

Here, (E_g, P, Δ, δ) are the model's parameters [9]: the energy gap, the matrix element of the pulse, the parameter of spin-orbital splitting and the above-mentioned Kildal parameter, respectively. The energy of carriers (ε) is counted from the top of the heavy holes band, k is the wave vector module, Θ is the

*Corresponding author: gp47@mail.ru

spherical angle, and $\eta = \frac{1}{2}c/a$ is the scalar parameter of tetragonal deformation determined by the two lattice constants.

The additional dependence of the Kildal parameter on η was taken into account according to the following formula [7]:

$$\delta(\eta) = \delta_s - 2b(1+\nu)(1-\eta)\left(1 - \frac{b(1+\nu)(1-\eta)}{\Delta}\right) \quad (1)$$

Here, δ_s is the structurally independent part of the Kildal parameter, ν – Poisson's factor, b – the constant of the deformation potential.
The set of calculation parameters for tetragonal phases is presented in following table [1, 2, 3, 5 and 7]

T a b l e 1

Parameter / Materials	E_g, eV	Δ, eV	P, eVm	δ_s, eV	b, eV	ν	η
$\mathbf{Zn_3P_2}$	1.50	0.11	$7.8 \cdot 10^{-10}$	0.058	3.51	0.474	0.9948
$\mathbf{Cd_3P_2}$	0.59	0.15	$7.2 \cdot 10^{-10}$	0.076	2.62	0.457	0.9909

The set of parameters for cubic phases was almost the same, save that: $\eta = 1$, $\delta_s = 0$, thus $\delta = 0$.

Results and discussion

First of all, the deformation's influence on the dependence of the Kildal parameter is much greater (from 6 to 10 times) than on the direct input of parameter $\delta(\eta)$ into equation (1) for both materials. This result was predictable. The parameter is included in the trace of the Hamiltonian, which is equal to the older coefficient at ε^3 in (1). At the same time, the parameter η is directly included only into the other coefficients of (1), but these originate from the non-diagonal elements of the Hamiltonian. Hence, the computing has just confirmed such supposition.

The solutions of secular equation (1) describe four energy band, viz. the conductivity band and three separate valence bands (as for tetragonal phases), in the order given in [2]. Let us to mark the three optical gaps between the valence bands and the conductivity band as A, B, C, in the ascending order of energies. These transitions form the edge of the fundamental absorption.

The plot presented below shows the dependences of changes of these gaps on the module of the wave vector for two directions: along the main crystalline axis and normal to it (upper and lower curves respectively as for B, C, and vice versa for A). These changes have been calculated for the tetragonal phases in relation to the cube phases. In other words, the changes are equal to deviations of A, B, C energies between the phases. Such a shift shall be observed after ordering the samples. As the obtained dependences are very similar qualitatively for both materials, only one of the couple has been shown.

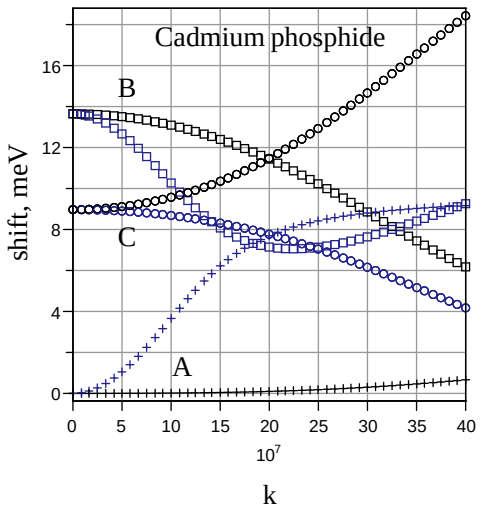

The magnitude of changes in cadmium phosphide is slightly greater than for zinc phosphide. Nevertheless the maximal shift for a degenerate sample with $k = 4 \cdot 10^8$ m^{-1} (i.e. with concentration of electrons of about $n \approx 2 \cdot 10^{24}$ m^{-3} and with the Fermi level located approximately $\varepsilon_F \approx 9$ meV over the bottom of the conductivity band) is no more than twice the well-known Burstein-Moss shift. At room temperature, the calculated changes have not exceeded $k_0 T \approx 26$ meV.

However, the effect may be more pronounced at low temperatures and above all of the low concentrations where the anisotropy of changes is progressively weakened and disappears completely. The following table presents the energy changes of A, B, C transitions in the limit: $k \to 0$.

Table 2

Energy changes, meV Materials	A	B	C
Zn_3P_2	0.0	11.3	7.1
Cd_3P_2	0.0	13.6	9.0

Thus, the influence of tetragonal deformation common for the investigated crystals is quite temperate and is mainly caused by dependence (2). Therefore, the parameter's direct inclusion in Hamiltonian (1) will generally be optional, if exactness of the computations should not exceed a few meV.

Acknowledgements

We gratefully acknowledge the informational support of the organizers and, first and foremost, that of Prof. Andrzej Ceynowa, Rector of the Gdansk University.

References

1. Pawlikowski J. 1982 *Phys. Rev. B* **26** (8) 4711
2. Cisowski J. 1982 *Phys. Stat. Sol.* **111** (1) 289
3. Sieranski K., Szatkowski J., Misiewicz J. 1994 *Phys. Rev.* **50** (11) 7331
4. Eichberger R., Eychmuller A., Giersig M., Kornowski A. and H. Weller 1996 *Journal of Phys. Chem.* **100** (30) 12467
5. Pistorius C.W.F.T., Clark J.B., Geotzer J. et all. 1977 *High Press. - High Temp.* **9** (4) 471
6. Chuiko G.P., Don N.L. and Ivchenko V.V. 2005 *Functional materials* **12** (3) 454
7. Chuiko G.P., Dvornik O.V. 2002 *Physics and Chemistry of Solid State* **3** (4) 682
8. Chuiko G., Don N., Dvornik O., Ivchenko V. 2003 *Moldavian Journ. of the Phys. Sciences* **1** (1) 88
9. Kildal H. 1974 *Phys. Rev.* **10** (12) 5082

Electrical and Optical Properties of Bismuth Telluride/Gallium Nitride Heterojunction Diodes

M. Y. Pang[1], W. S. Li[2], K. H. Wong[1]

[1] *Department of Applied Physics and Materials Research Centre, The Hong Kong Polytechnic University, Hunghom, Kowloon, Hong Kong, China*

[2] *Department of Electronic and Information Engineering, The Hong Kong Polytechnic University, Hunghom, Kowloon, Hong Kong, China*

Semiconducting bismuth telluride has a band-gap energy of about 0.15 eV at room temperature and is a good material for mid-infrared detection [1]. We grew bismuth telluride thin films on gallium nitride (on sapphire) by pulsed laser deposition at a substrate temperature of 300°C. The structural characteristics, surface morphology and transmission/absorption properties of these bismuth telluride thin films were respectively studied by X-ray diffraction, scanning electron microscopy and Fourier transform infrared spectroscopy. The chemical composition of as-deposited bismuth telluride thin films was determined by X-ray photoelectron spectroscopy and found to differ from that of the bulk target, changing from the stoichiometric Bi_2Te_3 to bismuth-rich. A bismuth-rich p-Bi_2Te_3/n–GaN/Al_2O_3 heterojunction was fabricated for photovoltaic detection of low energy photons. The wide band gap semiconducting n-GaN layer and the Al_2O_3 substrate acted as a window for IR transmission. A sensitive IR photo-response of the heterojunction was obtained by back-side illumination. The irradiation changes of the current-voltage characteristics allowed us to evaluate the series resistances, parallel resistance and ideality factor of the junctions. Our results suggest that bismuth telluride can be used in photovoltaic mid-infrared detection at room temperature.

References

1. S. K. Mishra, S. Satpathy, O. Jepsen, J. Phys.: Condense Matter, 9, 461 (1997)

Elastic Properties of Selected 2D and 3D Model Solids of Soft Molecules at Zero Temperature

J. W. Narojczyk*, K. W. Wojciechowski†

Institute of Molecular Physics, Polish Academy of Sciences,
M. Smoluchowskiego 17, 60-179 Poznan, Poland.

Modern technology often requires designing materials of special properties, not common in nature. An example is the class of materials showing anomalous (negative) Poisson's ratio [1, 2]. Such materials, called *auxetics* [3], have recently become a subject of increasing interest [4]. Effective design of such materials could be greatly improved if mechanisms controlling properties of elastic media were known in detail and well understood. Studies of simple model systems constitute an important step in this direction.

The present work is focused on studying the influence of disorder introduced on the microscopic level by atomic size polydispersity on the macroscopic elastic properties of simple models of molecular systems (see Fig.1).

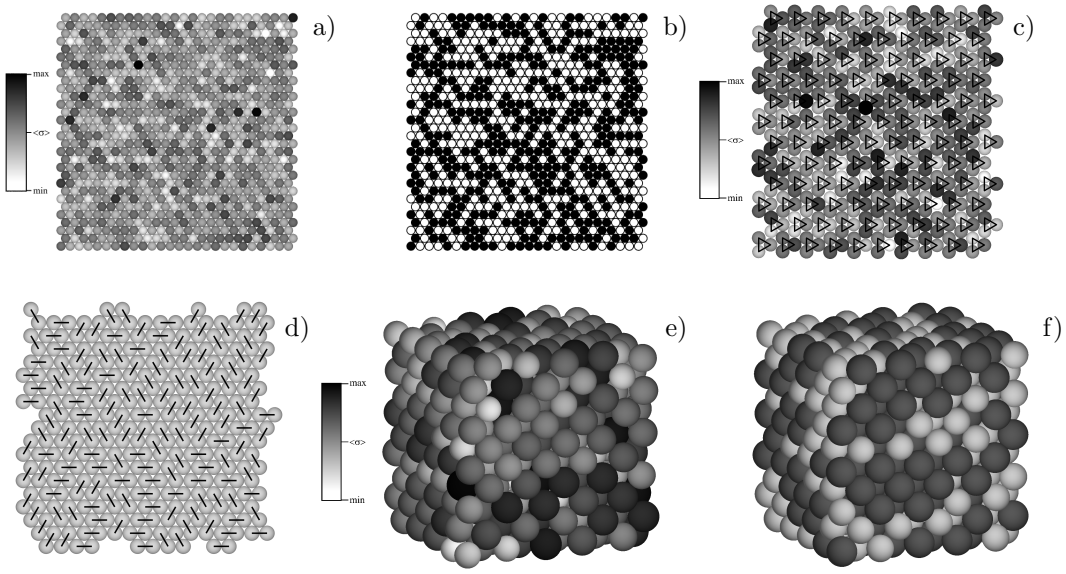

Figure 1: Examples of the studied systems: (a) polydisperse discs, (b) a binary mixture of discs, (c) polydisperse trimers, (d) dimers in the DC phase, (e) a polydisperse sphere system, (f) a binary mixture of spheres. The scales on the structures' left indicate distribution of atomic sizes in the system. In binary systems, atoms with diameters of less than σ are drawn in light gray, those with diameters in excess of σ are drawn in dark gray

The particles ('molecules') interact through site-site ('atom-atom'), n-inverse-power, pair potentials. Their interactions are assumed to be short-range, i.e. only the particles sharing a side of their Dirichlet polygons (in 2D) or a face of their Voronoi polyhedra (in 3D) are assumed to interact. Our investigations have been restricted to the static case, i.e. to the temperature of $T = 0$K. All the polyatomic molecules

*jwn@ifmpan.poznan.pl
†kww@ifmpan.poznan.pl

are rigid, i.e. the atoms forming them are placed at fixed distances from each other. The aperiodicity is introduced to the system either by dispersion of atomic sizes (in polydisperse and binary systems) or by degeneracy of the systems' ground state (for identical molecules).

Two kinds of atomic size distributions were studied: *polydisperse* systems and *binary mixtures*. In polydisperse systems, atomic sizes were generated according to the Gauss distribution function at a given standard deviation δ

$$\delta = \frac{\sqrt{\langle\sigma^2\rangle - \langle\sigma\rangle^2}}{\langle\sigma\rangle} \ , \tag{1}$$

where σ was the atomic diameter. In binary mixtures, the atomic size distribution function consisted of two Dirac delta functions of the same amplitude. This implies that there were only two possible values of atomic size in binary system, $\sigma(1-\delta)$ and $\sigma(1+\delta)$, fifty percent of each.

The elastic properties were determined for highly symmetric periodic and aperiodic structures at various densities of the systems with a simple computational method [5]. Systems of the same standard deviation were compared. The results obtained for:

- two-dimensional mono-atomic particles – *soft discs* [6],
- two-dimensional three-atomic particles – *soft trimers* [5],
- three-dimensional mono-atomic particles – *soft spheres* [7]

have been published earlier and are reviewed only briefly here. New results are reported for system of

- two-dimensional di-atomic particles, further referred to as *soft dimers*.

The studies have shown that, typically [6–9], Poisson's ratio increases with disorder increasing in the system and tends to its extreme possible value when the interaction potential tends to the hard-body one. It also follows from these studies that elastic properties of polydisperse systems and binary systems of the same δ and $\langle\sigma\rangle$ are very similar. This indicates that moments of the probability distribution of particle sizes higher than the second one weakly influence the system's elastic properties.

Acknowledgements

Part of the simulations was performed at the Poznan Supercomputing and Networking Center. The studies were partially supported by the Ministry of Science and Higher Education's grant no. N202 07032/1512.

References

[1] R. S. Lakes. Foam structures with a negative Poisson's ratio. *Science*, 235:1038–1040, 1987.
[2] K. W. Wojciechowski. Constant thermodynamic tension Monte Carlo studies of elastic properties of a two-dimensional system of hard cyclic hexamers. *Molecular Physics*, 61:1247–58, 1987.
[3] K. E. Evans, M. A. Nkansah, I. J. Hutchinson, and S. C. Rogers. Molecular network design. *Nature*, 353:124, 1991.
[4] K. W. Wojciechowski, A. Alderson, A. C. Brańka, and K. L. Alderson. Preface. *Physica Status Solidi (b)*, 242:497, 2005. see also other papers in that issue and references therein.
[5] J. W. Narojczyk and K. W. Wojciechowski. Elastic properties of two-dimensional soft polydisperse trimers at zero temperature. *Physica Status Solidi (b)*, 244:943–954, 2007.
[6] J. W. Narojczyk and K. W. Wojciechowski. Elastic properties of two-dimensional soft discs of various diameters at zero temperature. *Journal of Non-Crystalline Solids*, 352:4292–4298, 2006.
[7] J. W. Narojczyk and K. W. Wojciechowski. Influence of size polydispersity on the elastic constants of f.c.c. crystals of static soft spheres. submitted, 2007.
[8] K. W. Wojciechowski and J. Narojczyk. Influence of disorder on the Poisson's ratio of static solids in two dimensions. *Reviews on Advanced Materials Science*, 12(2):120–126, 2006.
[9] J. W. Narojczyk and K. W. Wojciechowski. Computer simulation of the Poisson's ratio of soft polydisperse discs at zero temperature. *Materials Science (Poland)*, 24(4):921–927, 2006.

The Magnetoelectric Effect in Cobalt/Lead Zirconate Titanate/Polyethylene Oxide Composites

K. H. Chau, Y. W. Wong, F. G. Shin

Department of Applied Physics, The Hong Kong Polytechnic University, Hung Hom, Hong Kong

The magnetoelectric effect was investigated in a 3-phase composite. The 0–3 connectivity composite consisted of cobalt (Co) powder and lead zirconate titanate powder (PZT) blended in a polyethylene oxide (PEO) matrix. Electric charge was induced at the electrodes on the sample's surface as an AC magnetic field was applied. The piezoelectric PZT is believed to have induced the surface charges as a result of the ferromagnetic Co produced magnetostriction coupled to the ceramic phase. The polymer PEO matrix enhanced the poling of PZT [1] and the induction of electric signals at the sample's electrodes [2]. This magnetoelectric composite can be fabricated by conventional polymer processing, such as extrusion or injection, to any shapes desired for magnetic sensing applications.

Acknowledgement

The authors acknowledge the support of an internal research grant from The Hong Kong Polytechnic University.

References

1. Wong C K and Shin F G 2006 *Journal of Materials Science* **41** (1) 229-249
2. Lam K S, Wong Y W, Tai L S, et al. 2004 *Journal of Applied Physics* **96** (7) 3896-3899

Optical Spectroscopy and Local Structure of Er^{3+} Luminescence Centres in Glasses of the $CaO–Ga_2O_3–GeO_2$ System

B. V. Padlyak[1]*, W. Ryba-Romanowski[2], R. Lisiecki[2]

[1] *Institute of Physical Optics of the Ministry of Education and Science of Ukraine*
23 Dragomanov Str., 79-005, Lviv, Ukraine

[2] *Institute of Low Temperatures and Structure Research of the Polish Academy of Sciences*
2 Okólna Str., 50-422 Wroclaw, Poland

Undoped and Er-doped glasses (amount of Er_2O_3 – 0.7 and 1.46 wt%) of high optical quality and chemical purity with garnet ($Ca_3Ga_2Ge_3O_{12}$ or $3CaO–Ga_2O_3–3GeO_2$) basic composition were obtained by high-temperature synthesis according to [1]. On the basis of Ga and Ge K-edge EXAFS analysis, the structural parameters (interatomic distances and coordination numbers) for Ga and Ge atoms in the undoped and rare earth (Eu, Ho, Er) doped glasses of $Ca_3Ga_2Ge_3O_{12}$ garnet compositions were obtained [2, 3]. It was shown in [3] that the introduction of rare-earth ions modifies the local structure around Ga atoms in the glass network, whereas the Ge-subsystem of the glass structure remains completely unaffected by the presence of rare-earth dopants.

It was also shown with EPR and optical spectroscopy that the erbium impurity is incorporated into the glass network exclusively as Er^{3+} ions ($4f^{11}$ electron configuration, $^4I_{15/2}$ free ion ground state). All the observed transitions of Er^{3+} ions in Er-doped glasses (amount of Er_2O_3 – 0.7 wt%) of $Ca_3Ga_2Ge_3O_{12}$ composition in the UV-visible spectral region were identified [4].

In the present work, the optical absorption, emission and luminescence excitation spectra, as well as luminescence kinetics, have been investigated and analyzed for the main transitions of the Er^3+ centers in glasses of $Ca_3Ga_2Ge_3O_{12}$:Er composition (amount of Er_2O_3 – 1.46 wt%). The Er^{3+} optical spectra were analyzed according to the standard Judd-Ofelt theory. As a result, the oscillator strengths, phenomenological intensity parameters (Ω_2, Ω_4, and Ω_6), radiative emission rates, branching ratios and radiative lifetimes for Er^3+ centers of the $Ca_3Ga_2Ge_3O_{12}$ glass were calculated and analyzed in comparison with the corresponding parameters of the $Ca_3Ga_2Ge_3O_{12}$:Er^{3+} garnet crystal and oxide glasses of different compositions. Decay curves for $^4S_{3/2} \rightarrow ^4I_{15/2}$ ($\lambda_{max} = 555$ nm), $^4F_{9/2} \rightarrow ^4I_{15/2}$ ($\lambda_{max} \approx 660$ nm), $^4I_{11/2} \rightarrow ^4I_{15/2}$, ($\lambda_{max} \approx 970$ nm) and $^4I_{13/2} \rightarrow ^4I_{15/2}$, $\lambda_{max} \approx 1.6$ μm) transitions of the Er^{3+} centers, obtained at room temperature, were satisfactorily described by a single exponent with lifetimes of 21.75, 2.02, 89.2 and 4202 μs, respectively. Experimental lifetimes are discussed and compared with those calculated using the Judd-Ofelt theory.

References

1. B. V. Padlyak, P. P. Buchynskii, *Patent of Ukraine*, No. UA 25235 A, October 30, 1998.
2. D. Chełstowski, A. Witkowska, J. Rybicki, B. Padlyak, A. Trapananti, E. Principi, Opt. Appl., V. XXXIII, No. 1 (2003) 125.
3. A. Witkowska, B. Padlyak, J. Rybicki, J. Non-Cryst. Solids, V. 352, No. 40–41 (2006) 4346.
4. B. Padlyak, O. Vlokh, K. Fabisiak, K. Sagoo, B. Kukliński, Opt. Mater. V. 28 (2006) 157.
5. A. Witkowska, B. Padlyak, J. Rybicki, Opt. Mater. (2007), in press.

*Corresponding author: bohdan@mail.lviv.ua

An FMR and DSC Study of Maghemite Nanoparticles in a PMMA Polymer Matrix

J. Typek[1], N. Guskos[1,2], A. Szymczyk[1], D. Petridis[3]

[1] *Institute of Physics, Szczecin University of Technology, Al. Piastów 17, 70-310 Szczecin, Poland*

[2] *Solid State Physics, Department of Physics, University of Athens, Panepistimiopolis, 15 784 Zografos, Athens, Greece*

[3] *Insitute of Materials Science, NCSR Demokritos, Aghia Paraskevi, 15 310 Athens, Greece*

Iron oxides are well-known magnetic materials, especially maghemite, γ-Fe_2O_3, which crystallizes in the cubic spinel structure. In recent years, magnetic oxide nanoparticles have attracted particular interest due to their unique magnetic properties arising from a complex interplay between the magnetic response of an individual particle and a multitude of inter-particle interactions. γ-Fe_2O_3 nanoparticles are used in catalysis and in magnetic recording media.

Many authors report on polymer-based iron oxide nanoparticles. Polymers may serve as excellent matrices for magnetic particles in synthesizing nanocomposite materials that combine the functionality and mechanical properties of the polymer with those of the magnetic filler. Magnetic properties of these systems are studied using magnetometer measurements, ^{57}Fe Mossbauer spectroscopy and magnetic resonance techniques. Experimental work on maghemite nanoparticles dispersed in polymeric matrices bearing different surface coatings has stressed the importance of surface effects, indicating that microstructure of the particles and the host medium can be significant factors determining the magnetic response of these systems.

In this paper, the thermal and magnetic properties of polymethylmethacrylate (PMMA) polymer samples filled with 5 and 10 wt% maghemite nanoparticles and agglomerates are investigated. Magnetic nanoparticles capped with oleic acid were prepared by a one-step method involving partial oxidation of Fe(II) in alkaline solutions by dilute H_2O_2. The reaction was conducted in the presence of oleic acid and under bi- phase conditions. The surface bond oleate groups can be fully exchanged with metacrylate units by refluxing in ethanol. The exchange reaction ensures the chemical bonding of methacrylate units to the surface of nanoparticles, which in turn undergo polymerization with the vinyl groups of the methyl mathacrylate. This procedure is expected to lead to grafting of the nanoparticles to the polymer chains.

The differential scanning calorimetry (DSC) technique was used to determine the glass transition temperature of the investigated samples. Measurements were made on a DSC-7 (Perkin-Elmer) apparatus. Samples were packed into hermetic aluminum DSC pans. Measurements were made over the temperature range of 20°C to 200°C at a heating rate of 10°C/min and under nitrogen flow. The glass transition temperatures, T_g, were taken as the midpoint of the change in heat capacity ($\Delta c_p/2$). Ferromagnetic resonance (FMR) measurements were recorded with a Bruker E 500 spectrometer of X-band (9.5 GHz) microwave frequency. The samples were cooled down to a given temperature in near-zero magnetic field. As is usually the case, the first derivative of power absorption was recorded as a function of the applied magnetic field. The temperature dependence of the FMR spectra in the 3.3–300 K temperature range was recorded using an Oxford Instruments ESP helium-flow cryostat.

The DSC thermographs showed that the glass transition temperature T_g for pure PMMA was 99.6°C, while it was 106.7°C for polymer/maghemite composites. The glass transition temperature of a polymer is defined as the temperature at which it becomes hard and brittle when cooled rapidly after heating. The weak secondary bonds that stick the polymer chains together get broken and the macromolecules start to move. The glass temperature, T_g, increases with the increase of nanoparticle concentration, probably due to branching when islands of nanoparticles are bonded to different polymeric chains. This reduces

the chains' mobility and, as a result, the glass transition temperature of the nanocomposites increases. In addition, the increased concentration of nanoparticles renders the nanocomposite more brittle, leaving even less free space for polymer macromolecules to move.

Our FMR study in the 3.3–300 K temperature range showed the presence of an asymmetric spectrum, analyzed in terms of two Gaussian-shaped components arising from assumed magnetic anisotropy of the nanoparticles. The FMR parameters (resonance field, line width, integrated intensity) were calculated and studied as a function of temperature. An analysis of the integrated intensity and the product of integrated intensity and temperature revealed the properties of magnetic interactions in the nanaoparticle system.

The Effect of γ-Irradiation on the Electric Properties of Chalcogenide Semiconductor Glass As_2S_3

H. M. Khlyap[1*], L. Pankiv[2], D. Labovka[2],
T. Kavetsky[2], V. Tsmots[2]

[1] *TU Kaiseslautern, Germany*

[2] *State Pedagogical University, Drohobych, Ukraine*

Room-temperature electric field-induced characteristics of a metal-semiconductor structure based on chalcogenide semiconductor glass, As_2S_3, have been studied before and after γ-irradiation. Experimental data showing considerable change of the threshold voltage observed in the current-voltage characteristics are presented. A possible explanation of these results is discussed in the framework of the random Poisson field model and according to the theory of current processes in chalcogenide glass semiconductors.

*Corresponding author: hkhlyap@yahoo.com

Magnetotransport Properties of Ferromagnetic Metal/Oxide Junctions

Y. K. Chan, W. F. Cheng, A. Ruotolo, C. W. Leung

Department of Applied Physics and Materials Research Centre, The Hong Kong Polytechnic University, Hunghom, Kowloon, Hong Kong, China

A magnetoresistive bi-layer junction was fabricated by pulsed laser deposition. A bottom electrode $LaNiO_3$ (LNO) layer was deposited on top of a (100) LAO substrate. A Co/$La_{0.7}Sr_{0.3}MnO_3$ (LSMO) junction was then fabricated on the LNO layer with the shadow masking technique. At low temperatures, the junction showed positive magnetoresistance (MR, defined as $(R(H)-R(0))/R(0)$) with a low in-plane field. By contrast, single LSMO and Co[1] layers showed negative MR under the same conditions, a clear sign of the giant magnetoresistive (GMR) effect. The MR ratio of GMR in Co/LSMO junctions at 20 K was about 0.5%, with a 3 kOe external field. Compared with conventional spin valves, the structure described here simplifies the fabrication process to simple deposition of a metallic ferromagnetic electrode on a ferromagnetic oxide layer, without the need for spacer layer deposition.

References

1. R. Ferré, K. Ounadjela, J. M. George, L. Piraux and S. Dubois, Phys. Rev. B 56, 14066 (1997)

Temperature Dependence of the FMR Spectra of Polymer Composites with Low Concentrations of Nanocrystalline Fe_3C/C Fillers

N. Guskos[1,2], M. Maryniak[2], J. Typek[2], A. Guskos[2],
I. Pełech[3], U. Narkiewicz[3], Z. Rosłaniec[4], E. Senderek[4]

[1] *Solid State Section, Departament of Physics, University of Athens, Panepistimiopolis, 15 784 Zografos, Athens, Greece*

[2] *Institute of Physics, Szczecin University of Technology, Al. Piastów 17, 70-310 Szczecin, Poland*

[3] *Institute of Chemical and Environment Engineering, Szczecin University of Technology, Pułaskiego 10, 70-322 Szczecin, Poland*

[4] *Institute of Materials Engineering, Szczecin University of Technology, Al. Piastów 19, 70-310 Szczecin, Poland*

Two different low concentrations of agglomerated magnetic Fe_3C/C nanoparticles (0.1 wt% and 0.3 wt%) were prepared as fillers for polymer nanocomposites using the in situ polycondensation reaction in poly(ether-ester) matrix. The samples were characterized using the XRD and SEM methods. The SEM pictures have shown that magnetic nanoparticles were agglomerated. Two types of agglomerates were detected according to their sizes: one below 100 nm and the other larger than 1 μm. The registered FMR (ferromagnetic resonance) spectra consisted of a superposition of two lines. One, more intense line was very broad, while the other was very narrow (Fig. 1).

The former was produced by larger agglomerates, while the latter originated from nano-scale agglomerates. The integrated intensities of these lines at room temperature were proportional to the concentrations of magnetic constituents [1]. A strong temperature dependence of the FMR spectra was observed and important differences were detected in comparison with the α-Fe/C nanosystem in the same matrix [2].

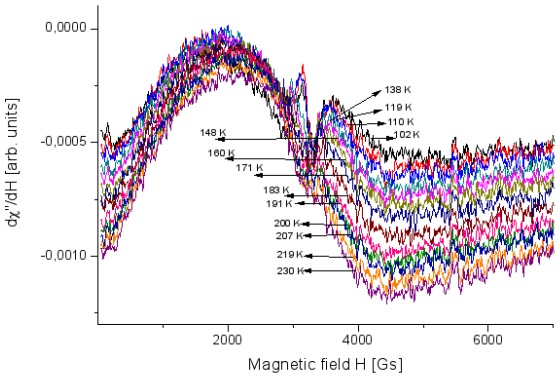

Figure 1: Temperature dependence of the FMR spectra of Fe_3C/C magnetic nanoparticles (0.3 wt%) in a nanocomposite matrix

References

1. M. Maryniak, N. Guskos, J. Typek, I. Kucharewicz, U. Narkiewicz, Z. Rosłaniec, M. Kwiatkowska, W. Arabczyk, and K. Adinis, Rev. Adv. Mater. Sci. **12**, 200 (2006).
2. N. Guskos, M. Maryniak, J. Typek, I. Pełech, U. Narkiewicz, Z. Rosłaniec, and M. Kwiatkowska, Solid State Phenomena **128**, 213 (2007).

Characteristics of Hetero-epitaxial $Cu_{2-x}Mn_2O$/Nb–$SrTiO_3$ p–n Junction

C. Y. Lam, K. H. Wong

Department of Applied Physics and Materials Research Centre,
The Hong Kong Polytechnic University,
Hunghom, Kowloon, Hong Kong, China

Mn-doped cuprous oxide, $Cu_{2-x}Mn_xO$ (CMO), is a p-type diluted magnetic semiconductor (DMS) with Curie temperature above room temperature [1]. We have grown CMO ($x = 0.03$) thin films, about 200 nm thick, on n-type semiconducting (001) Nb–$SrTiO_3$ (NSTO) single crystal substrates by pulsed laser deposition. The cubic crystalline phase of CMO layers was obtained in a narrow deposition pressure window of about 20 mTorr at a growth temperature of 650°C. X-ray diffraction and TEM studies of these heterostructures have revealed a cube-on-cube epitaxial relationship of $[CMO]_{001}/[NSTO]_{001}$. All the oxide p–n junctions with the size of 500×500 μm^2 were fabricated by the shadow masking technique. These junctions have shown highly asymmetric I–V characteristics. Their rectification ratio at room temperature is about 10^3 at ± 2 V. Leakage current density of 10^{-4} A/cm^2 at -1 V has been observed. No apparent junction breakdown has been recorded at reverse bias voltages down to -5 V. From the $1/C^2$–V plots, the forward bias turn on voltage has been ~ 1.4 V. The clear junction current rectifying properties are maintained up to 200°C. The rectification ratio appears to increase with temperature. Our results have demonstrated that epitaxial CMO films can be fabricated on lattice-matched cubic substrates. They are suitable DMS for above-room-temperature spintronic junction applications.

References

1. M. Wei, N. Braddon et al., Appl. Phys. Lett. 86, 072514 (2005)

Nanocrystalline $Co_{60}Fe_{30}Ni_{10}$ and $Co_{50}Fe_{35}Ni_{15}$ Alloys Obtained During Mechanical Synthesis: a Mössbauer Study

T. Pikula[1], D. Oleszak[2], M. Pękała[3], E. Jartych[1]

[1] *Department of Experimental Physics, Institute of Physics, Technical University of Lublin, Poland*

[2] *Faculty of Materials Science and Engineering, Warsaw University of Technology, Poland*

[3] *Department of Chemistry, Warsaw University, Poland*

Ternary Co–Fe–Ni alloys have interesting structural and magnetic properties, one of the most important being their good soft magnetic properties, especially in Co-rich compositions. This could lead to a number of applications. Mechanical alloying has been proposed as a potential technology of producing such bulk alloys. Co, Fe and Ni have similar atomic sizes and melting points, so they can easily form solid solutions in a wide range of chemical compositions.

In this work, the $Co_{60}Fe_{30}Ni_{10}$ and $Co_{50}Fe_{35}Ni_{15}$ alloy compositions were chosen for investigations, due to these alloys' location in the transitional area of the phase diagram. Moreover, these alloys have the same e/a ratio (number of valence electrons per atom). Samples were prepared from elementary powders in a high-energy planetary ball mill. X-ray diffraction, transmission Mössbauer spectroscopy and differential scanning calorimetry were used to characterize the alloys' structure and hyperfine interactions. Magnetic measurements were carried out as well in order to determine the studied alloys' effective magnetic moment, Curie temperature, saturation magnetization and coercive field.

The final products of the milling processes were solid solutions with a b.c.c. lattice and the average grain size of tens of nanometers. After heating to 993 K in the calorimeter, the mixture of two solid solutions (b.c.c. and f.c.c.) was obtained. At the same time, isothermal annealing at 1173 K resulted in both cases in the formation of a solid solution with an f.c.c. lattice. Mössbauer spectra obtained for specimens after mechanical alloying and thermal treatment were numerically fitted using hyperfine magnetic field distribution. It not only enabled monitoring the alloy formation process and estimating the values of hyperfine interaction parameters but also determination of the local atomic configuration in the nearest neighborhood of ^{57}Fe isotopes. The most probable configurations were found using extended binomial distribution.

The Effect of La and Er Impurities on the Structure and Critical Temperature of Bi-2223 Superconductors

A. Amirabadizadeh[1*], R. Tomari[1], H. Arabi[1], M. R. Alinejad[2]

[1] *Department of Physics, Faculty of Science, University of Birjand, Birjand, Iran*

[2] *Department of Physics, Faculty of Science, Ferdowsi University of Mashhad, Mashhad, Iran*

$(Bi_{1-x}Pb_x)Sr_2Ca_2Cu_3O_6$ compounds (Bi-2223) are the best high T_c superconductors, with a high critical temperature and current density. However, their preparation is difficult and dependent on the preparation technique. In this research, $Bi_{1.7}Pb_{0.3}Sr_{1.97}Ca_{2.03}Cu_{3.1}O_{10+x}$ compounds were prepared by the sol-gel technique. Er and La oxide was added to the samples and T_c was measured. The results have shown that increasing of impurities (up to ≈ 0.5%wt) T_c is not changed, with increasing the impurities the T_c decreases.

XRD measurements have shown that a transition phase from 2223 to 2212 occurs with increasing impurities. La^{+3} and Er^{+3} were formed separating domains which these domains were cased the 2212 phase being dominate with increasing of imparities.

*Corresponding author: ahmadamirabadi@yahoo.com

Magnetite Nanowire in MCM-41 Type Mesoporous Silica Templates

Z. Surowiec, M. Budzyński, M. Wiertel, J. Sarzyński

Institute of Physics, M. Curie-Skłodowska University,
Pl. M. Curie-Skłodowskiej 1, 20-031 Lublin, Poland

During the last few years, nanowires have attracted considerable attention due to their importance for fundamental studies and a wide range of their potential applications in nanodevices.

One of many methods of producing nanowires is embedding atoms in mesoporous ordered silica materials. The M41S mesoporous ordered silica materials were invented in 1992 by a group from Mobil Oil. One of such materials, characterized by uniform pore diameter, large pore volume and large surface area, is MCM-41. Hexagonal arrangement of the cylindrical pores is obtained in MCM-41 through the templating technique. Cylindrical micelles formed by a surfactant in alkaline medium are used as condensation centers for silica from tetraethylortho-silicate (TEOS) or alkali metal silicate. Accumulation of micellar rods leads to the creation of honeycomb-shaped micelle-templated silica. Using templates with alkyl chains of various length enables controlling pore diameters in the range from 2 to 10 nm.

Arrays of Fe_3O_4 nanowires embedded in mesoporous ordered silica were obtained by dissolving Fe^{3+} ions in the aqueous medium and their adsorption on internal and external surfaces, with the use of Fe-EDTA complex. Magnetite polycrystalline nanowires were characterized by means of X-ray diffraction and ^{57}Fe Mössbauer spectroscopy (MS). The average length of these nanowires was about 70nm and their diameter was about 3 nm. Mössbauer studies demonstrated that the composites consisted of very small Fe_3O_4 particles. Almost 80% of particles existed in a paramagnetic state.

POSTERS

Reduction of sintering time in preparation of high T_c superconductors based on Bi

A. Amirabadizadeh[1*], S. Memarzadeh[1], Sh. Poormand[2], H. Arabi[1], H. Farsi[3]

[1] *Department of Physics, Faculty of Science, University of Birjand, Birjand, Iran*

[2] *Research center of Kansaran Binalood center, Mashhad, Iran*

[3] *Department of Chemistry, Faculty of Science, University of Birjand, Birjand, Iran*

Bi-based superconductors are prepared by different methods [1,2,3], all of them requiring for a prolonged sintering process. In the solid state reaction method, calcination eliminates carbonates and produces an oxide. Until now, this stage has been performed on mixed starting powders of nominal composition Bi_2O_3, PbO, $SrCO_3$, $CaCO_3$ and CuO. We have produced BSCCO superconducting ceramics by the solid state reaction method with the calcination stage performed on $CaCO_3$ and $SrCO_3$, only in order to produce CaO and SrO separately. $CaCO_3$ was kept at 1100°C for 3 hours, while $SrCO_3$ was kept at 1000°C for 3 hours. The sintering stage was then performed on the Bi_2O_3, PbO, SrO, CaO and CuO powders at 840°C for 24 hours. We have thus considerably reduced the time required to obtain the product . We have studied the samples in terms of X-ray diffraction Scanning Electron Microscopy (SEM). The results have shown that we can obtain BSCCO-2223 and BSCCO-2212 superconducting ceramics with ease.

References

1. I. H. Gul, F. Amin, A. Z. Abbasi, M. Anis-ur-Rrehman, A. Maqsood, Physica C 449 (2006) 139
2. I. H. Gul, M. A. Rehman, M. Ali, A. Maqsood, Physica C 432 (2005) 71
3. A. Tampieri, G. Calestani, G. Celotti, R. Masini, S. Lesca, Physica C 306 (1998) 21

*Corresponding author: ahmadamirabadi@yahoo.com

Mixed Conductivity in Tungstenite-phosphate Glasses Containing Alkali Ions

R. J. Barczyński, T. Kamiński

Faculty of Applied Physics and Mathematics, Gdansk University of Technology,
Narutowicza 11/12, 80-952 Gdansk, Poland
jasiu@mif.pg.gda.pl

Many glasses containing transition metal oxides are electronic conducting semiconductors. When alkali ions are admixtured during preparation of the glass they also participate in the conductivity process, so that mixed conductivity phenomena are observed. In alkali free-transition metal oxide glasses, conductivity is described by small polaron hopping. The carrier concentration is constant and related to the concentration of transition metal ions in various valence states. At the same time, ionic conduction generally depends on the alkali concentration and carrier ions' mobility. Assuming that the motion of alkali ions and polarons is independent, the electrical conductivity may be expected to increase with increasing alkali content. However, real transition metal oxide glasses containing alkali exhibit quite variable electrical behavior, ranging from strong anomalies in conductivity of several orders of magnitude [1] at certain amount of alkali ions to conductivity weakly dependent on the alkali content [2].

In the process of glass formation, most transition metal oxides play the role of glass formers and their ions are built into the structural network. A characteristic feature of electrical conductivity in this family of glasses is a deep minimum in conductivity at certain concentrations of the alkali oxide [2]. A few possible explanations for particular families of glasses are given in the literature, but there is no general consensus on the origin of this specific shape of conductivity.

The aim of the presented work has been to find a clue on the mechanisms of conductivity anomalies in tungstenite-phosphate glasses containing alkali ions. In order to keep the transition metal oxide's content at a constant level, we prepared glasses containing the same amount of W_2O_3 and altered the ratio of P_2O_5 to Li_2O, Na_2O, K_2O or Rb_2O. We have found that no conductivity anomalies are present under conditions of constant concentration of tungsten ions and alkaline ions exhibit rather low mobility in the tungstenite network.

References

1. J. C. Bazan, J. A. Duffy, M. D. Ingram, and M. R. Mallace, *Solid State Ionics*, **86–88** (1996) 497
2. R. J. Barczyński, and L. Murawski, *J. Non-Cryst. Solids*, **307–310** (2002) 1055

Development of Plastic Deformations in Cu Monocrystals under Application of External Stress

M. Białoskórski[1,2], M. Rychcik-Leyk[1], G. Bergmański[1], J. Rybicki[1,2,3]

[1] *Department of Solid State Physics, Gdansk University of Technology, Narutowicza 11/12, 80-952 Gdansk, Poland*

[2] *TASK Computer Center, Gdansk University of Technology, Narutowicza 11/12, 80-952 Gdansk, Poland*

[3] *Institute of Mechatronics, Nanotechnology and Vacuum Technique, Koszalin University of Technology, Racławicka 15–17, 75-620 Koszalin, Poland*

Extensive MD simulations of plastic deformations of Cu monocrystals were performed in a configuration corresponding to scraping a thin surface layer of atoms (several lattice constants) with a rigid tool. The deformed regions' evolution was analyzed for various shapes of rigid tool, various scraping depths, crystal orientations and directions of scraping. Easy-slip planes and directions have been determined.

Local Structure in Liquid Ag and Cu: a Molecular Dynamics Study

G. Bergmański[1], J. Rybicki[1,2,3], S. Feliziani[4]

[1] *Gdansk University of Technology, Narutowicza 11/12, 80-954 Gdansk, Poland*

[2] *TASK Computer Centre, Narutowicza 11/12, 80-954 Gdansk, Poland*

[3] *Institute of Mechatronics, Nanotechnology and Vacuum Technique, Koszalin University of Technology, Racławicka 15–17, 75-620 Koszalin, Poland*

[4] *Istituto di Matematica e Informatica, Università di Camerino, Camerino (MC), Italy*

Molecular dynamics simulations of liquid Ag and Cu have been carried at various temperatures with the Sutton-Chen many-body potential [1, 2] using the nanoMD code [3]. A detailed analysis of the obtained atomic configurations was performed using a number of tool programs contained in the ANELLI package [4, 5].

We cooled liquid metals from 2000 K to the phase-transition temperature at average rates of 1.9×10^{13} and 1.6×10^{13} K/s (respectively for Ag and Cu). Then, the liquids were cooled down to room temperature at two rates, 2×10^{13} and 2×10^{11} K/s. The main structural results for both metals, viewed with bond orientation order analysis [6], are qualitatively similar.

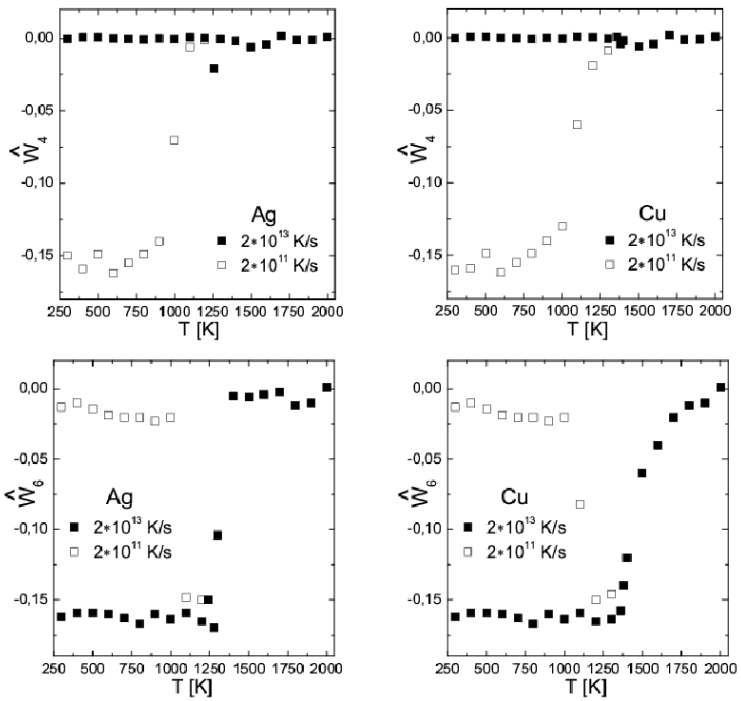

Figure 1: W_4 and W_6 parameters for Ag and Cu at various temperatures and cooling rates

Fig. 1 shows the values of the W_4 and W_6 parameter for Ag ad Cu at several intermediate temperatures. The changes in the parameter values during cooling suggest the appearance of an icosahedral local structure in the solid phase of the quickly cooled sample, and an fcc local structure in the slowly cooled sample.

References

1. T. Cagin, G. Dereli, M. Uludogan, M. Tomak 1999 *Phys. Rev.* **B 59** 3468
2. F. Cleri, V. Rosato 1993 *Phys. Rev.* **B 48** 22
3. M. Białoskórski, http://www.simgroup.task.gda.pl/staff.html
4. http://www.task.gda.pl/nauka/software/anelli/
5. J. Rybicki, G. Bergmański, G. Mancini 2001 *J. Non-Cryst. Solids* **293–295** 758
6. P. J. Steinhardt, D. R. Nelson, M. Ranchotti 1981 *Phys. Rev. Lett.* **47** 1275

Tensile Strength of Carbon Nanotubes

M. Białoskórski[1,2], J. Rybicki[1,2,3]

[1] *Department of Solid State Physics, Gdansk University of Technology, Narutowicza 11/12, 80-952 Gdansk, Poland*

[2] *TASK Computer Center, Gdansk University of Technology, Narutowicza 11/12, 80-952 Gdansk, Poland*

[3] *Institute of Mechatronics, Nanotechnology and Vacuum Technique, Koszalin University of Technology, Racławicka 15–17, 75-620 Koszalin, Poland*

Extensive classical Molecular Dynamics simulations of tensile strength of single-walled carbon nanotubes have been performed using the AIREBO force field.

About 30 nanotubes of radii from 2.8 Å ((0,7) nanotube) to 8.31 Å ((12, 12) nanotube) have been simulated systematically and the dependence of their tensile strength and stiffness moduli on the nanotube's radius has been determined. It turns out that (n, n) nanotubes are more mechanically resistant that $(n, 0)$ nanotubes.

The Structural Self-organization and Electrical Properties of Bicontained Thin Films

V. I. Bilozertseva[1]*, H. M. Khlyap[2], N. L. Dyakonenko[1], D. A. Gaman[1]

[1] *National Technical University "Kharkov Polytechnical Institute", 21 Frunze str., Kharkov, 61002 Ukraine*

[2] *University of Technology, 11 Diestel str., Kaiserslautern, 67657, Germany*

Investigations of multicomponent solid compounds allow us to expand the possibilities of their practical applications in modern electronics as replacements of elemental and binary materials. Amorphous chalcogenide semiconductor thin films containing alkali metals make it possible to vary the physical and chemical properties in a wide range. Bi-contained materials are not only considered to be attractive for structural studies (the question is still almost open), but also as a subject of electric investigations. These properties have not been studied until recently.

The present abstract describes some structural peculiarities of amorphous Li-Bi-Se thin films (40–100 nm thick) grown on glass substrates by the resistive evaporation technique and demonstrates their electric field-induced characteristics for the first time.

Layers were deposited under substrate temperatures of 300 K and 400 K. The deposition rate was estimated to be 0.1–0.5 nm/s. The electron-diffraction investigation demonstrated the layers' amorphous structure. The transmission electron microscopy and diffraction methods applied to study the films showed the crystal structure of films to have a cubic lattice of the bulk compound at $T_s = 400$ K.

The film's surface is sufficiently inhomogeneous, consisting of two structural units: globules and clusters. The surface of the $LiBi_3Se_5$ films is different: apart from the globules and clusters, their relief consists of micro crystals. Diffraction patterns observed in the images indicate the amorphous structure of layers. Polycrystalline $LiBi_3Se_5$ films were obtained under condensation at the substrate temperature of 400 K. Crystallization is connected with increased temperature of the substrate. As Ts increases, the mobility of atoms absorbed on the substrate also increases, resulting in the crystallization energy barrier being overcome. Even a small 3 K increase of the substrate temperature (40–600 K) due to focusing the electron beam causes the growth of separate needle-like crystallites, which means that a self-organization process taking place.

Electrical measurements were carried out under applied electric field of up to $4 \cdot 10^4$ V/m. An analysis of the experimental current-voltage characteristics has exhibited a quasi-tunneling mechanism of carrier transport: a two-step process under direct applied voltage and one-step transfer under reverse direction. These results suggest a considerable effect of the layer structure on carrier transport.

Thus, amorphous and polycrystalline Li-Bi-Se thin films of various composition were prepared by the resistive evaporation technique from a quasi-closed volume. Condensation on glass substrates at various temperatures of the substrate (300 K and 400 K) made it possible to obtain amorphous $LiBiSe_2$ films and polycrystalline $LiBi_3Se_5$ layers. The amorphous films' surface was globule-and-cluster in character. Room-temperature current-voltage characteristics of the amorphous films demonstrated tunneling and space charge-limited currents due to peculiarities of the film surface.

*Corresponding author: biloz@mail.ru

Quantum-numerical Parameterization for Quantum-classical Hybrid Methods for Metals

M. Bobrowski[1,2], J. Dziedzic[1], J. Rybicki[1,2,3]

[1] *Department of Solid State Physics, Gdansk University of Technology, Narutowicza 11/12, 80-952 Gdansk, Poland*

[2] *TASK Computer Center, Gdansk University of Technology, Narutowicza 11/12, 80-952 Gdansk, Poland*

[3] *Institute of Mechatronics, Nanotechnology and Vacuum Technique, Koszalin University of Technology, Racławicka 15–17, 75-620 Koszalin, Poland*

A numerical scheme is presented fitting the classical forces acting on flagged atoms to quantum mechanically calculated forces. The atoms in the system which will be treated quantum mechanically are localized and flagged. Likewise localized are atoms around them acting on their central flagged atom. Forces acting on the flagged atoms are calculated and used as reference for the classical forces of the Sutton-Chen potential. The potential is reparameterized by means of the nonlinear Levenberg-Marquardt procedure, using the standard parameters until they reproduce the actual forces. The "on the fly" fitting scheme was first proposed by Csanyi and his co-workers and applied successfully for vacancy diffusion and crack propagation in silicon. In our work, the scheme is applied to metallic systems using the TB algorithms of Papaconstantopoulos and his co-workers as the quantum-mechanical method and our own program for MD simulations. We have adapted it for various defects in copper and gold, as well as for nanocutting of copper with metallic nano-edges.

Acknowledgements

Supported by grant 1627/T11/2005/29 from the Polish State Committee for Scientific Research. Calculations were carried out with the resources and software at the Informatics Center of the Metropolitan Academic Network (IC MAN) at the Technical University of Gdansk and at the Department of Solid State Physics at the Technical University of Gdansk, Poland.

Nanocomposite SiO_2(Si) Films as a Medium for Non-volatile Memory

O. Bratus'*, A. Evtukh, V. Ievtukh, V. Litovchenko

Lashkarev Institute of Semiconductor Physics NAS of Ukraine, 41 pr. Nauki, Kiev, 03028 Ukraine

Nanocrystal memories have been proposed as a possible solution to the scaling problem of electronic nonvolatile memories. Ultimately, one is looking for nanoparticle memories to significantly decrease the voltage needed to write/erase memory without compromising its retention characteristics. An important problem for practical realization of non-volatile nanocrystal memory is the required technology. Several techniques of nanocrystal formation have recently been developed based on chemical vapor deposition (CVD) of Si nanocrystals onto oxidized Si substrates, ion implantation of Si or Ge into SiO_2, annealing of silicon-rich oxides, aerosol deposition, etc.

Two methods were applied in our work for nanocomposite SiO_2(Si) films containing Si nanocrystals (NCs) in dielectric SiO_2 matrix: (i) plasma-enhanced chemical vapor deposition (PE CVD) and (ii) pulse laser deposition (PLD). The C–V method was used to characterize the charging effects in the MIS structure (capacitor), with nanocomposite SiO_2(Si) film as an insulator.

The SiOx and SiO_2(Si) nanocomposite films obtained by the plasma-enhanced chemical vapor deposition method (PE CVD) were investigated. The SiH4/N2O ratio of gases during deposition was the main variable parameter, the others being power density of 0.11 W/cm^2, substrate temperature of T=100°C and the HF signal's frequency of of 13.56 MHz. After deposition, the thickness and refractive indices of the SiOx film were measured and determined by the laser ellipsometry method (λ=632.8 nm). Subsequent thermal annealing of the films promotes their transformation from SiO_x into SiO_2(Si) with silicon nanocrystals in the SiO_2 dielectric matrix.

The PLD method allowed us to obtain nanocomposite SiO_2(Si) with a mirror surface upon deposition in a vacuum chamber with residual gas pressure of 10^{-3} Pa for size separation of Si particles. A YAG:Nd^{3+} laser beam (wavelength 1.06 μm, energy and duration of pulse 0.2 J and 8 ns, frequency of their reiteration 25 Hz), working in the modulated soundness, scanned the target. The velocity of film deposition remained in the 2–20 nm/min range, while their thicknesses was 50–500 nm. Further from the axis of the erosion torch the thickness of the film decreased. The films grown at large distances from the torch axis were characterized by smaller dimensions of Si NC and their higher concentration. These regularities of formation of SiO_x films with Si NC structure are the result of their deposition from a backward, low-energy flood of erosion torch particles.

Formation of MIS structures was completed by sputtering aluminum films on the frontal side through the mask and the rearward surface. The Ohmic Al contact with the p-Si substrate was provided by thermal or laser annealing.

The C–V characteristic measurements were made with an AMTs-1530 C meter at a testing signal frequency of 1 MHz and voltage rate of 50 mV/s, in the −15 to +15 V range. The C–V characteristic measurements began from the voltage corresponding to depletion or inversion of the surface semiconductor layer (from positive gate voltages for p-type semiconductors and from negative gate voltages for n-type semiconductors), to the voltages corresponding to accumulation and continued in the reverse direction. The amplitude of the high- frequency signal was 20 mV. The charging effect was determined from C–V characteristics' shift at their measurements.

The typical C–V characteristics of structures under investigation are shown in Fig. 1. As a rule, the counterclockwise hysteresis was observed. This type of hysteresis suggests positive charging, at-

*Corresponding author: Bratus1981@ukr.net

tributable to hole trapping from the substrate accumulation layer (p-type substrate) into the nanocrystals of SiO_2(Si) films.

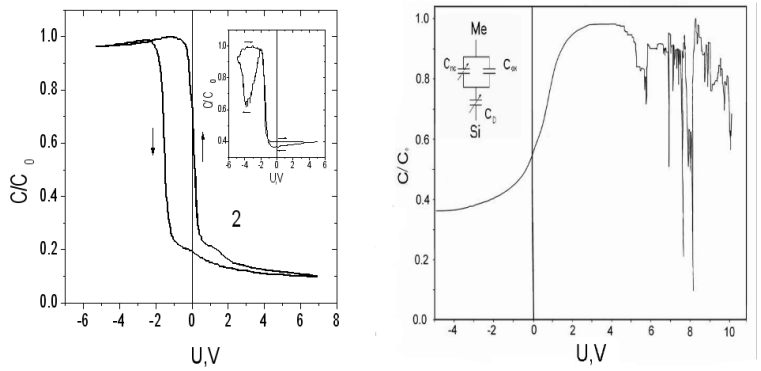

Figure 1: Typical C–V characteristics of MIS structures with nanocomposite SiO_2(Si) films: a) deposited by the PLD method on Si, p-type, b) deposited by the PE CVD method on Si, n-type (inserted the equivalent capacity circuit of the MIS structure).

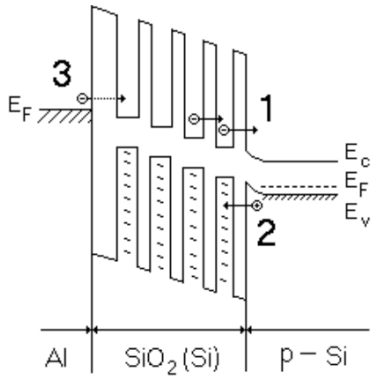

Figure 2: Energy band diagram of an MIS structure with nanocomposite SiO_2(Si) film and charge carrier transport processes: 1 – electron injection from NCs, 2 – hole tunneling from the semiconductor, 3 - electron injection from the metal electrode.

An important peculiarity of C–V characteristics is a decrease in capacitance under conditions of semiconductor surface accumulation. Some MIS structures experience a significant decrease of C in the accumulation region, an effect due to charging of Si nanocrystals under increasing gate voltage. In the accumulation region, almost all voltage applied in the insulator decreases. In this case, the electric field is high enough to promote hole or electron tunneling from the substrate/gate on Si NCs. It is possible to represent the equivalent capacity circuit of an MIS structure as containing three capacities (see insert in Fig. 1b): (i) the differential capacity of the semiconductor, CD, (ii) the capacity of insulator, C_{ox}, and (iii) the capacity of nanocrystals C_{nc}. Upon charge capture on NCs, C_{nc} decreases, an effect due to reduced quantity of uncharged NCs, i.e. a decreased number of available electron states reacting on small alternative signal at C–V measurements.

The value and sign of charge (ΔQ_d) captured in the insulator (SiO_2 (Si)) of an MIS structure due to the influence of electric field is determined from hysteresis of C–V characteristics at writing in two directions from inversion to accumulation and vice versa.

The maximal value of electric field's strength is reached in SiO_2(Si) films under conditions of semiconductor surface accumulation. As a rule, a negative value of the flat band voltage shift (ΔV_{FB}) is observed, evidence of effective positive charge being captured in Si NCs.

In the case of films prepared by the PLD method, the captured charge is greater for thinner SiO_2(Si)

films. As mentioned above, thinner films have smaller NCs. The greater charge captured for thinner films is attributable to the higher density of Si NCs. The Coulomb blockade effect is known to be significant for small NC (d<10 nm) and can inhibit charge capture, but in our case the influence of Si NCs density is dominant. As expected, the values of ΔV_{FB} and ΔQ_d increase with the increase of maximal electric fields.

Additional measurements were performed to clarify the sign and value of charge captured in nanocomposite SiO_2 (Si) films and the charge carrier transport mechanism. The maximal value of negative voltage was varied at fixed positive applied voltage and vice versa. The following results were obtained: (i) small negative charge was captured in the nanocomposite SiO_2 (Si) film under positive gate voltage, (ii) significant capture of positive charge was observed under negative gate voltage, while (iii) the difference between the positive and negative charge captured in both cases cannot be attributed to the reduction of the positive gate voltage in the semiconductor's depletion region.

On the basis of the obtained experimental results, a model of charge transport and capture in nanocomposite SiO_2 (Si) films has been proposed (Fig. 2). The capture of small negative charge under positive gate voltage appears to be a result of electron direct tunneling from the semiconductor's depletion or inversion layers. In the case of the negative gate bias, hole tunneling from the accumulation layer into the SiO_2(Si) film occurs. Direct tunneling is complicated by the high energy barrier for the hole ($\sim$4.6 eV). A possible mechanism for hole tunneling is resonance tunneling assisted by traps in the insulator's forbidden band (trap-assisted tunneling). In this case, theoretical calculations have shown the current of trap-assisted tunneling to be higher than the direct tunneling current by the same order of magnitude. The existence of traps localized in the forbidden SiO_2 band of the SiO_2 (Si) nanocomposite film is quite natural and attributable to the film's deposition conditions. Under greater negative gate bias, the influence of electron injection from the metal electrode becomes noticeable.

The Atomic Structure of a Silicon Nitride Thin Film on Si(111): a Computer Simulation

E. Chernonog, R. Balabay

Department of Physics, Krivoy Rog State Pedagogical University,
Prospekt Gagarina 54, 50055 Krivoy Rog, Ukraine

Si/SiO_2 and Si/Si_3N_4 systems are present in almost all devices of modern microelectronics, including SONOS structures (Silicon-Oxide-Nitride-Oxide-Silicon). In order to increase volumes available for saving information, the thicknesses of SONOS structures' layers is reduced to nanoscale. The features of technology producing such nanosized systems determine the nonstoichiometry of their chemical composition and the probability of Si, O or N precipitating generation into the dielectric phases. This leads to changes in the conductivity type of layers. Nowadays, data storage based on conducted nanoclusters (Si, Ge) in dielectrics is developed. Therefore, there is interest in research on the atomic structure and chemical composition of Si/SiO_2 and Si/Si_3N_4 interfaces with the thicknesses of layers of not more than 10 nm.

By means of computer modeling, we have created a model of an Si/Si_3N_4 system with free surfaces and layer thickness of 18.72 Å and 14.555 Å, respectively, the inter-atomic interactions being described by the Tersoff potential.

A real multi-atomic system was replaced with a limited cubic cell, with periodic boundary conditions imposed on a cube face with a 38.4 Å side in the x direction and a 34.32 Å side in the y direction. This choice of size depended first of all on the significant duration of relaxation time of large-volume systems. The prototype system was filled with atoms in positions approximate to those of an ideal crystal and contained 1920 atoms. The vacuum was simulated on a part of the Si and Si_3N_4 layers. Thus, a model of a continuous interface with free surfaces was obtained and the Si/Si_3N_4 interface was investigated. The equilibrium atomic configuration was determined using a Monte-Carlo procedure at the decrease of temperature from 1000 K to 300 K: 1000 shifts of the atomic system were made for every 50 K. The amplitude of shifts depended on temperature.

The following structural characteristics were used to analyze details of the atomic structure:

- Radial distribution functions,
- The energy of the atomic system,
- Three-body correlation functions,
- The value of bond-angle distributions,
- The arrangement of atoms in planes (100), (110) and (111),
- The spatial configuration of the atomic array, and
- The presence of Si precipitate as fractal clusters.

References

1. Tersoff J 1989 *Phys. Rev. B* **39** R5566

Vacuum-deposited poly(o-methoxyaniline) thin film: its structure and electronic properties

V. Cherpak[1], P. Stakhira[1], O. Aksimentyeva[2], Z. Hotra[1,3], B. Tsizh[4], D. Volynyuk[1], I. Bordun[1]

[1] *Lviv Polytechnic National University, S. Bandery 12, 79013 Lviv, Ukraine*

[2] *Ivan Franko Lviv National University, 8 Kyrylo and Mefodiy str., 79005 Lviv, Ukraine*

[3] *Rzeszów University of Technology, W. Pola 2, 35-959 Rzeszów, Poland*

[4] *Kazimierz Wielki University, Chodkiewicza 30, 85-064 Bydgoszcz, Poland*

Thin films of poly(o-methoxyaniline) (POMA) were formed by thermovacuum deposition in the 350–450°C temperature range, under pressure of 1×10^{-6} Torr. Structural properties of the vacuum-deposited POMA films were investigated with Fourier transform infrared spectroscopy (FTIR). The obtained results showed that the polymer was in its fully reduced state. Furthermore, FT–IR and UV–VIS spectra were similar to those observed for the emeraldine form of polyaniline.

A sandwich-type ITO/POMA/A1 device was formed and its dark I–V characteristics were measured in air at room temperature. Non-Ohmic rectifying behavior typical for metal/p-semiconductor interfaces (the Schottky barrier) was indicated.

Electrical impedance measurements in the frequency range between 10 Hz and 1 MHz were made. For low frequencies, the real part of conductivity $\sigma(\omega)$ was frequency-independent, while above the critical angular frequency it was described by an equation of the form $\sigma(\omega)^s$. A nomadic polarization model of quasi-one-dimensional solids was used to fit the experimental results.

Influence of the Technological Conditions of the LPE Process on the Morphology of Si ELO Layers

J. M. Olchowik[1], S. Gułkowski[1], K. Cieślak[1], I. Jóźwik[1], A. Fave[2], A. Kaminski[2]

[1] *Institute of Physics, Lublin University of Technology, Nadbystrzycka 38, 20-618 Lublin, Poland*

[2] *Institut des Nanotechnologies de Lyon (INL), UMR 5270 CNRS-ECL-INSA-UCBL No 5270, Institut National des Sciences Appliquees de Lyon, Bat Blaise Pascal, 7 avenue Jean Capelle, 69621 Villeurbanne Cedex, France*

Epitaxial lateral overgrowth (ELO) is a method of obtaining thin-film solar cells. It enables saving the material used in their production making PV modules more economical. Moreover, an ELO layer is partly separated from the growing substrate by SiO_2 overlayer which prevents the propagation of defects from the substrate into the ELO layer. This means that even silicon substrates of inferior quality can be used to fabricate quality solar cells.

Growing a continuous thin silicon layer on a specially prepared silicon growth substrate is the first step in obtaining photovoltaic (PV) modules. The morphology, quality and density of defects in this layer depend on various factors: the temperature and time of growth, the cooling rate, atmosphere, etc.

This work presents an analysis of the growth of silicon ELO layers under various conditions in horizontal and vertical LPE furnaces. The results can be used to determine the best growth conditions in order to obtain optimal Si layers for PV applications.

Application of Impedance Spectroscopy for Ferroelectric Thin Film Characterization

D. Czekaj, A. Lisińska-Czekaj, J. Czuber, T. Orkisz

University of Silesia, Department of Materials Science,
Śnieżna 2, 41-200 Sosnowiec, Poland

The present paper is a presentation of results of a study of barium strontium titanate ($Ba_{1-x}Sr_xTiO_3$ – BST) thin film capacitors fabricated by the spin-coating technique. Both pure and Mg-doped $Ba_{0.6}Sr_{0.4}TiO_3$ thin films were investigated. Morphological analysis using optical microscopy, scanning electron microscopy and atomic force microscopy were performed. The crystalline structure of BST thin films was examined through X-ray diffraction (XRD) analysis using a Philips PW 3710 X-ray diffractometer at room temperature.

Impedance spectroscopy results of the ceramic samples' AC response at room and elevated temperatures are given. The usual representation of impedance measurements (i.e. Z'' vs. Z') and alternative representations have been used to interpret the impedance spectra of BST thin films in order to separate the contributions of the bulk, grain boundary and electrode processes.

Acknowledgements

The present research was supported by the Polish Ministry of Education and Science from the funds for science in 2006–2009 as research project N507 098 31/2319.

Dynamical and Structural Properties of Titanium-decorated Fullerene: a Computer Simulation Study

A. Dawid*, A. Piątek, Z. Gburski

University of Silesia, Institute of Physics, Uniwersytecka 4, Katowice 40-007, Poland

Materials composed of titanium-decorated fullerene molecules are considered to be potential hydrogen-storage media [1–3].We have investigated the TiH_2 functionality group attached to double-bonded carbons of a pair of fullerene hexagons (Fig. 1). The simulation (by the MD method) was carried out with an NPT ensemble with periodic boundary conditions. We have chosen the Lennard-Jones potential as interaction between separate sites. We studied the system in a wide range of energies, from the solid to the gaseous state. The low energy, solid-state structure was determined. We calculated the Lindemann index (mean intermolecular length fluctuation) and specific heat as a function of energy. The velocity auto-correlation function and its Fourier transform of $C_{60}Ti_6H_{12}$ molecule were also calculated, analyzed and discussed.

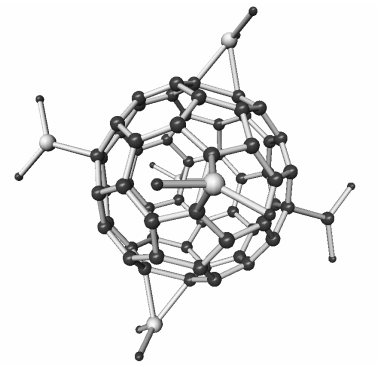

Figure 1: A TiH_2-decorated fullerene molecule

References

1. T. Yildirim, J. Iniguez and S. Ciraci *Phys. Rev. B* **72**, 153403 (2005)
2. T. Yildirim and S. Ciraci *Phys. Rev. Lett.* **94**, 175501 (2005)
3. E. Durgun S. Ciraci W. Zhou and T. Yildirim *Phys. Rev. Lett.* **97**, 226102 (2006)

*Corresponding author: dawid@us.edu.pl

Dynamical Properties of Potassium Ion K^+ Trapped in Fullerene C_{60} Cage: an MD simulation

A. Dawid*, A. Piątek, M. Sokół, Z. Gburski

University of Silesia, Institute of Physics,
Uniwersytecka 4, Katowice 40-007, Poland

We have simulated a nanosystem composed of endohedral fullerene $K^+@C_{60}$ molecules, possibly applicable in micro-electronic devices [1]. The interaction has been taken to be the full site-site pair-wise additive Lennard-Jones (LJ) potential, which generates both translational and anisotropic rotational motions of each endohedral fullerene molecule. We have used periodic boundary conditions with an NVT ensemble. Our atomically detailed MD simulations allow us to analyze the dynamics of a potassium ion inside a fullerene cage, as well as the motion of $K^+@C_{60}$ molecules. The physical quantities of the radial distribution function, the mean square displacement, the translational velocity correlation functions and their Fourier transforms, the librational frequency of K^+ ion inside a C_{60} cage, etc. have been calculated for several energies of the studied nanosystem.

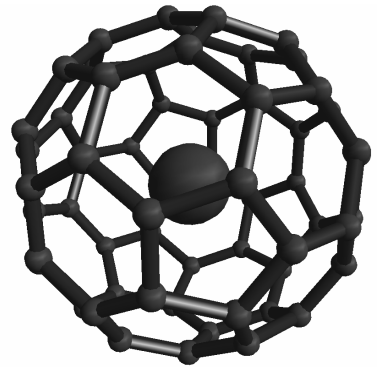

Figure 1: A K^+ ion trapped in a fullerene cage

References

1. J. W. Kang and H. J. Hwang *Journal of the Physical Society of Japan* **73**, (4) 1077-1081 (2004)

*Corresponding author: dawid@us.edu.pl

Properties of Endohedral Complexes of Low Molecular Weight Systems Encapsulated in Carbon Nanotubes: an MD Study

Z. Dendzik*, M. Sokół, W. Gwizdała

University of Silesia, Institute of Physics,
Uniwersytecka 4, 40-007 Katowice, Poland

The behavior of molecules confined in nanoscale pores is of great interest to biology, geology and materials science. The importance of carbon nanotubes as a confining medium is due to their extreme narrowness combined with considerable length, which brings about effects not observed in bulk systems [1–2].

We have used molecular dynamics simulation to study the properties of several low molecular weight systems encapsulated in single-walled carbon nanotubes of various diameters and chiralities. We have also assessed the influence of the encapsulated molecular systems on the phonon density of states of the nanotubes.

References

1. Zhao J, Buldum A, Han J and Lu J P 2002 *Nanotechnology* **13** 195
2. Kolesnikov I A, Zanotti J M, Loong C K, Thiyagarajan P, Moravsky A P, Loutfy R O and Burnham C J 2004 *Phys. Rev. Lett.* **93** 035503-1

*Corresponding author: dendzik@us.edu.pl

Effective Elastic Properties and Strong Ellipticity for Two-dimensional Elastic Media

A. R. Duda[1*], K. W. Wojciechowski[2†]

[1] *Institute of Theoretical Physics, Wroclaw University, Pl. Maxa Borna 9, 50-204 Wroclaw, Poland*

[2] *Institute of Molecular Physics, Polish Academy of Sciences M. Smoluchowskiego 17, 60-179 Poznan, Poland*

Effective elastic properties are obtained for all two-dimensional elastic symmetries. In particular, the effective Poisson's ratio is calculated in two ways: (i) as a quotient of an effective stiffness constants, (ii) by averaging an analytic expression for the Poisson's ratio over all possible rotations of the coordinate system. An analysis of the Poisson's ratio in the stability region of a certain two-dimensional elastic medium of high symmetry is presented and conditions under which the ratio reaches negative values (i.e. for auxetic media) are given.

Necessary and sufficient conditions of strong ellipticity for some two-dimensional elastic media of higher symmetries are also derived.

*ardud@ift.uni.wroc.pl
†kww@ifmpan.poznan.pl

Magnetic Films of Negative Poisson's Ratio in Rotating Magnetic Fields

M. R. Dudek*, K. W. Wojciechowski†

Institute of Molecular Physics, Polish Academy of Sciences
M. Smoluchowskiego 17, 60-179 Poznan, Poland

We model the mechanical properties of a thin magnetic film subjected to an external, rotating magnetic field with computer simulations. The film consists of a nonmagnetic polymer matrix with inclusions of magnetic nanoparticles (nanograins) of uniaxial anisotropy. The time evolution of the nanograins' magnetization is described by the Landau-Lifshits-Gilbert equation [1, 2, 3]. The Poisson's ratio [4] of the used matrix model is negative [5], i.e. the system expands laterally under a longitudinal stretching force. The nonmagnetic matrix, represented with a simplified two-dimensional bead-spring model with the beads interacting via the Lennard-Jones potential and connected by harmonic bonds, is simulated by applying the leap frog algorithm [6] to the Nosé-Hoover thermostat technique [7, 8]. However, in contrast to our earlier studies [9], magnetic nanoparticles do not form an anisotropic (e.g. square) lattice but a hexagonal structure known to be elastically isotropic for small deformations [4].

We show explicitly that magnetic nanoparticles affect the mechanical response of the nonmagnetic matrix. In particular, we have observed an interesting dynamical state of the nonmagnetic matrix when the in-plane rotating magnetic field is followed by successive shrinking and expansion of the matrix below a threshold value, ω_0, of the field frequency. This magneto-elastic coupling can be used to control the expansion/contraction of nonmagnetic matrices.

References

1. L. D. Landau and E. M. Lifshits, Phys. Z. Sovjetunion 8, 153 (1953)
2. T. L. Gilbert, Phys. Rev. 100, 1243 (1955)
3. M. I. Shliomis, Sov. Phys. Usp. 17, 153–169 (1975)
4. L. D. Landau and E. M. Lifshits, Theory of Elasticity, Pergamon Press, London, 1986
5. K. W. Wojciechowski, Phys. Lett. A 137, 60–64 (1989)
6. M. P. Allen and D. J. Tildesley, Computer Simulations of Liquids, Oxford University Press, Oxford, 1987
7. S. Nosé, Molec. Phys. 52, 255 (1984)
8. W. G. Hoover, Phys. Rev. A 31, 1695 (1985)
9. M. R. Dudek, B. Grabiec and K. W. Wojciechowski, Rev. Adv. Mater. Sci. 14, 14–34 (2007)

*mdudek@proton.if.uz.zgora.pl
†kww@ifmpan.poznan.pl

Degradation of Nano-cutting Tools: an MD Simulation

J. Dziedzic[1], M. Białoskórski[1,2], M. Rychcik-Leyk[1], J. Rybicki[1,2,3]

[1] *Department of Solid State Physics, Faculty of Technical Physics and Applied Mathematics, Gdansk University of Technology, Narutowicza 11/12, 80-952 Gdansk, Poland*

[2] *TASK Computer Centre, Gdansk University of Technology, Narutowicza 11/12, 80-952 Gdansk, Poland*

[3] *Institute of Mechatronics, Nanotechnology and Vacuum Technique, Koszalin University of Technology, Racławicka 15–17, 75-620 Koszalin, Poland*

High-precision finishing of surfaces is a process of significant technological importance. Difficulties caused by the small size of the system render its experimental analysis expensive and challenging. Since the length scales involved in today's technological processes are in the nanometer regime, it becomes possible to perform atomic-level computer simulations bridging on the sizes achievable in a laboratory.

We present the results of molecular-dynamics simulations of repeated interactions of a realistically-shaped cutting edge with a model, infinitely hard grain. The model edge is composed of several hundred thousand of atoms of an fcc metal, treated with the Sutton-Chen potential, moving at a constant speed of 20 m/s.

Plastic deformations appearing upon contact with the rigid obstacle are observed and described by means of stress and temperature fields and the atomic slip vector. Preferable slip planes are identified and the normal force experienced by the tool is investigated.

Transport Measurements of Ferromagnetic-superconductor Composite Bases on Open-pore $YBa_2Cu_3O_{7-\sigma}$, High-temperature Superconductors

P. Fiertek[1] , B. Andrzejewski[2], W. Sadowski[1]

[1] *Department of Solid State Physics, Faculty of Technical Physics and Applied Mathematics, Gdansk University of Technology, Narutowicza 11/12, 80-952 Gdansk, Poland*

[2] *Institute of Molecular Physics, Polish Academy of Sciences, Smoluchowskiego 17, 60-179 Poznan, Poland*

Very few studies have been carried out so far regarding the production methods and analysis of $YBa_2Cu_3O_{7-\sigma}$ high-temperature superconductors with open pores. The presented work widens our knowledge about this group of materials. Generally speaking, the physical properties of high-T_c superconductors are highly dependent on their macroscopic structure: e.g. the critical current density, J_c, of thin films exceeds by two orders of magnitude the J_c value calculated for bulks materials. The article presents $R(T)$ characteristics measured for various external magnetic fields ranging from 0 T to 1 T and various pore sizes.

Methane Decomposition and Formation of Carbon Filaments in the Presence of Nickel Catalysts

W. Gac[1], T. Borowiecki[1], A. Denis[1], L. Kępiński[2]

[1] *Departament of Chemical Technology, University of Maria Curie-Skłodowska, Pl. M. Curie-Skłodowskiej 3. 20-031 Lublin, Poland*

[2] *Polish Academy of Sciences, Institute of Low Temperature and Structure Research, Okólna 2, 50-422 Wroclaw, Poland*

Carbon-based materials have recently enjoyed great interest. Formation of carbon deposits on the surface of catalysts has been perceived for long time as undesirable. The nature of carbon deposits is related to the type of catalyst, its structural and surface properties, the type of metal, the size of crystallites or metal-support interactions, as well as the experimental conditions, including temperature and gas or liquid phase composition. Methane decomposition is a relatively cheap and simple method of producing pure hydrogen, directly applicable in modern energy production systems. We have investigated nickel catalysts obtained by various preparation methods and of various composition. In our recent work, we have dealt with nickel alumina catalysts modified with magnesia.

The catalysts were obtained by the co-precipitation method. Their properties were studied by the temperature-programmed reduction (TPR) and desorption (TPD) methods. Methane decomposition was studied by the thermogravimetric, transient temperature programmed reaction method and pulse oxygen adsorption using mass spectrometry. The nature of deposits formed under varying experimental conditions was investigated by the temperature-programmed oxidation method (TPO) and high-resolution transmission microscopy. It was found that the activity of catalysts was strongly related their composition and the temperature of reaction. We observed changes in the structure of carbon filaments. An increase of reaction temperature transformed the filled whiskers with axial carbon layers and metal crystallites on top to tubes with few parallel carbon layers. Deactivation of catalysts was related to incomplete removal of carbon species from the surface of nickel crystallites and formation of stable deposits covering the crystallites.

The Structure and Electrical Conductivity of Reduced Lead-germanate, Bismuth-germanate and Bismuth-silicate Glasses Modified with Potassium

J. Gackowska*, M. Gazda, K. Trzebiatowski, B. Kusz

Department of Solid State Physics, Gdansk University of Technology, Narutowicza 11/12, 80-952 Gdansk, Poland

The structure of lead-germanate, bismuth-germanate and bismuth-silicate glasses was modified with potassium in order to improve their mechanical properties. Studies of the potassium modification's influence on the glasses' structure and electrical properties were performed with AFM, DSC and conductivity measurements. It has been observed that the potassium modification improves the mechanical and technological properties of glasses, while at the same time slightly deteriorating their electrical properties.

*Corresponding author: asia@mif.pg.gda.pl

Electronic Conduction in (Bi,Pb)-Sr-Ca-Cu-O Granular Superconductors

M. Gazda, B. Kusz, T. Klimczuk, L. Murawski

Faculty of Applied Physics and Mathematics, Gdansk University of Technology, Narutowicza 11/12, 80-952 Gdansk, Poland

Granular superconductors are very interesting materials thanks to their untypical electrical properties due to the presence of Coulomb effects, electron tunnelling, Josephson coupling of granules and various aspects of disorder. This paper is a study of the electrical properties of (Bi,Pb)-Sr-Ca-Cu-O granular superconductors obtained by the solid state crystallization method. The materials may be considered as a system of granules of a high-temperature superconductor embedded in an insulating matrix. The studied granules ranged from 10 nm to 40 nm in size. The materials, which contained granules in their superconducting state below the transition temperature, had three types of temperature dependence of resistivity. These composed of very small granules (10 nm) of the superconducting phase exhibited hopping conductivity exponential dependence. In the samples containing relatively large granules of the 2212 phase (above 30 nm), the bulk superconducting state was achieved. The intermediate materials were characterized by an unusual temperature dependence on resistivity, incompatible with the known models of electronic transport in granular materials.

Electronic Correlations in Fermionic Lattice Models

M. Matlak[1], B. Grabiec[2], S. Krawiec[1]

[1] *Institute of Physics, University of Silesia, Uniwersytecka 4, 40-007 Katowice, Poland*

[2] *Institute of Physics, University of Zielona Góra, Prof. Z. Szafrana 4a, 65-516 Zielona Góra, Poland*

We investigate two-site electronic correlations within a generalized Hubbard model as representative of a broad class of fermionic lattice models. The considered model incorporates the conventional Hubbard model (with hopping between nearest neighbors, t, and Coulomb repulsion/attraction, U, as parameters) supplemented with inter-site Coulomb interactions (with parallel spins, $J^{(1)}$, and antiparallel spins, $J^{(2)}$, as parameters) and the term responsible for the hopping of intra-site Cooper pairs (parameter V), similarly as in the Kulik-Pedan-Penson-Kolb (KPPK) model. As the first step, before moving to the real lattice, we consider the exactly solvable dimer problem. We find the eigenvalues, E_α, and eigenvectors, $|E_\alpha\rangle$, of the dimer and represent each partial Hamiltonian, $E_\alpha|E_\alpha\rangle\langle E_\alpha|$ ($\alpha = 1, 2, \ldots, 16$), in the second quantization with Hubbard and spin operators. Thus, each energy level has its own Hamiltonian (or partial Hamiltonian) ascribed, describing the various two-site interactions that can be active only when this level is be occupied by electrons. A typical feature is the appearance of two generalized t–J interactions ascribed to two different levels so that their coupling constants do not disappear even in the case of $U = J^{(1)} = J^{(2)} = V = 0$ and are equal to $\pm t$. In the large-U case, when $J^{(1)} = J^{(2)} = V = 0$, there is only one t–J interaction with the coupling constant equal to $4t^2/U$, the same as in the case of a real lattice. We demonstrate that the competition between magnetism (ferromagnetism and antiferromagnetism) and superconductivity (intra-site and inter-site pairings) is a universal feature of all fermionic lattice models, as it exists even when $U = J^{(1)} = J^{(2)} = V = 0$ but $t \neq 0$. We also demonstrate that the same types of electronic interactions are additionally scattered between different energy levels and, therefore, their thermodynamical activities are dependent on the occupation of these levels. This feature qualitatively explains the origin of the model's phase diagram. As the next step, we consider the case of a real lattice which can be decomposed into a set of interacting dimers. We thus show that the above-mentioned competition between magnetism and superconductivity appears automatically also in this general case. This in turn creates a delicate problem of symmetry breaking discussed in the paper, introducing the order parameters in four competitive channels: ferromagnetic, antiferromagnetic and two different superconducting pairings). The resulting presented in this paper may be relevant not only in solid state physics but for quantum dots and nanosystems.

Organized Photoelectretic Films Based on Carbazole Polymers

A. P. Shpak[1], Yu. A. Kunitskiy[2], Yu. M. Barabash[3], M. I. Rakitin[4], D. A. Grynko[4]

[1] *G. V. Kurdyumov Institute for Metal Physics, National Academy of Science of Ukraine, Academican Vernadsky 36, Kyiv-142, 03680 Ukraine*

[2] *Technical Centre NAS of Ukraine, Pokrovskaya 13, 04070 Kiev, Ukraine*

[3] *Institute of Physics of National Academy of Sciences of Ukraine, Prospekt Nauky 46, 03650 Kyiv, Ukraine*

[4] *Institute of Semiconductor Physics of National Academy of Sciences of Ukraine, Prospekt Nauky 41, 03650 Kyiv, Ukraine*

The properties of carbazole-based polymer coatings as template media are discussed. Trapped and localized carriers may produce electrets of strong electric field localized near the film's surface. Thin films of 300–800 nm thicknesses were deposited by solution spinning. Coatings and films of 10–500 nm thicknesses were deposited by polymerization in vacuum from the vapour phase. Coatings so obtained contain carbazole groups of varying coordination depending on the deposition method. The films' electretic state was obtained with the electrophotography technique and was maintained for a few months. The density of localized charge depends strongly on the film's deposition method.

Modeling Thin Si Layers' Growth on a Partially Masked Si Substrate

S. Gułkowski[1], J. M. Olchowik[1], P. Moskvin[2*]

[1] *Institute of Physics, Lublin University of Technology, Nadbystrzycka 38, 20-618 Lublin, Poland*

[2] *Zhitomir State Technological University, Chernyakhovs'kogo 103, 10005 Zhitomir, Ukraine*

This paper presents a numerical simulation model of epitaxial silicon layers laterally overgrown from the Sn solvent's liquid phase. A two-dimensional diffusion equation has been solved and concentration profiles of Si in an Si-Sn rich solution during the growth process have been constructed. The epilayer's thickness and width were obtained from the concentration gradient at both ELO faces for various growth parameters. An aspect ratio was calculated for these results.

*Corresponding author: moskvin@us.ztu.edu.ua

The Ageing Effect in Nanocrystalline TiC/C: an EPR Study

N. Guskos[1,2*], T. Bodziony[2], J. Typek[2], G. Żołnierkiewicz[2], M. Maryniak[2], A. Biedunkiewicz[3]

[1] *Solid State Physics, Department of Physics, University of Athens, Panepistimiopolis, 15 784 Zografos, Athens, Greece*

[2] *Institute of Physics, Szczecin University of Technology, Al. Piastów 17, 70-310 Szczecin, Poland*

[3] *Institute of Material Engineering, Szczecin University of Technology, Al. Piastów 17, 70-310 Szczecin, Poland*

A TiC/C nanocrystalline material, titanium carbide TiC dispersed in a carbon matrix, was prepared in a non- hydrolytic sol-gel process. The temperature dependence of the material's electron paramagnetic resonance (EPR) spectra was studied in the 3.5–60 K range. Two asymmetric EPR lines was recorded for a fresh sample at temperatures below 70 K, arising from Ti^{3+} complexes (Fig. 1a). One year later, an additional EPR line appeared, while a narrow line attributed to conduction electrons vanished (Fig. 1b). The existence of the paramagnetic centers connected with trivalent titanium ions was due to the disordering processes, while the appearance of an additional line was attributable to the oxidation processes which could form new trivalent titanium complexes. The disappearance of the narrow EPR line suggests that the oxidation process (ageing effect) could influence the electrical properties of titanium carbide.

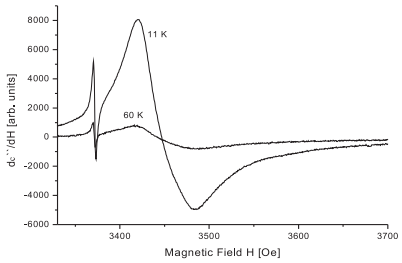

Figure 1a

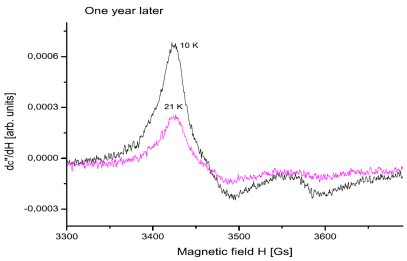

Figure 1b

*Corresponding author: ngouskos@phys.uoa.gr

Magnetic properties of TiC_x/C nanoparticles

N. Guskos[1,2*], V. Likodimos[1], S. Glenis[1],
G. Żołnierkiewicz[2], C. L. Lin[3], A. Biedunkiewicz[4]

[1] *Solid State Physics, Department of Physics, University of Athens, Panepistimiopolis, 15 784 Zografos, Athens, Greece*

[2] *Institute of Physics, Szczecin University of Technology, Al. Piastów 17, 70-310 Szczecin, Poland*

[3] *Deparment of Physics, Temple University, Philadelphia, PA 19122, USA*

[4] *Institute of Material Engineering, Szczecin University of Technology, Al. Piastów 17, 70-310 Szczecin, Poland*

Two samples of the nanocrystalline titanium carbide (TiC/C) dispersed in a carbon matrix have been prepared by the nonhydrolytic sol-gel process with different concentration. The magnetic properties have been studied by dc magnetization and electron paramagnetic resonance (EPR) measurements. Both samples exhibit a transition to the superconducting state below 3.5–3.7 K, identified by the low field magnetization and the superconducting-like hysteresis loops. The superposition of a ferromagnetic-like signal is further observed at both the paramagnetic and superconducting regimes, indicative of an additional magnetic phase. EPR measurements have shown the presence of trivalent titanium complexes. It is suggested that the presence of non-stoichiometry may lead to the formation of various titanium(III) complexes that influence both magnetic and transport properties.

*Corresponding author: ngouskos@phys.uoa.gr

ESR Study of the C_{60}·2ferrocene Crystalline Complex

N. Guskos[1,2*], A. G. Soldatov[3], G. Żołnierkiewicz[2], V. Likodimos[1], S. Glenis[1]

[1] *Solid State Physics, Department of Physics, University of Athens, Panepistimiopolis, 15 784 Zografos, Athens, Greece*

[2] *Institute of Physics, Szczecin University of Technology, Al. Piastów 17, 70-310 Szczecin, Poland*

[3] *Joint Institute of Solid State and Semiconductor Physics, NAS Belarus, Minsk, Belarus*

Single crystals of $C_{60}(Fe(C_5H_5)_2)_2$ grown from a benzene solution of a stoichiometric mixture of fullerene, C_{60}, and ferrocene, $Fe(C_5H_5)_2$, by slow evaporation of the solution at 300 K [1], are studied by electron spin resonance (ESR) in the temperature range of 90–290 K. At room temperature, the ESR spectrum of the complex consists of a very narrow resonance line at $g = 2.0030(1)$, with line width of $\Delta H = 1.2(2)$ Gs, superimposed on a broad resonance background of line width over 1 T due to ferromagnetic particles. Both the resonance field (g-factor) and the ESR intensity of the narrow resonance line display a marked temperature variation, attributable to the orientational ordering of the C_{60} molecules.

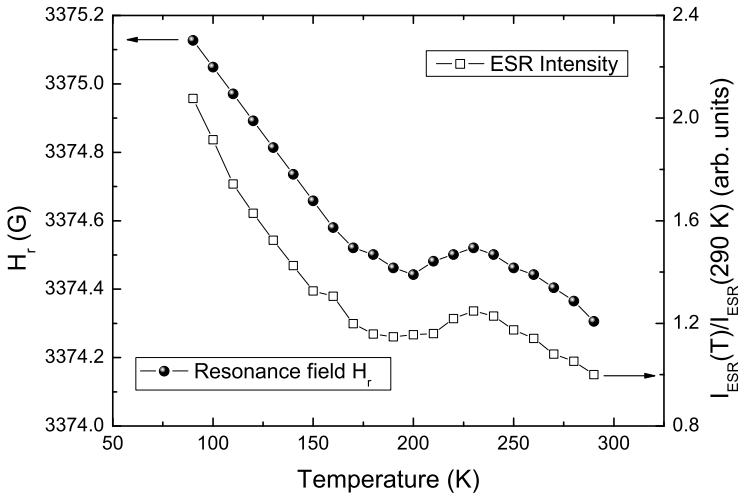

References

1. Soldatov A G, Goranov V A, Szpilevskyj E M, Tuna F, Safronova E G and Fedotova V V, Proc. 4th Int. Symp. "Fullerenes and fullerene-like structures", June 20-23, 2006, Minsk, pp. 285–291.

*Corresponding author: ngouskos@phys.uoa.gr

Adaptation of Nanoporous Alumina Dielectric and Copper Interconnections in Thin-film Temperature Microsensors

P. Hamolka*, V. Sokal, I. Vrublevsky, V. Parkoun

Department of Micro- and Nanoelectronics, Belarusian State University of Informatics and Radioelectronics, 6 Brovka str., 220013 Minsk, Republic of Belarus

Progress in electronic technologies and such advantages as small dimensions and weight and high thermosensitivity have resulted in rapid development of a new type of sensors: film temperature sensors. The main problem of manufacturing film temperature sensors is co-ordination of elastic properties of the thermosensitive material with the protective insulating coating. This problem can be solved by using nanoporous alumina as a material for protective insulating coating in film temperature sensors. An important feature of nanoporous alumina is its low elastic modulus of about 90–140 GPa, with the value of 340–380 GPa for non- porous alumina [1, 2]. This feature allows a reduction of mechanical stresses arising in film structures during the heating and cooling cycle. Thus, the long-term stability of electric characteristics of such film sensors is improved.

Electrochemical deposited copper has been used as a thermosensitive material in film sensors. Electrochemical deposition of Cu enables high purity of films and so high reproducibility of measurements. We have investigated the possibility of joint adaptation of the creation processes of nanoporous alumina and thin-film copper interconnections. Included in this work are the results of studying the effect of anodizing voltage and anodizing solution on the volume expansion of porous alumina formed in oxalic acid. A micromechanical profiler with computer signal processing was used for these studies. A SEM study of film structures and resistivity measurements were carried out as well.

The Cu lines in the studied film sensors were built in nanoporous alumina. The following processes were used: vacuum deposition of 1.8 micron thick aluminum on an insulating substrate, formation of nanoporous alumina by anodizing the aluminum, formation of trenches in the alumina using a local etching and, finally, vacuum deposition of a Ta barrier layer and filling the trenches by electrochemical deposition of Cu. The Ta layers have good adhesive properties on dielectric substrates and are often used as barrier layers for Cu interconnective metallization [3].

Cu temperature sensors were manufactured over an area of 2×5 mm with electric resistance of 50 Ohm and a protective dielectric based on nanoporous alumina. The film sensors' electric characteristics were studied in the temperature range from -60 to 160°C.

References

1. Sokol, I. Vrublevsky, V. Parkoun, K. Moskviechev, Anal. Bio. Chem. 375 (2003) 968.
2. Z. Xia, L. Riester, B.W. Shedon, W.A. Curtin, J. Liang, A. Yin, J.M. Xu, Rev.Adv.Mater.Sci. 6 (2004) 131.
3. M. Traving, I. Zienert, E. Zschesh, G. Schindler, W. Steinhoegl, M. Engelhardt, Appl. Surf. Sci. 252 (2005) 11.

*Corresponding author: zapad3@tut.by

Small-signal Spectra of Complex Capacitance Obtained at an Organic–Organic Heterojunction

G. Jarosz

Gdansk University of Technology,
G. Narutowicza 11/12, 80-952 Gdansk, Poland
zofia@mifgate.pg.gda.pl

This presentation will be focused on electric properties of organic heterojunctions formed from phthalocyanine and the perylene dye. The discussion will be based on experimental results of small-signal spectra of complex capacitance (or impedance/admittance) and direct current curves. The analysis will be enhanced by the effect of bias on small-signal capacitance spectra and additionally supported by the effect of illumination. A direct relation between low frequency response and direct current curves will be verified.

Systems with organic heterojunctions formed from phthalocyanine acting as the p-type material and the perylene dye playing the role of the n-type material have been the subject of 20 years' extensive research due to their possible application in photovoltaic cells [1–3]. The issue of particular importance for the progress in this field is description of the electric properties of such devices, since the theory successfully applied to inorganic systems is often unable to describe those with organic materials.

Small-signal impedance/capacitance spectroscopy appears to be a method particularly well-suited for this research since it can be applied directly to the organic device under polarization by external voltage. It has been well established in investigations of inorganic systems, but seems not to have been appreciated in investigations of organic devices. The most important question in the analysis of thin organic systems is the difference between dielectric relaxation of the lattice itself, occurring throughout the volume of organic materials, from dielectric effects resulting from interfacial processes or injected charge carriers. An analysis of both parts of small-signal impedance/capacitance spectra obtained under polarizing bias will indicate in which frequency region the barrier effect occurs and simultaneously provide other information on the electrical properties of organic devices.

Acknowledgements

This work was supported with means granted for science by the Polish Ministry of Education and Science for years 2006–2009, under Program No. 3T11B06530.

References

1. Tang C. W., Appl. Phys. Lett. 48 (1986) 183.
2. Wöhrle D., Kreienhoop L., Schurpfeil G., Elbe J., Tennigkeit B., Hiller S., Schlettwein D., J. Mater. Chem. 5 (1995) 1819–29.
3. R. Signerski, J. Non-Cryst. Solids 352 (2006) 4319.

Interdigitated Back-contact Solar Cells with Optimized Back-surface Passivation

I. Jóźwik[1,2], P. Papet[1], A. Kaminski[1*], E. Fourmond[1], F. Calmon[1], M. Lemiti[1]

[1] *Institut des Nanotechnologies de Lyon, INSA, Batiment Blaise Pascal, 7 avenue Jean Capelle, 69621 Villeurbanne Cedex, France*

[2] *Institute of Physics, Lublin University of Technology, Nadbystrzycka 38, 20-618 Lublin, Poland*

The presented results concern a study of interdigitated back-contact solar cells' (IBC SC) emitter passivation by way of comparison of full- and point-contact solar cells and two types of passivation layers (SiN and SiO_2), as well as various values of the emitter sheet's resistance. In comparison with full contacts cells, fabrication of contacts in the form of points does not influence significantly the values of parameters of the I–V characteristics of highly doped emitters; however, an improvement of Rsh is observed for a few point contact solar cells. A similar effect has been observed for sheet emitters of greater resistance, as well as strong degradation of the dark current after the last annealing of the cell. We have attributed this effect to short-circuiting of an excessively thin emitter.

*Corresponding author: anne.kaminski@insa-lyon.fr

Electrophysical Properties of Nanoscale $NaBiTe_2$ Thin Films

S. S. Avotin[1], V. I. Bilozertseva[1], D. A. Gaman[1], N. L. Dyakonenko[1], A. A. Mamalui[1], L. G. Petrenko[1], H. M. Khlyap[2]

[1] *National Technical University "Kharkov Polytechnical Institute", Kharkov, Ukraine*

[2] *University of Technology, Kaiserslautern, Germany*

The structure, phase composition and electro-physical properties of nanoscale $NaBiTei_2$ thin films obtained by resistive evaporation from a Knudsen cell and condensation on glass substrates are investigated. XRD analysis and current-voltage characteristics measured at room temperature are shown. Mechanisms explaining the experimental time and temperature dependencies of electrical conductivity are discussed. Results of numerical analysis of experimental data are included.

Thin Film Parameter Modeling by Spectra Envelope Functions of Light Reflection and Transmission

P. S. Kosobutskyy[1*], O. P. Kushnir[2]

[1] *The Institute of Applied Mathematic and Fundamental Sciences, National University "Lvivs'ka Politekhnika", PB 4544, Lviv-53, 79053, Ukraine*

[2] *Lviv State Agrarian University, V. Velikogo 1, Dubljany, Lviv region, 80381, Ukraine*

The problem of reflection and transmission of an electromagnetic wave in a plane parallel layer is considered to be classical and well-studied. Nevertheless, a number of new regularities in the scope of the problem have been found recently. This paper explores new applications of Fabry-Perot spectroscopy in nondestructive testing of monolayer structures' parameters. Let us express light reflectance, R, and transmittance, T, through their values in extremes $(R,T)_{\substack{\max\\\min}}$ as:

$$R=\frac{R_{\substack{\max\\\min}}\mp\left(\frac{a}{b}\right)^2\left(\frac{\sin}{\cos}\right)^2\frac{\phi_{12}-\Delta}{2}}{1\mp\left(\frac{a}{b}\right)^2\left(\frac{\sin}{\cos}\right)^2\frac{\phi_{12}+\Delta}{2}},\qquad T=\frac{T_{\substack{\max\\\min}}}{1\pm\left(\frac{b}{a}\right)^2\left(\frac{\cos}{\sin}\right)^2\frac{\phi_{12}+\Delta}{2}},$$

where functions

$$R_{\substack{\max\\\min}}=\left(\frac{\sigma_{12}\pm\Theta}{1\pm\sigma_{12}\Theta}\right)^2$$

are the envelope functions of extremes for reflection spectra, while

$$T_{\substack{\max\\\min}}=\frac{n_3}{n_1}\frac{T_{12}T_{23}}{(1\mp\sigma_{12}\Theta)^2}\frac{\Theta}{\sigma_{23}}$$

are the envelope functions of extremes for transmission spectra,

$$T_{12,23}=\tilde{t}_{12,23}\tilde{t}^*_{12,23}\,,\quad\left(\frac{a}{b}\right)^2=\frac{4\sigma_{12}\Theta}{(1\pm\sigma_{12}\Theta)^2}\,,\quad\Theta=\sigma_{23}\exp\left(-\mathrm{Im}\tilde{\delta}\right),\quad\Delta=\phi_{23}-\mathrm{Re}\tilde{\delta}\,,\quad\tilde{\delta}=\frac{4\pi d}{\lambda}\left(n_2-i\chi_2\right),$$

$\tilde{r}_{12,23}=\sigma_{12,23}\exp(i\phi_{12,23})$ are the Fresnel amplitude coefficients corresponding to 12 and 23 interfaces. Here, transparent and optically uniform semi-infinite media with refraction indices $n_{1,3}$are separated by a plane parallel layer with thickness d and complex refraction index $\tilde{n}_2=n_2-i\chi_2$.The difference between envelope functions equals

$$\Delta R=R_{\max}-R_{\min}=2\Theta\frac{1-\sigma_{12}^2}{1-\sigma_{12}^2\Theta^2}\cdot 2\sigma_{12}\frac{1-\Theta_{23}^2}{1-\sigma_{12}^2\Theta^2}\,.$$

For a single-monolayer structure, parameters σ_{12},σ_{23} and Θ can be rewritten by coefficients $(R,T)_{\max,\min}$ as follows

$$\sigma_{12}=\frac{1+\sqrt{R_{\max}R_{\min}}}{\sqrt{R_{\max}}+\sqrt{R_{\min}}}\pm\sqrt{\left[\frac{1+\sqrt{R_{\max}R_{\min}}}{\sqrt{R_{\max}}+\sqrt{R_{\min}}}\right]^2-1}\,,\quad\Theta=\frac{\sqrt{R_{\max}}-\sigma_{12}}{1-\sqrt{R_{\max}}\sigma_{12}}\,,\ \sigma_{12}\Theta=\frac{\sqrt{T_{\max}}-\sqrt{T_{\min}}}{\sqrt{T_{\max}}+\sqrt{T_{\min}}}\,.$$

*Corresponding author: petkosob@polynet.lviv.ua

The 2π-periodicity of Fabry-Perot interference spectra in coordinate plane $R, \mathrm{Re}\tilde{\delta}$ allows us to express the area restricted by the contour of a maximum less the area restricted by the envelope function of the adjacent minima with the structural parameters as

$$S = 2\int_{\pi}^{3\pi} [R(\theta) - R_{\min}] d\theta \,, \quad \theta = \frac{\mathrm{Re}\tilde{\delta}}{2} \,.$$

Superconducting Properties of NbN–SiO_2 Disordered System Obtained by Ammonolysis of Nb_2O_5–SiO_2 Sol-Gel Derived Coatings

B. Kościelska[1], W. Jurga[2]

[1] *Faculty of Applied Physics and Mathematics, Gdansk University of Technology, Narutowicza 11/12, 80-952 Gdansk, Poland*

[2] *Institute of Molecular Physics, Polish Academy of Science, Smoluchowskiego 17, 60-179 Poznan, Poland*

Studies of superconducting properties of NbN–SiO_2 films are reported. In order to obtain such films, sol-gel derived Nb_2O_5–SiO_2 coatings were nitrided at 1200°C. As suggested by X-ray diffraction (XRD) and X-ray photoelectron spectroscopy (XPS), the nitridation process leads to the formation of disordered structures, with NbN metallic grains dispersed in the insulating SiO_2 matrix. The electrical resistivity was measured with the conventional four-terminal method in the temperature range from 5 to 280 K. All the samples exhibited negative temperature coefficients of resistivity. The samples' superconducting properties were examined with magnetically modulated microwave absorption (MMMA). The superconducting transition depended on the NbN/SiO_2 molar ratio as well as on the film's thickness.

Structural Analysis of NbN–SiO_2 Films Obtained by Ammonolysis of Nb_2O_5–SiO_2 Sol-Gel Derived Coatings

B. Kościelska[1], A. Winiarski[2]

[1] *Faculty of Applied Physics and Mathematics, Gdansk University of Technology, Narutowicza 11/12, 80-952 Gdansk, Poland*

[2] *Faculty of Mathematics, Physics and Chemistry, Silesian University, Bankowa 14, 40-007 Katowice, Poland*

Sol-gel derived $x\mathrm{Nb_2O_5}$–$(100-x)\mathrm{SiO_2}$ films (where x = 100, 80, 60, 50, 40, 20, 0 mol%) were nitrided at various temperatures: 800, 900, 1000, 1100 and 1200°C. As a result of ammonolysis, structural transformations occurred in the films. These transformations were studied using X-ray diffraction (XRD), atomic force microscopy (AFM) and X-ray photoelectron spectroscopy (XPS). The XRD results have shown that temperatures below 1100°C are too low to obtain a pure NbN phase in the samples. The AFM observations indicate that the formation of an NbN phase and the size of NbN grains are related to the silica content in the layer. NbN grains become more regular and larger with increasing niobium content. The maximum grain size, about 100 nm, was observed for x = 100. Preparation of Nb_2O_5–SiO_2 sol-gel derived layers and the subsequent nitridation is a promising method of controlling the amount of crystalline NbN in amorphous matrices. It follows from our XPS results that a small amount of Nb_2O_5 persists in the films after nitridation at 1200°C and nitrogen reacts not only with Nb_2O_5 but also with SiO_2.

Thermodynamic Stability of Degenerate Crystals (Aperiodic Solids) of Hard Dimers in Three Dimensions

M. Kowalik*, K. W. Wojciechowski†

Institute of Molecular Physics, Polish Academy of Sciences, Smoluchowskiego 17, 60-179 Poznan, Poland

Phase transitions in molecular system play an important role both in fundamental researches and practical applications. Computer simulations allow one for precise locations of the transitions and provide effective methods for investigating their underlying mechanisms.

To locate a phase transition between any two phases it is sufficient to know the exact values of their free energies. For over twenty year, very simple [1, 2], but precise [3] method of determining the free energy of model solid has been used. In simulations, however, only finite-size systems are dealt with for obvious reasons. Thus, in order to estimate the free energy in the thermodynamical limit *precisely*, its asymptotic dependence on the number of particles N in the sample has to be known. Hoover [4] pointed out that for *harmonic* systems the leading term has the form $-\ln N/N$. Recently, it was shown that also in an extremely *anharmonic* system – hard spheres – N-dependence has the same character [5]. The question arises, whether that result, obtained for an 'atomic' system, can be extended to molecular systems. To answer the question, we numerically investigated the free energy and its N-dependence of one of the simplest molecular models – an extremely *anharmonic* system of hard dimers in three dimensions.

The choice of the system requires a comment. The hard dimer, which consist of two adjacent hard spheres (each of the diameter σ), separated by the distance $D = \sigma$, constitutes a crude model of a diatomic molecule and the simplest non-convex body as well. It is also worth adding that it was used to model molecular solids [6] and as a starting point in studies of polymers [7, 8, 9]. One of the most unusual features of the hard dimer system and one of main reasons of our interest in the system is, however, its solid phase. Namely, in the whole range of the densities where the solid phase is *thermodynamically* stable, it is *aperiodic*, both in two [10, 11, 12, 13] and three dimensions [14]. In that phase, which has been coined a *degenerate* crystal [12], while 'atoms' of the dimers form (at close packing) the fcc lattice, the molecular centres of mass and orientations are *not* periodic.

In the present work we determine accurately the free energy of the degenerate crystalline phase of the dimers and compare it to values obtained for some (metastable) crystalline structures of the dimers.

References

1. Frenkel D and Ladd A J C 1984 *J. Chem. Phys.* **81** 3188
2. Frenkel D and Smit B 1996 *Understanding molecular simulations*, Academic Press
3. Tretiakov K V and Wojciechowski K W 1999 *Phys. Rev. E* **60** 7626
4. Hoover W G 1968 *J. Chem. Phys.* **49** 1981
5. Polson J M, Trizac E, Pronk S, and Frenkel D 2000 *J. Chem. Phys.* **112** 5339
6. Singh V K and Khanna K N 2004 *Phys. Stat. Solidi B* **241** 1832
7. Vega C, McBride C, and MacDowell L G 2001 *J. Chem. Phys.* **115** 4203
8. Vega C, McBride C, and MacDowell L G 2001 *Phys. Rev. E* **64** 011703
9. Largo J, Maeso M J, Solana J R, Vega C, and MacDowell 2003 *J. Chem. Phys.* **119** 9633

*kowalik@ifmpan.poznan.pl
†kww@ifmpan.poznan.pl

10. Wojciechowski K W, Frenkel D, and Brańka A C 1991 *Phys. Rev. Lett.* **66** 3668
11. Wojciechowski K W 1991 *Mod. Phys. Lett.* **5** 1843
12. Wojciechowski K W 1992 *Phys. Rev. B* **46** 26
13. Wojciechowski K W, Brańka A C, and Frenkel D 1993 *Physica A* **196** 519
14. Vega C, MacDowell L G, and McBride C 2004 *J. Mol. Liquids* **113** 37

Thermal Conductivity of Proton Glassy Crystals: Clathrate Hydrates

A. I. Krivchikov, O. O. Romantsova, O. A. Korolyuk

B. Verkin Institute for Low Temperature Physics and Engineering of the National Academy of Sciences of Ukraine, Kharkov, Ukraine

Clathrate hydrates are open polymorphous crystal structures related to ordinary ice. They are formed by introducing one kind of molecules ("guests") into the cavities of a crystal frame consisting of another kind of molecules ("hosts"). The "guest" particles can be atoms of inert gases or small molecules (e.g. methane, tetrahydrofuran). Under natural conditions clathrate hydrates were discovered as clathrate hydrates of methane forming vast deposits at the oceans' bottom and in the Earth's interior or as hydrocarbon clathrates plugging the insides of gas and oil pipelines in the Arctic latitudes.

Most of the thermodynamic and dynamic properties of gas clathrate hydrates are similar to the properties of ice Ih crystal. However, the very low thermal conductivity of clathrate hydrates decreases with temperature and the $\kappa(T)$ curve has a plateau in the temperature interval in which this occurs in glasses. The understanding of the causes responsible for the glass-like behavior in gas hydrates will be helpful in finding a microscopic mechanism of thermal transport in disordered solids.

The thermal conductivity of the methane [1], tetrahydrofuran (THF) [2] and xenon [3] hydrates was measured using the steady-state technique in a wide temperature interval (2–170 K). The thermal conductivity of these hydrates was typically observed for disordered substances. Three different qualitative models were used to explain the thermal conductivity's glass-like behavior: large unit cells leading to a limited phonon mean free path. Proton disorder of the host lattice or a coupling between the guest and host vibrations in the low frequency region, in turn leading to effective phonon scattering.

The thermal conductivity of the xenon hydrate in the interval from 50 to 100 K shows an anomaly, where the thermal conductivity increases by almost 50% with decreasing temperature. A similar behavior of $\kappa(T)$ was found in the THF hydrate prepared through slow cooling or with a KOH impurity. These anomalies of the thermal conductivity are explicable qualitatively on the basis of two approaches: resonant scattering or the proton-order processes in the clathrate hydrates' lattice.

The results are discussed in the context of theoretical calculations and phenomenological models of phonon scattering by local modes.

References

1. Krivchikov A I, Gorodilov B Ya, Korolyuk O A, Manzhelii V G, Conrad H, Press W 2005 *JLTP* **139** (693)
2. Krivchikov A I, Gorodilov B Ya, Korolyuk O A, Manzhelii V G, Romantsova O O 2005 *Phys. Chem. Chem. Phys.* **7** (728)
3. Krivchikov A I, Gorodilov B Ya, Korolyuk O A, Manzhelii V G, Romantsova O O, Conrad H, Press W, Tse J S and Klug D D 2006 *Phys. Rev. B* **73** 064203

Patterned Test Samples for Scanning Near-Field Optical Microscopes Prepared by Electron Beam Lithography

R. Krutohvostov[1], A. Kuzmin[1], R. Kalendarev[1], V. Zauls[1], I. Shorubalko[1,2]

[1] *Institute of Solid State Physics, University of Latvia, 8 Kengaraga st., LV-1063 Riga, Latvia*

[2] *Solid State Physics Laboratory, ETH Zürich, Schaffmattstrasse 16, CH-8093 Zürich, Switzerland*

We propose a new approach to fabrication of submicron scale test structures for calibration of Scanning Near-Field Optical Microscopes (SNOM) operating in the luminescence or Raman modes. For this purpose, samples of $ZnWO_4$ thin films on a Si/SiO_2 substrate were prepared by magnetron sputtering and coated with Al through a PMMA mask patterned by the electron lithography (EBL) technique, achieving submicron patterns with high accuracy. Al structures were used to screen areas of the $ZnWO_4$ layer, thus enabling mapping the samples in terms of its luminescence with high contrast.

$ZnWO_4$ was chosen because of its stability and identifiability by its luminescence and Raman spectra. The optical properties of $ZnWO_4$ were studied using the scanning confocal Raman microscopy and photoluminescence spectroscopy techniques.

Acknowledgements

This research has been supported by the European Social Fund.

Composition of Ge^+ and Si^+ Implanted SiO_2/Si Layers: the Role of Oxides in Nanocluster Formation

H. Krzyżanowska[1], H. Bubert[2], J. Żuk[1]

[1] *Institute of Physics, Maria Curie-Skłodowska University, Pl. M. Curie-Skłodowskiej 1, 20-031 Lublin, Poland*

[2] *Institute for Analytical Sciences, Bunsen-Kirchhoff Str. 11, 44 139 Dortmund, Germany*

Group IV semiconductor nanoclusters embedded in SiO_2 matrices are artificially engineered materials which have recently received attention because of their potential for developing integrated optoelectronic devices directly on silicon substrates. SiO_2 is a very important optical material fully compatible with the existing Si technological base.

Samples were prepared by means of Ge^+ and Si^+ ion implantation into thermally-grown, 500 nm thick SiO_2 layers on an Si substrate. The implanted structures were subsequently annealed in the temperature range from 500 to 1200°C in dry nitrogen.

X-ray photoelectron spectroscopy (XPS) was used to examine the atomic content of the implanted SiO_2/Si layer. Atomic concentration/depth profiles could be obtained with a combination of the XPS technique and the noble gas-induced sputtering process. In particular, XPS analysis allowed us to identify elemental Ge and Si, as well as GeO_2 precipitations in the SiO_2 matrices.

With respect to the germanium-implanted samples, the presence of a subsurface GeO_x zone (about 100 nm thick) predicted in kinetic 3-dimensional lattice simulations has been confirmed. The composition of the modified SiO_2 layer depended strongly on the annealing temperature. The possibility of Ge nanocrystal formation appeared at high annealing temperatures (above 1000°C), but the intermediate step of Ge oxide formation seems to have been necessary for the creation of Ge nanoclusters.

In the case of Si^+ implanted samples, non-stoichiometric silicon oxide lines have been noticed in the XPS spectra of the SiO_2 layer. No evidence of a line connected to Si–Si bonding has been observed. This suggests that Si–O bonds are more energetically preferential than the Si–Si ones. Thus, the formation of silicon nanocrystals in a SiO_2 matrix remains a challenge.

Hydrogen and Oxygen Concentration Analysis of Porous Silicon

H. Krzyżanowska[1], A. P. Kobzev[2], J. Żuk[1], M. Kulik[1]

[1] *Institute of Physics, Maria Curie-Skłodowska University, Pl. M. Curie-Skłodowskiej 1, 20-031 Lublin, Poland*

[2] *Joint Institute for Nuclear Research, Frank Laboratory of Neutron Physics, 141980 Dubna, Moscow Region, Russia*

Porous silicon (PSi) has attracted growing interest for the last two decades because of its important potential applications. The knowledge of atomic composition of porous Si layers is essential for constructing such devices as gas sensors and biomedical implants. Concentration depth profiles of atoms in PSi layers depend both on experimental conditions of porous samples' preparation (the type and orientation of Si wafers, the etching solution, current density, anodization time) and on the time of exposition to air after their electrochemical processing.

This work is a systematic study of low- and medium-porosity PSi samples aged in air for over one year. This range of porosities (25–66%) has not been studied before by reason of technological difficulty of preparing this kind of samples. PSi supported layers were obtained on p^+-type, (111)-oriented Si substrates.

In particular, hydrogen and oxygen concentration depth profiles are the most interesting. Hydrogen is incorporated into the pores' walls during electrochemical etching. This phenomenon plays an essential role in PSi formation, especially for highly-doped p^+-type Si substrates. Oxygen is bonded on enormous inner surfaces of PSi by the natural oxidation process when samples are exposed to air.

The contents of hydrogen in near-surface layers was determined by the elastic recoil detection (ERD) method with a 2.3 MeV ^{4}He ion beam. Very precise oxygen depth distribution was obtained using nuclear reaction $^{16}O(\alpha,\alpha)^{16}O$ with the narrow, 10 keV-wide resonance line for a 3.045 MeV ^{4}He ion. Changing the energy of the ^{4}He ion from 3.045 to 3.200 MeV (with a step of 10 keV) enables scanning oxygen concentration across the depth of about 100 nm. At the energy of 3.045 MeV, resonance occurs on the sample's surface and, with increasing energy of α particles, we can observe a resonance line in deeper layers. In this way it is possible to determine the amount of oxygen in a thin layer with high precision. The maximum of H content in PSi has been observed at the depth of 200–600 nm, while the highest oxygen concentration is typical for 200 nm-thick subsurface layers. The highest obtained ratio of H/Si atomic concentrations has reached the value of 2 for PSi samples of 66% porosity, compared with $N_H/N_{Si} = 0.27$ in the case of the 25% PSi.

Coherent Fourier Analysis in Diagnostics of Amorphous and Nanocrystalline Materials

Yu. A. Kunitskiy, M. Yu. Barabash, Ya. A. Nechitaylo, V. Dementjev

Technical Centre NAS of Ukraine, Pokrovskaya 13, 04070 Kiev, Ukraine

The coherent Fourier technique is quite effective in analysis of electronic-microscopic and optical pictures. Optical Fourier analysis has been demonstrated to be a synthesis of diffraction and microscopic techniques. According to this approach, material structure is identified with the first transfer function of a data processing system with the help of which the sample's structural parameters are expressed as a two-dimensional distribution, $f(x, y)$, of nigrescence on photographic film or plate. The transfer function is adjustable through varying enlargement with a transparent electronic microscope (TEM) in a light or dark field, through scanning or optical microscopes. Optical Fourier spectroscopy is maximally efficient when the information on the sample's structure to be processed is contained in the photographic object, conditions of its obtaining being determined by individual research objectives. It would be appropriate to study the structure of amorphous and micro-crystal films on the basis of analysis of optical Fourier spectrums of electronic-microscopic patterns in order to:

1. study the geometric parameters of discretization of Fraunhofer's diffraction patterns (FDP) for the purpose of determining statistical structural parameters of samples and establishing general structural parameters typical for non-crystal materials, material characteristics of particular substances, as well as a range of structural parameter fluctuations depending on techniques and modes of obtaining and processing the materials and substances, their chemical composition and external conditions (temperature, pressure, radiation, etc.),

2. develop accurate analytical models and patterns for planar environments to describe the FDP structure quantitatively and develop an analytical procedure for model Fourier spectrum excitations corresponding to real structural parameters and

3. establish correlations between structural parameters at various levels and the physico-chemical properties of materials to enable forecasting such properties and synthesis of materials and substances of desirable properties.

Self-organizing Processes in Ion-plasma Condensed Nanomaterials

A. P. Shpak[1], O. V. Sobol[2], Yu. A. Kunitskiy[3], M. Yu. Barabash[3], Ya. A. Nechitaylo[2], V. Dementjev[3]

[1] *G. V. Kurdyumov Institute for Metal Physics, National Academy of Science of Ukraine, Academican Vernadsky 36, Kyiv-142, 03680 Ukraine*

[2] *Technical University "Kharkov Polytechnical Institute", Frunze 21, Kharkov, 61002 Ukraine*

[3] *Technical Centre NAS of Ukraine, Pokrovskaya 13, Kiev, 04070 Ukraine*

Super-rapid quenching characteristic for condensation from high-energy ion-plasma fluxes is an effective way of structure milling and obtaining materials with cluster- and nano-structures. This is promoted by the development of high strains peculiar to the formation process of condensed materials under ion bombardment.

All peculiarities of the surface state are revealed at sizes characteristic for the nano-structural range from 1 to 50 nm, as the meaning of volume is practically lost there (i.e. the fractal dimensionality of such structures becomes less than 3). This causes the appearance of non-linear processes defining the bifurcation nature of size effects that follows by changing the properties of condensed materials. At the foundations of the formation process of such structures lies the phenomenon of self-organization in crystals with non-equilibrium imperfections (radiation defects).

Ordering processes under radiation of particles bombarding the growing coating may be divided into two levels: (i) subsurface (including the surface), where thermally and radiation stimulated ordering occurs at the energy of incident particles of less than 1 keV, and (ii) volume ordering, involving interaction ofhighly energetic implanted atoms or ions. Considering the efficiency of influence on the ordering processes, the former is more favorable due to the presence of weakened bonds and an amount of gaseous impurity atoms in the subsurface layers, stimulating the formation of small, relatively low-bonded structural forms.

The coatings obtained through condensation from ion-plasma fluxes (magnetron and triode schemes of sputtering) with energy of the film forming particles characteristic for the first level, have shown a strong tendency towards self-organization of the structure under the action of locally concentrated energy. In this case, the two leading mechanisms are high energetic crystallite boundaries (due to a large amount of broken bonds) and strain energy, especially in coatings with high adhesive bonding with the substrate. The high level of free energy in condensate grain boundaries (including electronic non-uniformity due to impurity atoms being forced out of the volume) results in the emergence of a spatially ordered cell-shaped structure (nearly regular six-angular shape) under volume strains. In the case of compressive strains in the self-organizing coating and relatively weak adhesion to the substrate, this factor results in material volume squeeze out and formation of a 3D ordered structure.

Theoretical models describing such processes are proposed, based on consideration of several stages of transformation in non-equilibrium systems and in general conformity with the current ideas of synergetic.

Diagnostics of Nanomaterials

Yu. A. Kunitskiy, S. Yu. Smyk, M. Yu. Barabash, Ya. A. Nechitaylo, V. Dementjev

Technical Centre NAS of Ukraine, Pokrovskaya 13, 04070 Kiev, Ukraine

The theoretical fundamentals of fractal structure diagnostics are reviewed. Possible applications of this diagnostic method in investigations of various nanosystems, including composite multi-level fractal aggregates, are considered. Current knowledge of fractal aggregation phenomena and fractal development in various nanosystems is presented. Possible investigation methods for nanostructural materials used in high technologies are analyzed, with a focus on the small-angle scattering technique. Physical properties of the following fractal substances are considered: nanopowders, sol-gel nanocomposites, silica gel, aerogel, polymeric solutions, gels and composites, colloids, microporous materials, inorganic and organic-inorganic nanocomposites.

The use of coherent Fourier analysis in processing electron microscopy images of amorphous and nanocrystalline structures can be successful enough and yield quantitative estimates of their structural heterogeneity as well as spatial distribution of nanoparticles and nanoparticles' size, so that the anisotropy of their shape can be investigated in dependence on their composition, forming conditions and heat treatment conditions. Information concerning an object's statistical parameters can obtained using the synthesized Fraunhofer diffraction patterns, plots of isofrequency curves and model structures. Improved, coherent Fourier spectroscopy is informative enough for studying the mechanisms and kinetics of relaxation as well as crystallization of amorphous alloys.

Thermal synthesis of CdTe films from elementary components

V. Kusnezh*, G. Ilchuk, V. Ukrainets, R. Petrus', A. Danylov

Department of Physics, National University "Lvivs'ka Politekhnika", 12 S. Bandera Street, Lviv, 79013, Ukraine

The possibilities of synthesizing cadmium telluride (CdTe) semiconductor films by annealing thermally deposited films of metallic cadmium (Cd) with thickness d≈1 μm on glass substrates ($75 \times 2 \times 2$ mm) and in tellurium (Te) vapor have been studied. The experiment in annealing- tellurization (tellurium transfer at a plate with cadmium and the expected synthesis of CdTe) was preceded by theoretical analysis of partial pressures of Te vapor above Te_{sol}, cadmium above Cd_{sol}, Te above $CdTe_{sol}$ and Cd above $CdTe_{sol}$ for the case of congruent sublimation and by the proper choice of thermal conditions of annealing. The annealing-tellurization process ($\tau = 6$ h) was conducted in a vacuum, sealed quartz ampoule in a two-zone furnace, in which the plate with Cd (zone of deposition, $t_2 = 255°$C) and the Te source ($t_1 = 307°$C) were positioned. The resulting film changed its color from silvery, characteristic for a cadmium, to dark brown and had slightly uneven distribution of optical density.

With the use of the SEM-102-02 scanning electronic microscope (Selmi, Ukraine, $U = 20$ kV, magnification 2000 times) the surface morphology of the original Cd films and films in vapor of tellurium was explored in the secondary electron beam and their qualitative and quantitative composition was determined (within the accuracy of up to 5 wt%) from the spectra of characteristic X-ray radiation ($1 \times 1 \times 1$ μm excitation volume). The image analysis of the original Cd film showed it to consist of disordered elongated Cd granules of average size 5×20 μm. The analysis of characteristic spectra of the original sample Cd-glass showed no impurity elements in the cadmium layer within the device's precision range.

An attempt to study the surface of the Cd tellurization film by means of secondary electrons was unsuccessful, possibly due to its electrization and substantial growth of resistance. The characteristic spectrum analysis of the tellurization film confirmed the change in its chemical composition in comparison with the original Cd film. Apart from Te (23.51 wt%) and cadmium (12.94 wt%), there were Si (44.07 wt%) and Na (19.49 wt%) lines in the spectrum, the basic elements of a glass substrate. This is evidence of a considerable reduction in film thickness, due to the partial evaporation of Cd in the process of tellurization and penetration of the electron beam into the glass. In order to identify the CdTe compound in the tellurization film, the spectral distribution of its optical transmission was investigated. In the spectrum of transmission, the region of fundamental absorption was observed with an edge of 1.44 eV, coinciding with the band gap width data for monocrystalline CdTe.

Thus, physical and chemical grounds for the new technology of CdTe film fabrication have been established (the tellurization method).

*Corresponding author: w_kusnierz@polynet.lviv.ua

Balance of Thermodynamic Restrictions as Basis for Production of Multicomponent Nanoheterosystems

V. V. Kuznetsov*, E. A. Kognovitskaya

St. Petersburg Electrotechnical University "LETI",
Prof. Popov str., 5, St. Petersburg, 197376, Russia

Obtaining nanoheterostructures of multicomponent solid solutions from the liquid phase is based on preliminary analysis of the technological possibilities. One of the primary factors defining these possibilities are thermodynamical restrictions. First of all, these restrictions are connected with the existence of a large miscibility gap in multicomponent antimonides, determined by the internal strains at growing temperatures. Another very important factor is the so-called fusibility restriction. The essence of this restriction is that, at any temperature above the melting point of the most fusible component of the solid solution, there is such a solid phase composition range for which the equilibrium liquid phase cannot be found.

It is also necessary to take into account the substrate generated external elastic strains induced at the heterointerface in the case of lattice mismatch (Δa), well known [1] to play a very important stabilizing role in the nanoheterosystem. Therefore, the mutual effect of the fusibility restriction and thermodynamic instability decreases the composition areas of solid solutions of multicomponent A^3B^5 antimonides that can be fabricated by LPE.

Notably, the elastic strains also influence the fusibility restriction area. Here, the role of elastic strains depends on the sing of the heteropair lattice mismatch (f). An analysis of the calculation results of liquid isotherms (carried out for the $Ga_xIn_{1-x}P_yAs_zSb_{1-y-z}$/InAs system at $T = 773$ K) has shown that the area of the fusibility restriction decreases when $f < 0$ and increases when $f > 0$.

At the same time, elastic strains can be taken into account through the stabilization factor, q. The elastic contribution to the total energy balance shifts the phase equilibrium and, hence, modifies the composition of the solid solution. Calculations of the stabilization factor have been carried out for $Al_xGa_yIn_{1-x-y}P_zAs_{1-z}$ solid solutions lattice-matched to GaAs and for $Ga_xIn_{1-x}P_yAs_zSb_{1-y-z}$ matched to GaSb and InAs. An analysis of the obtained results has shown that the stabilization factor is negative in the area of thermodynamic instability. This is due to the variation in the curvature of the composition dependence of the solid solution's free energy leading to a change of the Δa sign.

In conclusion, LPE growth parameters for multicomponent A^3B^5 nanoheterostructures are defined by mutual dependencies of thermodynamic restrictions.

References

1. Kuznetsov V. V., Moskvin P. P., Sorokin V. S., Nonequilibrium Effects in Liquid-Phase Heteroepitaxy of Semiconductor Solid Solutions, Moscow: Metallurgiya, 1991

*Corresponding author: phone: +7(812)346-17-23, fax: +7(812) 346-27-58, e-mail: vvkuznetsov@inbox.ru

Luminescent Properties of Sm-Doped Polycrystalline ZrO_2

S. Lange[1]*, I. Sildos[1], M. Hartmanova[2], J. Aarik[1], V. Kiisk[1]

[1] *Institute of Physics, University of Tartu, Riia 142, 51014 Tartu, Estonia*

[2] *Institute of Physics, Slovak Academy of Sciences, Dubravska cesta 9, 845 11 Bratislava 45, Slovak Republic*

Their wide band-gap (≈ 5–6 eV), high refractive index, good transparency up to vacuum ultraviolet, good mechanical properties and low phonon energies make zirconia and hafnia increasingly popular hosts for doping with rare earth (RE) ions. Although successful RE-activation of matrices has been reported by several authors [1, 2, 3], the nature of RE optical centers and the host sensitization mechanism is yet to be fully understood. A possible reason might be that preparation of high-quality crystalline samples is complicated by the size mismatch between RE ions and those of the host metal. A sol-gel method is usually employed. The charge mismatch is also responsible for the sophisticated nature of RE optical centers due to charge compensation effects.

The aim of the present work was to perform laser spectroscopic investigations (within the 5–300 K range) of Sm-activated ZrO_2 material prepared by directional solidification of melt [4]. It was focused on elucidating the host-quest energy transfer process at various photo-excitation energies and identifying the possible contribution of various lattice defects. An annealing treatment was performed to control the presence of defects, the nanocrystallite size, the stabilization of the monoclinic and tetragonal phases (monitored via micro-Raman spectra) and the luminescence efficiency.

A tunable OPO laser was used at various emission wavelengths (210, 230, 320 and 405 nm) in order to achieve both direct and indirect photo-excitation of Sm ions. The photoluminescence (PL) emission characteristic for Sm ions in trivalent charge state was found. The highest relative emission efficiency was recorded while exciting the sample with a wavelength of 230 nm. The decay curves of Sm^{3+} emission were typically long-lasting (several ms) and non-exponential in nature, whereas under direct excitation of ions almost single-exponential decay of the PL emission was observed ($\tau \approx 1$ ms). In order to clarify further the ions' excitation path, time-resolved spectroscopy was used to record the PL spectra in various stages of decay. No evidence of intrinsic host lattice emission usually found in high-quality crystalline and nano-crystalline zirconia was found under band-to-band excitation [5]. This was most likely due to high dopant concentration (4 mol%) which introduced substantial structural changes (defects) in the host and thus prevented the formation of self-trapped excitons in the material.

The obtained results were compared with samples prepared by atomic layer deposition (ALD) followed by ion implantation [3]. Due to the relatively good emission properties, the materials' potential for applications in luminescence, scintillating and gas-sensing will be evaluated.

Acknowledgements

The work was partially supported by the Estonian Science Foundation (Grant Nos 6999 and 6660).

References

1. E. De la Rosa-Cruz, L. A. Diaz-Torres, P. Salas, R. A. Rodriguez, and G.A. Kumar 2003 *J. Appl. Phys.* **94** 3509–3515
2. R. Reisfeld, M. Zelner, and A. Patra 2000 *J. Alloys Comp.* **300** 147–151

*Corresponding author: sven.lange@mail.ee

3. V. Kiisk, I. Sildos, S. Lange, V. Reedo, T. Tätte, M. Kirm and J. Aarik 2005 *Appl. Surface Science* **247** 412–417
4. M. Hartmanova, J. Schnaider, V. Navratil, F. Kundracik, H. Schulz, E. E. Lomonova 2000 *Solid state Ionics* **136–137** 107
5. M. Kirm, J. Aarik, M. Jürgens, I. Sildos 2005 *Nuclear Instruments and Methods in Physics Research A* **537** 251–255

Electronic Transport Properties of New N-(p-R-phenacyl)-1,7-phenanthrolinium Bromides in Thin Films

L. Leontie[1*], I. Druță[2], T. Dăniloaia[2], N. Apetroaei[1], V. Nica[1], G. I. Rusu[1]

[1] *Faculty of Physics, "Al. I. Cuza" University, Department of Solid State Physics, 11 Carol I Blvd., 700506 Iași, Romania*

[2] *Faculty of Chemistry, "Al. I. Cuza" University, 11 Carol I Blvd., 700506 Iași, Romania*

The electrical conductivity, σ, and thermoelectric power, S, of six newly synthesized high-resistivity organic salts, N-(p-R-phenacyl)-1,7-phenanthrolinium bromides (T compounds, Scheme 1), have been investigated as a function of temperature.

Thin film samples ($0.11 \leq d \leq 2.21$ μm) deposited from ethanol solutions onto glass were used (an immersion technique).

It was established that samples of stable structure and reproducible electronic transport properties could be obtained if the films were submitted, after deposition, to heat treatment within the temperature range from 297 up to 513 K.

A structural investigation of the organic samples was performed with XRD, while their surface morphology was examined by the AFM technique, corroborated by optical microscopy.

The studied organic salts behaved like typical n-type polycrystalline semiconductors. Their activation energy of electrical conduction, E_a, remained in the 1.58–1.82 eV range, while the ratio of charge carrier mobilities, b, ranged from 1.09 to 1.25.

Correlations between the semiconducting parameters (activation energy of electrical conduction, ratio of carrier mobilities, etc.) and the compounds' molecular structure have been discussed using limit structures and taking $+E$ into account, as well as the $-I$ and $+I$ effects of the substituents. Electronic transport in actual organic compounds is strongly influenced by both their capacity to enable extended conjugation systems and the packing capability of the respective monomolecular layers, allowing planar configurations. The nature and position of the substituents within a molecule play an important role in the electrical conduction mechanism, since they affect significantly the extent of the π conjugation and, hence, the values of activation energy.

In the higher temperature range (360–513 K), the model based on band gap representation is suitable for explanation of electronic transfer in the investigated compounds, while Mott's variable-range hopping (VRH) conduction model may be conveniently used for lower temperatures.

The investigated compounds are also promising for thermistor applications.

References

1. Leontie L, Druta I, Furdui B, Rusu G I 2007 *Prog. Org. Coat.* **58** 303.
2. Căplănuș I, Rusu M, Rusu G G and Leontie L 2007 *Mater. Chem. Phys.* **101** (1) 77.
3. Leontie L and Danac R 2006 *Scripta Mater.* **54** (2) 175.
4. Leontie L, Rusu G I 2006 *J. Non-Cryst. Solids* **352** (9-20) 1475.
5. Leontie L, Druta I, Danac R, Prelipceanu M and Rusu G I 2005 *Prog. Org. Coat.* **54** (3) 175.

*Corresponding and presenting author: phone: +40-32-201168; fax: +40-32-201150/201201; e-mail: lleontie@uaic.ro

6. Leontie L, Druta I, Danac R, and Rusu G I 2005 *Synth. Metals* **155** (1) 138.
7. Goser K, Glosekotter P, Dienstuhl J 2004 *Nanoelectronics and Nanosystems: From Transistors to Molecular and Quantum Devices*, Springer Verlag, Berlin.
8. Leontie L, Roman M, Brinza F, Podaru C, Rusu G I 2003 *Synth. Metals* **138** 157.
9. Leontie L, Olariu I and Rusu G I 2003 *Mater. Chem. Phys.* **80** 506.
10. Farchioni R, Grosso G (Eds) 2001 *Organic Electronic Materials: Conjugated Polymers and Low Molecular Weight Organic Solids*, Springer Verlag, Berlin-Heidelberg-New York.
11. Rusu G I, Căplănuș I, Leontie L, Airinei A, Butuc E, Mardare D and Rusu I I 2001 *Acta Mater.* **49** 553.
12. Swenberg C E, Pope M 1999 *Electronic Processes in Organic Crystals and Polymers*, 2nd Ed., Oxford Univ. Press, Oxford.
13. Mahler G 1996 *Molecular Electronics*, Marcel Dekker, New York.
14. Brédas J L, Salaneck W R (Ed), Wegner G (Ed) 1994 *Organic Materials for Electronics*, Elsevier, Amsterdam.

Luminescent Materials: Tb(III) Ions-noble Metal Nanostructures-oxide Xerogel

B. Lipowska*, A. M. Kłonkowski

Faculty of Chemistry, University of Gdansk,
Sobieskiego 18, 80-952 Gdansk, Poland

Unlike bulk, nanosized particles often display many unusual properties, strongly dependent on their size, shape and surface configuration. Research in this area is mainly motivated by the possibility of designing nanostructured materials that possess novel electronic, optical, magnetic, photochemical and catalytic properties. Extensive studies have been performed for Ag and Au nanoscaled particles because of their attractive optical properties [1].

Many preparation methods regarding matrices containing nanoparticles of metals and procedures for metal nanostructures can be found in literature. In our work, we used such reduction agents as UV radiation [2], KBH_4 [3] and $CANa_3$ [4] to obtain nanostructures of noble metals.

The aim of the present work has been to present the influence of Ag and Au nanoparticles on the luminescence of Tb(III) ions incorporated in an SiO_2 matrix. We have observed the enhancement of Tb(III) emission in the presence of Ag nanostructures owing to the surface plasmon resonance (SPR) effect for materials prepared by the sol-gel method. General luminescence quenching occurs in the same matrix with Tb^{3+} ions in the presence of Au nanoparticles.

In order to remove O–H oscillators' quenching luminescence of Tb(III), the samples consisting of metal nanoparticles and Tb(III) ions entrapped in SiO_2 matrix were thermally treated. A variety of reduction techniques, material preparation procedures (one-pot or impregnation) and matrix modifications produce very interesting luminescent materials.

References

1. W. Chen, J. Zhang, Scripta Materialia **49** (2003) 321
2. T. Sato, H. Onaka, Y. Yonezawa, J. Photochem. Photobiol. A: Chem. **127** (1999) 83
3. T. Hayakawa, K. Furuhashi, M. Nogami, J. Phys. Chem. **108** (2004) 11301
4. S. K. Ghosh, A. Pal, S. Kundu, S. Nath, T. Pal, Chem. Phys. Lett., **395** (2004) 366

*Corresponding author: l_becia@poczta.onet.pl

Fabrication and Multi-properties of $BiFeO_3$ Ceramics

A. Lisińska-Czekaj[1], D. Czekaj[1], Ł. Madej[2]

[1] *University of Silesia, Department of Materials Science, Śnieżna 2, 41-200 Sosnowiec, Poland*

[2] *University of Silesia, Institute of Materials Science, Bankowa 4, 40-007 Katowice, Poland*

A very promising approach to creating novel high-performance materials is to combine different physical properties in one material in order to achieve rich functionality. Therefore, multiferroics – materials which are simultaneously (ferro)magnetic and ferroelectric, often also ferroelastic or ferrotoroidic – attract considerable attention nowadays, both due to the interesting physics involved and to their potentially important practical applications in spintronics, information storage devices such as multi-state non-volatile memories, sensors, phase shifters, amplitude modulators and optical wave devices. Recently, multiferroism has been observed in several perovskite-type materials, incl. $BiFeO_3$, $YMnO_3$, $BiMnO_3$.

The present study describes our attempts to synthesize bismuth ferrite ($BiFeO_3$), a high-performance ceramic material, and characterize its multiferroic properties. Thermogravimetry, differential thermal analysis and X-ray diffractometry was utilized to characterize the process of $BiFeO_3$ synthesis from simple oxide powders, Bi_2O_3 and Fe_2O_3. The mixed oxide method followed by hot-pressing sintering was utilized to fabricate ceramic samples. Impedance spectroscopy results of their AC response are presented and studies of their magnetic properties are reported. Both dielectric and magnetic investigations were carried out at temperatures up to 600°C.

Acknowledgements

The present research was carried out as part of the scientific activity of the University of Silesia's Department of Materials Science, research project no. BS/KM/317/2007.

Structural transformations in thin films of the GaSb-Ge system

N. Yu. Lutsyk, O. G. Mykolaychuk

Lviv National University, Physical Faculty, Chair of Physics of Metals,
8 Kyrylo and Mefodiy str., 79005 Lviv, Ukraine

Films of the GaSb–Ge system of thickness near 500 Å were prepared using the flash vacuum evaporation method. Ceramic, glass and spalling NaCl monocrystals served as substrates. The structure, substructure, concentration areas of metastable solid solutions and an amorphous state, as well as the kinetics of structural transformations depending on the technological conditions of evaporation of thin films of the GaSb–Ge system were studied by the electronography and transmission electron microscopy methods. The GaSb–Ge system's equilibrium in the massive state is represented by a diagram of the eutectic type, while the mutual solubility of components of the molar composition does not exceed 1%. The composition of films is more conveniently represented using the $(GaSb)_{1-x}(Ge_2)_x$ formula because, in the investigated system, solid thin-film solutions are formed by substitution.

The temperature of a substrate maintained during a film precipitation process has a dominant effect on the structural formation of the examined films. Films of all the examined compositions, precipitated on substrates at room temperature, were amorphous. Threefold GaSb coordination in the distribution of proximate atoms was observed in amorphous films. At Ge_2 concentrations of about 20%, a transfer from threefold to tetrahedral coordination was observed. Amorphous films crystallized in heat, but no phases of a solid solution were observed. The initial crystallization phases were GaSb crystal grains. The growth of crystallite sizes of GaSb took place with increasing temperature. The speed of continuous heating has an essential influence on the density and size of GaSb crystallites formed in the amorphous semiconductor matrix based on Ge.

Non-uniform amorphous films formed with increasing substrate temperature. Areas of initial ordering on a GaSb basis were observed. With further increase of substrate temperature, polycrystalline films of a metastable solid solution of the substitution formed on the isotropic substrates, while textured and epitaxial films formed on spalling NaCl monocrystals. In the case of epitaxial films, a weak modulation of a composition detected with transmission electron microscopy was observed. Disorder of solid solutions was observed on GaSb and Ge phases at temperatures in excess of 700.

Luminescence Kinetics in Silica Gel Doped with Tb^{3+} Ions and ZnS:Mn^{2+} Nanocrystals

S. Mahlik[1*], M. Zalewska[2], A. M. Kłonkowski[2], M. Godlewski[3,4], M. Grinberg[1]

[1] *Institute of Experimental Physics, University of Gdansk, Wita Stwosza 57, 80-952 Gdansk, Poland*

[2] *Faculty of Chemistry, University of Gdansk, Sobieskiego 18, 80-952 Gdansk, Poland*

[3] *Institute of Physics, Polish Academy of Sciences, Al. Lotników 32/46, 02-668 Warsaw, Poland*

[4] *Department of Mathematics and Natural Sciences, College of Science, Cardinal S. Wyszyński University, Warsaw, Poland*

We present the results of photoluminescence, luminescence kinetics and time-resolved spectroscopy of SiO_2 doped with Tb^{3+}, SiO_2 doped with ZnS:Mn^{2+} nanocrystals (quantum dots), and SiO_2 doped with ZnS:Mn^{2+} and additionally co-doped with Tb^{3+}. The materials were excited with a YAG:Nd pulse laser and an OPO system, which gave 30 ps pulse excitation in the 210–400 nm spectral range. The luminescence was detected by a streak camera. The purpose of this research was an analysis of the kinetics of Tb^{3+} and Mn^{2+} intra-shell luminescence and elucidation of energy transfer processes between the ZnS nanocrystals, Mn^{2+} ions and Tb^{3+} ions.

The luminescence of pure SiO_2 under 335 nm excitation consists of a broad band emission peaked at 450 nm decaying non-exponentially with an average decay time of the order of 2 ns. This luminescence has been attributed to the intrinsic emission of SiO_2.

The luminescence of the SiO_2 gel doped with ZnS:Mn^{2+} consists of two emission bands. One of them is a fast decaying band peaked at 430 nm, a combination of the intrinsic SiO_2 emission, decaying within 2 ns, and additional luminescence related to ZnS:Mn^{2+}, decaying slightly faster. The other, a slow decay band, is peaked at 600 nm and is related to the $^4T_1 \rightarrow {}^6A_1$ intra-shell transition of Mn^{2+} ions replacing Zn^{2+} ions in ZnS quantum dots. The decay time of this emission is approximately equal to 1.9 ms. It should be mentioned that the emission decay monitored at 600 nm also has a slow decay component. This fast component may be related to the tail of the fast decaying broad emission peaked at 430-450 nm, which extends spectrally below 600 nm.

In the case of SiO_2 containing ZnS:Mn^{2+} nanocrystals additionally doped with Tb^{3+}, no emission related to Mn^{2+} has been observed under pulse excitation. The only luminescence observed is due to the fast decaying SiO^2 emission and the sharp luminescence lines related to $^5D_3 \rightarrow {}^7F_5$, $^5D_3 \rightarrow {}^7F_4$, $^5D_4 \rightarrow {}^7F_6$, $^5D_4 \rightarrow {}^7F_5$, $^5D_4 \rightarrow {}^7F_4$ and $^5D_4 \rightarrow {}^7F_3$ intra-shell transitions of Tb^{3+} ions, decaying within 1 ms. The lack of the Mn^{2+} emission is related to the efficient energy transfer from ZnS:Mn^{2+} nanocrystals to Tb^{3+} ions.

*Corresponding author: fizmgr@univ.gda.pl

Photoacoustic Spectrum of a New, Twelve-coordinated Ho(III) Hydrazone Complex

N. Guskos[1,2*], J. Typek[2], J. Majszczyk[2], M. Maryniak[2], D. Paschalidis[3]

[1] *Solid State Section, Department of Physics, University of Athens, Panepistimiopolis, 15 784 Zografos, Athens, Greece*

[2] *Institute of Physics, Szczecin University of Technology, Al. Piastów 17, 70-310 Szczecin, Poland*

[3] *Department of Chemistry, Aristotle University, Thessaloniki, Greece*

A new, twelve-coordinated holmium(III) compound, $[Ho(NO_3)_3(PBH)_2]NO_3 \cdot 1.5H_2O$, has been prepared and studied by high-resolution photoacoustic spectrometry (PAS). The spectroscopic parameters of the obtained photoacoustic lines attributed to the f–f transitions were analyzed and compared with the parameters of a similar tenfold-coordinated holmium(III)-complex, $[Ho(NO_3)_2(PicBH)_2]$. Computer fitting of the obtained spectra allowed us to decompose them into Gaussian components and calculate the spectral parameters of each transition. Of the five observed f-f transitions, the $^5I_8 \rightarrow ^5G_6$ $^5I_8 \rightarrow ^5G_6$ and $^5I_8 \rightarrow ^5G_3$ transitions appeared to be the most sensitive to change of ligand coordination. The charge-transfer $\pi \rightarrow \pi^*$ and $n \rightarrow \pi^*$ transitions registered in the UV part of the photoacoustic spectrum exhibited significant variation due to the change of the coordination number and the shift of ligands towards greater wavenumbers.

Acknowledgements

This work was partially supported by the European Union – European Social Fund and from Poland Governments Science Budget 2007–2008 under a research project.

*Corresponding author: ngouskos@phys.uoa.gr

The Three-dimensional Conserved-order-parameter Ising Model with $M = 0.95$: a Monte-Carlo Wang-Landau Approach

I. A. Hadjiagapiou, A. Malakis, S. S. Martinos

Section of Solid State Physics, Department of Physics,
University of Athens, Panepistimiopolis,
Zografos GR 157-84, Athens, Greece

The critical region properties of the conserved-order-parameter three-dimensional Ising model with constant magnetization of $M = 0.95$ were studied by means of the Monte Carlo Wang-Landau algorithm. The study was carried out in the appropriate restricted but dominant energy subspaces. Using the evaluated density of states for the current model, the main effort was focused on the specific heat and Binder energy cumulant for lattices with linear size $30 \leq L \leq 120$, in order to asses whether this version of the Ising model belonged to the same universality class as the normal one. This was achieved by estimating the values for the thermal critical exponent, y_t, and critical temperature, T_c, by applying finite-size scaling analysis.

TiO_2 Thin Films as Sensing Gas Materials

D. Mardare[1*], N. Iftimie[1,2], D. Luca[1]

[1] *Al. I. Cuza University, Faculty of Physics, 11 Carol I Blvd., 700506, Iași, Romania*

[2] *National Institute of Research and Development for Technical Physics, 47 Mangeron Blvd., 700050, Iași, Romania*

Among many interesting applications of titanium dioxide (TiO_2) films, such as multilayer optical coatings, optical waveguides, photodecomposition of environmental pollutants, solar cells, electronic devices, etc. [1, 2], such films can detect a large category of harmful gases affecting our environment and, as a consequence, the quality of our life. As suggested in literature, undoped TiO_2 thin films respond significantly and very rapidly to the reducing gas ethanol and to H_2, while doping with Ce, Y, Sr and Tb render them sensitive to ethanol only [3].

Semiconducting gas sensors change their electrical conductivity when exposed to varying gas atmosphere. The mechanism usually depends on the operating temperature, which depends on the sensor material's properties and on the gas atmosphere. Nanosized grains of the sensing materials are preferred, as they increase the specific surface exposed to the gas [4].

In this paper, we discuss the influence of some deposition parameters (substrate nature, doping, etc.) on the phase composition and morphology of titanium oxide films and, consequently, on their gas-sensing properties. The sensitivity of these films and their optimum operating temperatures were investigated for some reducing gases (methane, acetone, ethanol and liquefied petroleum gas). Several methods were used for preparing films with different structural and electrical properties (sol-gel, spray pyrolisis, dc reactive magnetron sputtering). We have observed chemical methods usually producing rougher films, with greater specific area surfaces and better sensing properties.

The films' structure and microstructure were respectively investigated with X-ray diffraction (XRD) and Atomic Force Microscopy (AFM).

TiO_2 films were exposed to various concentrations of gases at elevated temperatures in order to evaluate the gas sensitivity of ZnO gas sensors. The electric resistance of the films in test gases, R_g, and in pure air, R_a, was measured and the gas sensitivity, defined as:

$$S = \frac{\Delta R}{R_a} = \frac{|R_a - Rg|}{R_a}$$

was calculated.

Correlations with the structure and morphology of TiO_2 films were made.

References

1. Bange K, Ottermann C R, Anderson O, Jeschkowski U, Laube M and Feile R Thin Solid Films 1991 197 279.
2. Katayama K, Hasegawa K, Takahashi Y and Akiba T Sens Actuat A, 1990 24 55.
3. Tang H, Prasad K, Sanjines S, Levy F Sens Actuat B 1995 26-27 71.
4. Shimizu Y, Egashira M MRS Bull 1999 24 18.
5. Hey-Jin Lim, Deuk Yong Lee, Young-Jei Oh, Sens Actuat A 2006 125 405.
6. Rezlescu N, Iftimie N, Rezlescu E, Doroftei C, Popa P D Sens Actuat B 2006 114 427.

*Corresponding author: dianam@uaic.ro

Magnetic Properties of a PEE PEN Matrix with Maghemite Nanoparticles

N. Guskos[1,2], M. Maryniak[2]*, J. Typek[2], A. Guskos[2], R. Szymczak[3], E. Senderek[4], Z. Rosłaniec[4], D. Petridis[5], K. Aidinis[6]

[1] *Solid State Section, Department of Physics, University of Athens, Panepistimiopolis, 15 784 Zografos, Athens, Greece*

[2] *Institute of Physics, Szczecin University of Technology, Al. Piastów 17, 70-310 Szczecin, Poland*

[3] *Institute of Physics, Polish Academy of Sciences, Al. Lotników 36/42, Warszawa, Poland*

[4] *Institute of Materials Science and Engineering, Szczecin University of Technology, Al. Piastów 17, 70-310 Szczecin, Poland*

[5] *Instytute of Materials Science, NCSR, Demokritos, 153 10 Aghia Paraskevi, Athens, Greece*

[6] *Applied Physics Section, Department of Physics, University of Athens, Panepistimiopolis, 15 784, Greece*

Two samples were prepared containing γ-Fe_2O_3 magnetic nanoparticles dispersed at the concentrations of 0.1% and 0.3% in a poly(ether-ester) multiblock copolymer (PEE PEN) matrix. The polymer filler was in powder form, consisting of 10 nm size magnetic nanoparticles arranged in 2–3 μm long and 100 nm thick agglomerates. The samples were characterized by XRD and TEM spectroscopy. TEM showed the concentration of magnetic nanoparticles to be homogenous in both samples. The temperature dependence of the dc magnetization revealed that the blocking temperature was about 100 K and the ZFC mode at low magnetic fields uncovered the presence of the matrix's critical points. The ferromagnetic resonance (FMR) measurements were carried out in the 4.2 to 300 K temperature range. An intense resonance absorption line from γ-Fe_2O_3 was recorded, with a slightly asymmetric line shape. The derivative spectra were fitted to two Lorentzian lines. The resonance lines at 280 K were centered at H_r = 2997(2) and 3217(2) Gs with line widths ΔH = 1164(1) and 1185(1) Gs for samples with concentrations of 0.1% and 0.3%, respectively. The integrated FMR intensities of the two samples were almost the same. All the FMR parameters showed anomalous behavior connected with the presence of the matrix's critical points. Tab. 1 shows the $\Delta H_r/\Delta T$ gradient in the various temperature regions. The above values are higher for lower concentrations at higher temperatures, while the opposite effect is observed for lower temperatures. It has been demonstrated that the concentration of magnetic nanoparticles could play an important role in the behavior of FMR spectra.

Table 1

Concentration	$\Delta H_r/\Delta T$ (280 K > T > 110 K) [Gs/K]	$\Delta H_r/\Delta T$(95 K > T > 40 K) [Gs/K]
0.1 %	0.84	8.57
0.3 %	0.69	21.24

Acknowledgements

This work was partially supported by the European Union – European Social Fund and from Poland Government's Science Budget 2007–2008 under a research project.

*Corresponding author: michalmaryniak@gmail.com

Phase Separation in $La_{0.54}Sm_{0.11}Ca_{0.35}$ $Mn_{1-x}Cu_xO_3$ Manganites

N. Cornei[1], C. Mita[1], M. L. Craus[1,2], O. Mentre[4], N. Tancret[4], F. Abraham[4]

[1] *Department of Chemistry, "Al. I. Cuza" University, Iași, Romania*

[2] *Institute of Research and Development for Technical Physics, Iași, Romania*

[3] *Joint Institute of Nuclear Research, Dubna, Russia*

[4] *Ecole Nationale Supérieure de Chimie Lille, UCCS, Lille, France*

$La_{1-x}Ca_xMnO_3$ manganites have a rich electronic diagram, depending on the average size of A places and the nature of interaction among Mn cations. Phase separation between FM and AFM regions was observed near $x = 0.5$. The substitution of Mn with other transition cations produces a change of Mn-O-Mn interactions, followed by a corresponding change in the electronic phase diagram. We have synthesized a new row of manganites of $La_{0.54}Sm_{0.11}Ca_{0.35}$ $Mn_{1-x}Cu_xO_3$ (LSCMCO) nominal composition. The samples were prepared by the sol-gel method. The gel was calcinated at 800°C for 17 h and than sintered in air at 1200°C for 10 h. The sintered samples were monitored through X-ray powder diffraction, IR and DR spectrophotometry, magnetic and electric measurements to study the effects of the Mn-site substitution on their electronic and magnetic structure. The lattice constants, atomic positions, Mn-O distances and Mn-O-Mn angles were determined with the DICVOL, POWDERCELL and FULPROF programs. The structure can be described by a Pnma unit cell (Fig. 1).

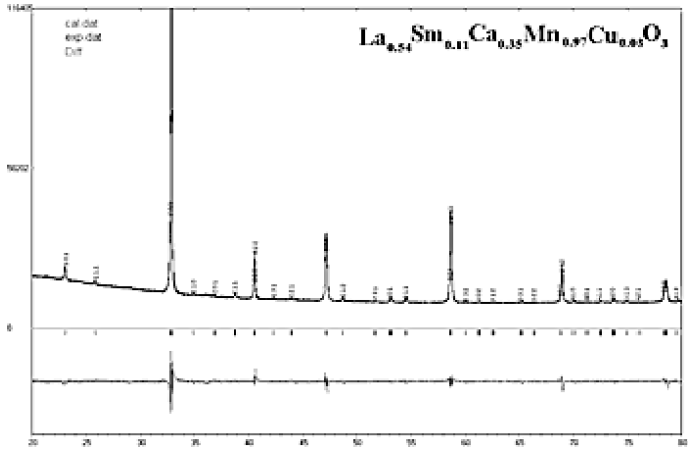

Figure 1: The diffractogram of LSCMCO ($x = 0.03$)

Slight dependence of the lattice parameters on the Cu amount in the sample was observed. Analysis of the FT-IR and UV-Vis spectra reflected a minor decrease of oxygen disorder and Mn^{3+} concentration with the decrease of the Jahn-Teller effect. We have discussed the dependence of the transition from the metal to the insulator behavior (Fig. 2) and the modification of FM/AFM concentrations in terms of tight-binding approximation (TBA). In agreement with the TBA theory the bandwidth depends strongly on Mn-O distances and Mn-O-Mn bond angles.

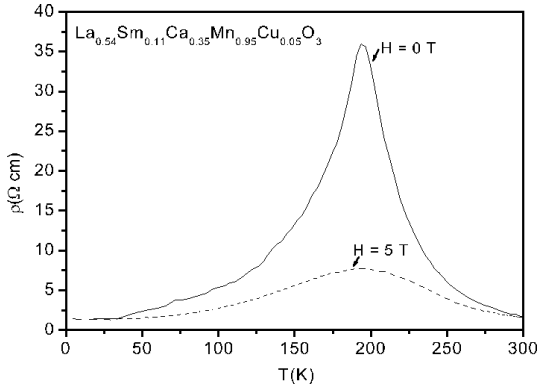

Figure 2: The variation of resistivity vs. temperature of LSCMCO ($x = 0.03$)

References

1. Papavassiliou G, Fardis M, Belesi M, Pissas M, Panagiotopoulos I, Kallias G, Niarchos D, Dimitropoulos C and Dolinsek J 1999 *Phys. Rev. B* **59** 6390
2. Pi Li, Zheng Lei, and Zhang Yuheng 2000 *Phys. Rev.B* **61** 8917
3. Dubroka A 2006 *Phys. Rev.B* **73** (1) 22440

Thermodynamic Software of a $Cd_XHg_{1-X}Te$ Solid Solution Obtained for Infrared Optoelectronics by Means of LPE

P. Moskvin[1]*, V. Khodakovsky[1], J. M. Olchowik[2], W. Sadowski[3]

[1] *Zhitomir State Technological University, Chernyakhovs'kogo 103, 10005 Zhitomir, Ukraine*

[2] *Institute of Physics, Lublin University of Technology, 20-618 Lublin, Poland*

[3] *Gdansk University of Technology, Narutowicza 11/12, 80-952 Gdansk, Poland*

Heterostructures based on $Cd_XHg_{1-X}Te$ solid solution for optoelectronic devices are obtained by LPE methods. An important experimental and theoretical problem is finding the most efficient growing parameters of the epitaxial process.

The first approximation while constructing a thermodynamic model of phase formation by LPE is based on the system's phase equilibrium data. An analysis of experimental results concerning phase equilibrium has shown that it is possible to achieve satisfactory thermodynamic description only if a model is included of the associated solutions with a set of complexes in the liquid phase. It is possible to explain and describe the complicated form of liquidus lines in initial binary systems and a moderate pressure of the system's main components only through a complex interaction between associates of different composition in the liquid phase. The developed thermodynamic model enables satisfactory description of the experimental data on the p–T–X equilibrium in ternary and initial binary systems in a wide interval of temperatures and pressures. LPE kinetics in the system was based on the theory of diffusion-limited growth. According to this theory, the growth of a solid solution is limited by diffusion transition of a substance to the interface. The mathematical problem of three-component material crystallization consists of a differential diffusion equations in the form of Stefan's problem, while the equations of phase equilibrium within the framework of the polyassociative solutions model serve as boundary conditions. The formulated problem was solved by numerical methods. Our experimental data and other available in the literature on the LPE process in Cd-Hg-Te systems were described precisely.

The heterojunction between the $Cd_XHg_{1-X}Te$ solid solution and a substrate of initial binary compounds is characterized by the presence of differences in the materials' crystal lattice constants. Therefore, a solid solution layer grows under elastic strain. In order to estimate this factor in an analysis of the system's phase equilibrium, the coherent phase diagram own melt – strained solid solution on a massive substrate from initial compound has been analyzed. The contact supercooling producing the quasi-equilibrium state in the system has been demonstrated to be close to 1 K. So insignificant degree of contact supercooling in the system reduces the growth rate and the thickness of layers insignificantly. Thus, the high thermodynamic stability of a growing solid phase composition change caused by the occurrence of elastic energy in the system is also insignificant. Such conclusions about the influence of elastic deformations in the growth process follow from data calculated with or without elastic energy in the system.

A kinetic analysis of the grown layers in various time-temperature regimes (step cooling, equilibrium cooling and supercooling techniques) has been performed and satisfactory description of the growth process has been achieved, both for layer thickness and the growing solid solution's composition. Thus, the obtained results have proved the applicability of the developed thermodynamic software in descriptions of crystallization of solid solutions . The applied mathematical software can be used to choose the most favorable growth conditions for layers of desirable parameters.

*Corresponding author: moskvin@us.ztu.edu.ua

Concentration Fluctuations in Liquid Bi–Zn Alloys

S. I. Mudry*, V. Sklyarchuk, Yu. Plevachuk, A. Yakymovych

Department of Metal Physics, Ivan Franko National University,
8 Kyrylo and Mefodiy str., 79005 Lviv, Ukraine

Binary systems with a miscibility gap in the phase diagram are interesting because, when cooled from the liquid state, they produce finely dispersed alloys. Besides, the alloys of these systems, whose concentration and temperature are close to the critical one, attract researchers' attention due to fundamental interests. It is therefore of great importance to study the concentration fluctuations near miscibility and their influence on physical properties. Such fluctuations affect the stability of liquid-liquid equilibrium and promote the formation of variously sized structural units, including nanoscale ones.

In this work, results of viscosity measurements of Bi–Zn binary melts are presented. Measurements of the viscosity coefficient were carried out with using a high-temperature viscometer. The Shvidkovskiy approach was used to calculate the coefficient of dynamical viscosity. The temperature dependences of the viscosity coefficient were obtained for molten alloys containing 15, 20 and 91.9 at% of Bi. The concentrations of melts corresponded with different points of the miscibility gap. The obtained temperature dependences were compared with those for the liquid components, Bi and Zn. Experimental results indicate anomalous behavior of the viscosity-temperature dependences, especially for the melt corresponding to the critical point concentration (15 at% Bi). The maximum was observed at the temperature of $T \approx 850$ K, whereas at other temperatures viscosity varied according to an exponential dependence. Such maxima are not commonly observed in temperature dependences for other liquid metals and alloys. With the content of Bi-atoms increasing to 20 at%, the maximum was significantly reduced but persisted.

The temperature dependences of viscosity were also used to calculate the activation energy values. An analysis of changes in viscosity with temperature and calculated values of activation energies allowed us to estimate the concentration fluctuations near the miscibility gap. The maximum, which appears in the experimental temperature dependence of viscosity is attributable to significant fluctuations in concentration accompanied by an increase in the structural unit size.

*Corresponding author: mudry@physics.wups.lviv.ua

Phase Transformations in a $La_{1-x}Nd_xNi_{3.5}Al_{1.5}$-$H_2$ ($x = 0.1$; 0.2) System

A. M. Trostianchyn[1], I. I. Bulyk[1], I. V. Trostianchyn[2], S. I. Mudry[2*]

[1] *Karpenko Physico-Mechanical Institute of National Academy of Sciences of Ukraine, Naukova 5, 79601 Lviv, Ukraine*

[2] *Department of Physics of Ivan Franko National University of Lviv, 8 Kyrylo and Mefodiy str., 79005 Lviv, Ukraine*

Interaction in a $La_{1-x}Nd_xNi_{3.5}Al_{1.5}$–$H_2$ ($x = 0.1$ and 0.2) system were studied from room temperature up to 950°C, with the initial hydrogen pressure of 5 MPa, by means of differential thermal and X-ray phase analyses. The heating of two-phase alloys ($x = 0.1$ and 0.2) in hydrogen results in their disproportionation at 530 and 560°C, respectively, and the formation of NiAl and unidentified amorphous products. The single-phase $La_{0.9}Nd_{0.1}Ni_{3.5}Al_{1.5}$ alloy decomposes in hydrogen at 900°C into a hydride of rare-earth metals and intermetallic Ni_3Al; traces of NiAl and a $CaCu_5$-type hydride structure were also observed. Heating the disproportionated samples in vacuum to 520–550°C leads to their recombination into a homogenized phase of a $CaCu_5$-type structure. The increased neodymium content shifts the reaction equilibrium in the $La_{1-x}Nd_xNi_{3.5}Al_{1.5}$–$H_2$ system in the recombination direction.

Conditions, phase composition and lattice parameters of interaction products of $La_{1-x}Nd_xNi_{3.5}Al_{1.5}$ ($x = 0.1$ and 0.2) alloys and hydrogen under the initial pressure of 5 MPa.

Alloy	Treatment	T, °C	Phase	Lattice parameters, nm	
				a	c
$La_{0.9}Nd_{0.1}Ni_{3.5}Al_{1.5}$	Initial state		$CaCu_5$ t. st.		
			NiAl	0.51043(4)	0.4067(4)
				0.2876(2)	-
	Heating under H_2	600	NiAl	0.2908(6)	-
	Heating under H_2	900	NiAl	0.2898(1)	-
	DR*	400	$(La,Nd)H_x$	0.5683(6)	-
	DR*	550	$CaCu_5$ t. st.	0.5078(2)	0.4086(3)
	Homogenization**		$CaCu_5$ t. st.	0.5138(3)	0.4101(4)
	Heating under H_2	600	$(La,Nd)H_x$	0.5616(4)	-
			Ni_3Al	0.35761(8)	-
	Heating under H_2	900	$(La,Nd)_1(Ni,Al)_5$	0.5387(1)	0.8558(5)
			$(La,Nd)H_x$	0.5621(1)	-
			Ni_3Al	0.35985(5)	-
			NiAl	0.28681(8)	-
	DR*	900	$CaCu_5$ t. st.	0.5127(1)	0.4089(1)
$La_{0.8}Nd_{0.2}Ni_{3.5}Al_{1.5}$	Initial state		$CaCu_5$ t. st.	0.5053(2)	0.4081(3)
			NiAl	0.2875(2)	-
	Heating under H_2	600	NiAl	0.2896(5)	-
	Heating under H_2	900	NiAl	0.2901(3)	-
	DR*	350	$(La,Nd)H_x$	0.5438(5)	-
	DR*	520	$CaCu_5$ t. st.	0.5106(6)	0.4099(8)
	DR*	600	$CaCu_5$ t. st.	0.5110(2)	0.4085(2)

Notes: t. st. – type of structure; * – desorption, recombination of disproportionated products obtained by heating in hydrogen to 600°C; ** – homogenized by means of Solid-HDDR.

*Corresponding author: mudry@physics.wups.lviv.ua

Dielectric Relaxation in Polyurethane Networks Nanostructured in Situ by Metal Complexes

Yu. M. Nizelskij

Institute of Macromolecular Chemistry, NAS of Ukraine,
Kharkovskoe Shosse 48, 02160 Kyiv, Ukraine
nizelskij@mail.ru

Dielectric relaxation spectroscopy of metal-containing polyurethane (MPU) networks nanostructured *in situ* by polyheteronuclear metal organic complexes has revealed significant increase in direct current conductivity as compared with the original metal-free PU matrix.

An analysis of MPU's temperature dependences of conductivity at a direct current justifies assuming its ionic character. The description of experimental data by curves constructed on the basis of the Fogel-Taman-Falcher equation shows the influence of free volume on charge transmission. If the small content of metal ions (0.01–0.05 wt%) and coordination immobilization of metal complexes in a PU matrix are taken into account, we can assume that the most possible current carriers are protons. Taking into account the dependence of charge transfer on the MPU's free volume, of the increased mobility of protons has been related to increased mobility of polymeric chains due to the structurization of the PU matrix. This assumption is in agreement with a shift in the relaxation of conductivity of the MPU toward higher frequency electric modules. It is also confirmed by the absence of dipole relaxations in the 10^2–10^6 Hz frequency range at temperatures from −40 up to 120°C.

Both the value and relaxation of MPU conductivity are sensitive to the complexes' structure (see table) and the presence of additional complexing agents in the reaction mixture. Solvents with various ability of complex formation, 1,4-dioxane, CH_2Cl_2, N,N-dimethylformamide (DMFA), were used as additional complexing agents capable of influencing the structurization process. PUs obtained using various solvents and in situ immobilized coordination complexes can be ordered as follows according to direct current increases: PU-Cu_2ZnNCS (1,4-dioxane) < PU-Cu_2ZnNCS (CH_2Cl_2) < PU-Cu_2ZnNCS (DMFA).

The conductivity of modified PUs is very sensitive to the metal ion content in metal-containing modifiers.

References

1. Formation of nanostructures in polyurethane with *in situ* polymer immobilized metal complexes, N. V. Kozak, Yu. M. Nizelskij, V. I. Shtompel, N. V. Mnikh, O. I. Grischuk, Nanosystems, nanomaterials, nanotechnologies 2005, **3**, No2 – P.445-464 (in Ukrainian)

Nanostructurization in Polyurethanes Containing Polymer-immobilized Coordination Metal Complexes in Situ

Yu. M. Nizelskij

Institute of Macromolecular Chemistry, NAS of Ukraine,
Kharkovskoe Shosse 48, 02160 Kyiv, Ukraine
nizelskij@mail.ru

Polymer-immobilized mono- and polyheteronuclear metal complexes were obtained in situ in structurally homogeneous polymer nanocomposites based on cross-linked polyurethane (PU). Aggregation of these metal complexes was shown by the EPR method to be hindered by complexation with polar groups of the polymer matrix. The obtained systems included organic nanoscale structures (self-similar micro heterogeneities typical for PU) and metal-containing coordination junction points. The nanoscale dimensions of these aggregates was demonstrated by X-ray scattering and scanning electronic microscopy (SEM). The profile values of their structural parameters were estimated using small-angle X-ray scattering as follows: periodicity of uniform electronic density scattering elements, D, heterogeneity range, l_p, and interface width, E (for a two-phase system), are all of the nanoscale order of magnitude. SEM microphotos of the cryogenic cross-brake surface of metal-containing PU films demonstrate the presence of heterogeneities of 10 to 100 nm linear dimensions.

According to the wide angle X-ray scattering (WAXS) data, all the analyzed metal-containing PUs are amorphous. At the same time, the formation of their microstructure depends on the spatial symmetry of coordination junction points and the structure of polyheteronuclear metal complexes. According to the X-ray and SEM data, as well as those of optical transmission microscopy, the presence of 5% metal chelate complex in PU leads to the saturation of coordination-able sites of the polymer matrix and to a partial separation of the metal-containing phase.

It has been shown that metal-containing PU matrices differ essentially in their polymer chain mobility, electric and thermomechanical properties, depending on the symmetry and quantity of ionic centers (1 to 7) in the coordination metalorganic modifier. Due to the immobilization of metal complexes in PUs, chain mobility increases, an effect demonstrated with the EPR and DSC methods. Increasing polymer chain mobility increases the conductivity of some of the PUs to the semiconducting level. This effect was demonstrated with the static two-electrode method and dielectric relaxation spectroscopy (DRS).

Effects of Nitrogen Addition on the Structure and Properties of a–C:H Layers on Polycarbonate Substrates

R. Nowak*, S. Jonas

AGH University of Science and Technoloy, Faculty Materials Science and Ceramics, Al. Mickiewicza 30, 30-059 Cracow, Poland

Polycarbonate (PC) possess many commercial applications. However, its use is still limited to non-abrasive and chemical-free environments, due to its poor hardness, low scratching resistance and high susceptibility to chemical attacks. To overcome this limitation, PC may be coated with hydrogenated amorphous carbon layers. Such a–C:H layers have very attractive properties, including good hardness, infrared transparency, chemical inertness, low friction coefficients and biocompatibility. The addition of nitrogen to the structure reduces the internal stress and improves the tribological properties of a–C:H layers.

In this work, a–C:N:H layers were deposited from a mixture of CH_4/N_2 gases by Plasma-Enhanced Chemical Vapor Deposition (RF CVD 13.56 MHz). Effects of nitrogen's incorporation in the structure and the tribological properties of the deposited layers were investigated. The structure of layers was characterized through X-ray Photoelectron Spectroscopy and Fourier Transform Infrared spectroscopy (FTIR). The layers' friction coefficient, wear resistance and surface topography were respectively estimated with a tribometer in the ball-on-disc configuration and atomic force microscopy (AFM). The results indicate that the content of incorporated nitrogen has considerable effect on the film's properties. The IR spectra of the obtained layers have demonstrated the presence of nitrogen bonded to carbon and hydrogen. The formation of the following bonds has been confirmed: –C≡N, $–NH_2$, $–C–NH_2$, >C=NH, all of them typical for a–C:N:H layers. The surface of layers has been estimated by AFM to be smoother with the increase of the N/C fraction. The tribological tests have shown that the layers reduce the friction coefficient of the polycarbonate (up to 50 %) and improve its wear resistance considerably.

*Corresponding author: rafnowak@agh.edu.pl

Influence of the Gas Atmosphere During the LPE Process on the Morphology of Si ELO Layers

J. M. Olchowik[1], S. Gułkowski[1], K. Cieślak[1], K. Zabielski[1], I. Jóźwik[1], A. Rudawska[2]

[1] *Institute of Physics, Lublin University of Technology, Nadbystrzycka 38, 20-618 Lublin, Poland*

[2] *Departement of Production Engineering, Lublin University of Technology, Nadbystrzycka 38, 20-618 Lublin, Poland*

Epitaxial growth of thin layers from the liquid phase can be achieved with solutions saturated in various ambient gases. Most often this process takes place in vacuum or a gaseous atmosphere of hydrogen or argon. According to the experimental data, the morphology of the crystallized layers is determined by the ambience in which the process occurs.

The cohesion energy responsible for the processes of epitaxial lateral deposition on the substrate's surface depends on the surface free energy, which is a measure of attraction of the solution's atoms by the substrate atoms. In the case of crystallization of an epitaxial lateral layer of Si on a substrate partially masked with a dielectric, the chemical potentials of atoms in the neighboring phases (determining the interface's evolution) influence the relaxation velocity of the saturated liquid phase and the horizontal and vertical growth rate.

The aim of our investigation was to analyze experimentally the influence of ambient gases used during LPE growth on the cohesion of the Sn:Si solution with substrates applied for the lateral epitaxial growth of Si layers. This work presents a comparative temperature analysis of the wetting angle of surfaces such as Si, SiO_2 and SiN_x by the Sn:Si solution.

Fluorophores and Noble Metal Nanostructures on Mesoporous Silica as Recognition Materials for Cations

M. Orłowska[1*], K. Kledzik[1], R. Ostaszewski[2], A. M. Kłonkowski[1]

[1] *Faculty of Chemistry, University of Gdansk, Sobieskiego 19, 80-952 Gdansk, Poland*

[2] *Institute of Organic Chemistry, Polish Academy of Sciences, Kasprzaka 44, 01-224 Warsaw, Poland*

The prepared recognition materials are key components of optical chemical sensors that selectively detect ions of particular metals. Such recognition elements could find applications in many fields, including environmental protection and medicine.

The recognition materials consist of mesoporous silica with organically functionalized surfaces [1, 2], which supports covalently grafted fluorophore molecules. Mesoporous silica exhibits sharp pore-width distribution, with pore sizes from 2 to 8 nm. The prepared MCM-48 matrix has a three-dimensional cubic structure, while MCM-41 exhibits a hexagonal array of uni-dimensional channels [3]. Fluorophore molecules consist of three functional parts: the fluoro group (pyrene), a receptor with O and N donor groups, and the anchoring (carboxyl) group.

The organo-functionalized silica supports were modified by noble metal nanoparticles, such as Au and Ag. This modification enhanced the fluorophores' fluorescence intensity in comparison with the recognition materials without noble metals. The effect is due to the *surface plasmon resonance* (SPR) of silver and gold nanoparticles [4].

Fluorescence intensity of the recognition element after complexation of various metal ions was examined. Every metal ion modified the fluorophore's fluorescence intensity, but the most significant effect was observed with Cu(II) ions. After complexation of Cu(II) ions, the emission decreased due to the *photo-induced electron transfer* (PET) effect [5]. Experiments have shown that fluorophores grafted on mesoporous silica modified by noble metal nanoparticles selectively recognize Cu(II) ions mixed in aqueous solutions with other metal ions. Thus, the prepared material can be treated as a chemical recognition element for Cu(II) ions.

References

1. A. Simon, T. Cohen-Bouhacina, M. C. Porté, J. P. Aimé, C. Baquey, J. Colliod Interf. Sci. **251** (2002) 278
2. J. Y. Kim, S. H. Park, J.-S. Yu, Opt. Mater. **21** (2002) 349.
3. P. Behrens, A. Glace, Ch. Haggenmüller, G. Schechner, Solid St. Ions **101–103** (1997) 255.
4. E. Hutter, J. H. Fendler, Adv. Mater. **19** (2004) 1685.
5. R. A. Bissel, E. Calle, A. P. de Silva, Chem. Soc. Perkin Trans. **2** (1992) 1559

*Corresponding author: maja_orlowska@o2.pl

Isolated Mn^{2+} Centers and Clusters in Mn-Doped Glasses of the $CaO–Ga_2O_3–GeO_2$ System

B. V. Padlyak

Institute of Physical Optics of the Ministry of Education and Science of Ukraine
23 Dragomanov Str., 79-005, Lviv, Ukraine

The EPR, UV-visible optical spectra (absorption, luminescence excitation, emission) and luminescence kinetics of Mn^{2+} impurity centers in Mn-doped glasses of the $CaO–Ga_2O_3–GeO_2$ system have been analyzed. EPR spectra of the as-synthesized Mn-doped glasses consist of three broad bands with effective g-factors: $g_{\text{eff}} \cong 4.3$, $g_{\text{eff}} \cong 3.0$, and $g_{\text{eff}} \cong 2.0$. The observed spectra have been attributed to Mn^{2+} ($3d^5$, $^6S_{5/2}$) isolated ions in octahedral sites with a broad distribution of crystal field parameters and small clusters of Mn^{2+} ions [1]. Optical spectroscopy [2] has demonstrated the manganese impurity to be incorporated into octahedral sites of the $CaO–Ga_2O_3–GeO_2$ glass network as Mn^{2+} and Mn^{3+} ions. The intense broad absorption band with a maximum about 460 nm is related to the spin-allowed $^5E_g \rightarrow {}^5T_{2g}$ transition of Mn^{3+} ions in trigonally distorted octahedral sites of the $CaO–Ga_2O_3–GeO_2$ glass network. The spin-forbidden weak absorption lines of Mn^{2+} ions were not observed on the background of Mn^{3+} strong absorption band. The observed luminescence band with a maximum about 650 nm can be explained in the framework of the transition $^4T_{1g} \rightarrow {}^6A_{1g}$ of Mn^{2+} ions in trigonally distorted octahedral sites.

The Mn^{2+} luminescence decay curve can be adequately described by a two-exponential approximation with different lifetimes ($\tau_1 = 12.4$ ms, $\tau_2 = 3.98$ ms at $\lambda_{\text{exc}} = 300$ nm), corresponding to two types of Mn^{2+} centers in the glass network. On the basis of the obtained results and the referenced data, it has been demonstrated that the longer lifetime ($\tau_1 = 12.4$ ms) belongs to isolated Mn^{2+} centers (about 64%), whereas the shorter lifetime ($\tau_2 = 3.98$ ms) belong to pairs and small clusters of Mn^{2+} centers (about 36%), coupled by magnetic exchange interaction. The presence of exchange-coupled $Mn^{2+}–Mn^{2+}$ pairs and Mn^{2+} clusters in the glass structure is confirmed by magnetic susceptibility measurements. Possible local structure of isolated Mn^{2+} centers in the $CaO–Ga_2O_3–GeO_2$ glass network is considered and discussed.

References

1. B. V. Padlyak, A. Gutsze, EPR Study of the Impurity Paramagnetic Centres in ($CaO–Ga_2O_3–GeO_2$) Glasses, Appl. Magn. Reson. 14 (1998) 59–68.
2. B. Padlyak, O. Vlokh, B. Kukliński, K. Sagoo, Spectroscopy of the Mn-Doped Glasses of $CaO–Ga_2O_3–GeO_2$ System, Ukr. J. Phys. Opt. 7, No. 1 (2006) 1–10.

Growth, Optical and Magnetic Properties of $PbMoO_4$, Pure and Doped with Co^{2+} Ions

D. Piwowarska[1], S. M. Kaczmarek[1*], M. Berkowski[2]

[1] *Institute of Physics, Technical University of Szczecin, 48 Al. Piastów, 70-310 Szczecin, Poland*

[2] *Institute of Physics, Polish Academy of Sciences, Al. Lotników 32/46, 02-668 Warsaw, Poland*

Lead molybdate single crystals were grown by the Czochralski technique under optimized conditions. As the starting charge stoichiometry is well known to be an important factor for controlling the optical transmission characteristics of pure and doped lead molybdate crystals. The starting polycrystalline lead molybdate material used for crystal growth was prepared by mixing the constituent oxides, i.e. PbO and MoO_3. In order to grow stoichiometric crystals, the constituent powders were mixed in the 1:1 molar ratio. A pull rate of 2.5 mm/h and a crystal rotation rate of 20 rpm were employed to grow crystals 20 mm in diameter and 60 mm long. A platinum crucible 50 mm in diameter and 50 mm long, was used in the experiment. A photograph of an ingot is shown in Fig. 1.

Figure 1: A $PbMoO_4$ single crystal

For the optical transmission measurements, crystal plates were cut from the crystal ingots and their faces were polished optically. The optical transmission spectra of the polished crystal plates were recorded over the wavelength range of 190–3200 nm by a Perkin-Elmer Lambda-2 spectrophotometer. EPR spectra were recorded to investigate the introduced paramagnetic centers for their symmetry and magnetic interactions using a standard X-band Bruker E500 EPR spectrometer with the field range of 0–1.4 T and the microwave field modulation of 100 kHz.

We have also analyzed the possibility of doping crystals with transition metal ions, especially cobalt ones. For three Co doped $PbMoO_4$ single crystals, starting concentrations of cobalt ions in the melt were 0.2 wt%, 0.5 wt% and 1 wt% with respect to molybdenum.

*Corresponding author: skaczmarek@ps.pl

Microsegregation in Liquid Pb-based Eutectics

Yu. Plevachuk[1*], V. Sklyarchuk[1], A. Yakymovych[1], G. Gerbeth[2], S. Eckert[2]

[1] *Ivan Franko National University, Department of Metal Physics, 8 Kyrylo and Mefodiy str., 79005 Lviv, Ukraine*

[2] *Forschungszentrum Dresden-Rossendorf, P. O. Box 510119, 01314 Dresden, Germany*

Lead-based eutectics continue to be interesting due to their various practical applications. Pb–Bi and Pb–Mg eutectics are considered to be good liquid-metal coolants for nuclear power systems [1, 2]. Pb–Sn and Pb–Sn–Bi eutectics are widely used as low-temperature solders. Although these systems have been extensively studied, the measurements of their eutectic region reveal anomalous temperature dependences of some physical properties. It has been shown that molten metallic alloys undergo a number of structural transformations from the initial microheterogeneous state just after melting up to the true solution state [3].

As has been shown in theoretical studies (see [4] and references therein), a regular solution becomes thermodynamically unstable when approaching the eutectic temperature, T_e. Areas of stability and instability have been determined, separated by spinodal and binodal lines. It has been shown theoretically that a maximum temperature of instability did not exceed $2T_e$. Having passed this temperature upon cooling, the regular solution becomes metastable. Further transition to the irregular state is possible either through the fluctuation processes or under external fields.

The anomalies of temperature dependences of various physical properties (incl. resistivity, internal friction or density), such as hysteresis and a divergence of the heating-cooling curve have been observed in various eutectic systems [3, 5, 6]. In the present work, the temperature dependence of electrical conductivity, $\sigma(T)$, thermoelectric power, $S(T)$, and viscosity, $\eta(T)$, of Pb-based eutectic and near-eutectic systems have been studied. An anomalous behavior of the physical properties of liquid binary Pb–Sn, Pb–Bi, Pb–Mg and ternary Pb–Bi–Sn melts has been revealed well above the liquidus. The anomalies' temperature range reaches hundreds degrees and depends on the sample's composition. The results are interpreted in the context of the assumption that microsegregation areas formed by micro and nanoclusters exist in eutectic and near-eutectic systems.

References

1. Power Reactor and Sub-Critical Blanket Systems with Lead and Lead–Bismuth as Coolant and/or Target Material 2003 (Vienna: IAEA) (IAEA TECDOC-1348) http://www.iaea.org/inis/aws/fnss/fulltext/tecdoc1348.pdf
2. Subbotin V I et al. 2002 *Atomic Energy* **92** (1) 29.
3. Dahlborg U, Calvo-Dahlborg M, Popel P, Sidorov V 2000 *Eur. Phys. J.* **B14** 639.
4. Kalashnikov E V *Technical Physics* 1997 **67** 330.
5. Zu F Q, Zhu Z G, Zhang B, Feng Y, Shui J P *J. Phys.: Condens. Matter* 2001 **13** 1145.
6. Xi Y, Zu F Q, Li X F et al. *Physica Letters A* 2004 **329** 221.

*Corresponding author: plevachuk@mail.lviv.ua

Electrical Conductivity and Photoconductivity Studies of TiO_2 Sol-Gel Thin Films and the Effect of N-Doping

K. Pomoni[1*], A. Vomvas[1], Chr. Trapalis[2]

[1] *Department of Physics, University of Patras, 265 00 Patras, Greece*

[2] *Institute of Materials Science, National Centre for Scientific Research "Demokritos", 153 10, Ag. Paraskevi, Attiki, Greece*

A comprehensive study of the conductivity of sol-gel nanocrystalline TiO_2 thin films is presented, both undoped (heat treated in 450, 500 and 600°C) and N-doped (heat treated in 500 and 600°C), in vacuum and in air, in dark and as a function of illumination time and light intensity, in an effort to better understand the influence of light on the transport properties of undoped and N-doped TiO_2.

A comparison of the dark conductivities of the undoped samples in vacuum and in air emphasizes the role of either the adsorbed oxygen (450°C) or water (500 and 600°C). Predictably, the addition of N reduces this influence.

At room temperature, the transient photoconductivity appears to be very sensitive to the environment for almost all samples. In vacuum, the rise and decay of p is slow, which suggests that the thermal release of electrons from traps dominates. In air, the rise and the decay are much faster, indicating that the predominant mechanism is recombination. However, in the case of the N-doped sample heat-treated at 600°C, the presence of nitrogen influences the photoconductivity behavior, revealing much longer saturation and decay times.

*Corresponding author: pomoni@physics.upatras.gr

Low-Temperature Optical Spectra of CdTe Thin Films

I. Virt[1,4], V. D. Popovych[1], I. S. Bilyk[1], R. V. Gamernyk[2], Yu. P. Gnatenko[3], P. N. Bukivskii[3]

[1] *Drogobych State Pedagogical University, 24 Ivan Franko str., 82100 Drogobych, Ukraine*

[2] *Lviv National University, 8 Kyrylo and Mefodiy str., 79005 Lviv, Ukraine*

[3] *Institute of Physics, National Academy of Science of Ukraine, 46 Pr. Nauki, 03028 Kyiv, Ukraine*

[4] *University of Rzeszów, Rejtana 16A, Rzeszów 35-959, Poland*

In this work, we present the results of investigations of low-temperature (4.5 K) optical properties of CdTe thin films prepared by the pulse laser deposition (PLD) method. Films were deposited by using a YAG:Nd laser with the power of 1 J, pulse duration of 10 ns and repetition frequency of 1 Hz on CdTe single crystalline substrates heated to about 250°C. An argon laser (wavelength $\lambda = 488$ nm) was used to excite photoluminescence (PL). We recorded PL and reflection spectra for both thin films and substrates (back side of the samples).

An extremely sharp doublet, consisting of two close peaks at 779.3 and 779.8 nm, dominates the exciton emission region of the substrates' PL spectra. They are attributable to recombination of excitons bound to neutral acceptors (A^0X-lines): Cu and Ag residual impurities. The prominent feature (D^0X-line) at 778 nm has been known due to the recombination of an exciton bound with a neutral hydrogenic donor. The low-wavelength shoulder of this line is connected with the exciton bound with another donor. Two weak emissions at 776.5 and 777.3 nm are practically coincident with the maximum and minimum positions of the exciton reflection curve. This structure is identified as the transverse and longitudinal components of the polariton (i.e. exciton-photon interaction). Its presence is evidence of high structural perfection of the CdTe substrates. The long-wavelength shoulder at 781.2 is due to the emission of multi-exciton acceptor complexes, while the nature of the line at 783.6 is not clear. Notable is the emission's weakness in the edge and deep-level regions, which is also evidence of high quality of substrates.

The PL spectra of the deposited films differ significantly from those of the substrates. D^0X-lines become more intensive than A^0X ones. The features at 780.8 and 781.2 nm are due to the presence of multi-exciton complexes and the broad band with a maximum at about 7915 nm is their LO-phonon replica. Another broad band with a maximum at about 802.2 nm appears in the edge emission region. This band is actually composed of conduction band-acceptor (e, A^0) emission and a shallow donor-acceptor (DAP) recombination. The acceptor has a complex character involving a cadmium vacancy, V_{Cd}. The band at about 813.5 nm is composed of the e, A^0-LO and DAP-LO lines. The well-structured deep emission band becomes dominant in the whole PL spectrum of the films. It is known to be a sum of two components. One is the so-called Y-line with a zero-phonon transition at 839.5 nm, associated with radiative recombination of excitons trapped by the fields of extensive defects (i.e. dislocations). The other, with a zero-phonon line at 852 nm, is associated with transitions from shallow donors to the A-center in the form of a cadmium vacancy-shallow donor $(V_{Cd}\text{-}D)^-$ complex. The presence of a deep emission band is the cause of the undistinguished character of the exciton reflection spectrum of the PLD obtained CdTe films.

Absorption Spectra of Pentacene Layers Formed by the PLD Method

P. Potera[1]*, M. Kuzma[1], I. Stefaniuk[1], I. Virt[1], G. Wisz[1], O. Aksimentyeva[2]

[1] *Institute of Physics University of Rzeszów, Rejtana 16A, 35-310 Rzeszów, Poland*

[2] *Lviv Ivan Franko National University, 79005 Lviv, Ukraine*

Organic solids are promising materials for electronic devices, since they demonstrate properties comparable with those of amorphous silicon. Recently, pentacene thin layers have been studied widely due to their outstanding properties suitable for application in field-effect transistors. The electronic properties of pentacene thin films and their stability depend strongly on the film's structure and ordering. Crystal defects, grain boundaries and disorder dominate charge transport properties in the obtained layers. However, single crystalline layers of pentacene have not been grown until now. In the present paper, we study the absorption properties of pentacene layers grown by the PLD method. We find that the layers obtained using the second harmonic of laser radiation exhibit optical properties suggestive of better ordering. Pentacene layers were grown by the ordinary pulse laser deposition (PLD) method. A pulsed YAG: Nd^{3+} laser was used with the maximal energy of 0.4 J in the pulse. The pulse duration was 40 ns and the repetition time was 3 s. Two laser wavelengths were used, the first harmonic of 1064 nm and the second one of 532 nm. The target in the shape of a tablet was prepared from pressed pentacene powder. The target and the substrates were placed in a quartz tube in a vacuum chamber preserving small volume in which the material was working. Layers were deposited on glass substrates with an ITO layer and KCl, BaF_2 or Al_2O_3 substrates. All the glass/ITO substrates used had the same thickness and optical properties. The target-substrate distance was 0.5–3.0 cm. Layers were deposited at room temperature. The samples' description and the technological parameters of the deposition process were collected. The absorbance spectra were registered with a UNICAM UV- 300 spectrophotometer in the wavelength region of 400 to 800 nm. The internal reflection losses were disregarded. The glass/ITO substrate practically did not influence the layers' optical properties. In the absorbance spectrum of the thinnest layer the structure of absorption was absent, probably because pentacene concentration in the layer was very small due to the smaller number of pulses in connection with small energy density. The absorbance measurements of layers prepared on glass/ITO substrates with PLD have shown that the layers deposited using the second harmonic are of higher quality than those of the first harmonic. This confirms the thesis that laser wavelength plays an important role in the PLD method applied to polymer layer growth. Studies in the dependence of other PLD parameters, such as substrate temperature, are necessary to grow pentacene layers of high crystal quality.

*Corresponding author: ppotera@univ.rzeszow.pl

Stability and Phase Changes in Thin Layers of Rare-earth Metals/Iron and Other Binary Compounds

V. Prysyazhnyuk

Department of Metal Physics, Ivan Franko Lviv National University,
8 Kyrylo and Mefodiy str., 79005 Lviv, Ukraine

Thin films of binary compounds such as rare-earth metals-iron ($GdFe_2$, Gd_2Fe_{17}) were obtained by thermal vacuum evaporation of a polycrystal charge. In order to enable structural examination, a 500–600 Å thick films on were precipitated NaCl and KCl chips. The films' thickness was determined with an optical interferometer. The temperature of substrates carriers varied from 300 to 500 K. Structural research of the films was carried out with an electron microscope. The thermal resistance and kinetics of crystallization of amorphous condensates were explored through straight heating in the microscope's column at the rate of 5–30 K/min.

Temperature stability in the temperature dependence of substrates was investigated. Phase transformations were observed during crystallization of amorphous films. At room temperature of substrates (T_s) amorphous films are formed, amorphous-crystalline at $T_s = 300$–500 K, and polycrystalline at $T_s > 500$ K. Formation of two phases, Gd_6Fe_{23} and a–Fe, was observed upon crystallization of Gd_2Fe_{17} amorphous films. In the films obtained at substrate temperatures > 500 K, 3 phase sets were present: a hexagonal Gd_2Fe_{17} phase of the Th_2Ni_{17} structural type, a rhombohedral Gd_2Fe_{17} phase of the Th_2Zn_{17} structural type, and a hexagonal $GdFe_5$ phase of the $CaCu_5$ structural type. Films of the $GdFe_2$ compound were shaped in the reference for massive state $GdFe_2$ to cubic structure with face-centered lattice.

Fuzzy Logic Modeling of Surface Treatment Processes

J. Ratajski[1], J. Dobrodziej[2], T. Suszko[1], A. Mazurkiewicz[2]

[1] *Institute of Mechatronics, Nanotechnology and Vacuum Technique, Koszalin University of Technology, Racławicka 15–17, 75-620 Koszalin, Poland*

[2] *Institute for Sustainable Technologies – National Research, Pułaskiego 6–10, 26-600 Radom, Poland*

The intensive development of surface engineering inspired by the needs of industry is connected with continuous research including the building of models illustrating physical and chemical phenomena in order to effectively design and control the surface treatments processes.

The difficulty of in-situ measurements giving information on the changes taking place on the surface and inside the basis material (or in layers of multifunctional materials) during a surface treatment process creates many problems in elaborating analytical models describing numerically the relations between physical and chemical phenomena and the features of the obtained surface layers.

The lack of adequate analytical models and calculation problems motivate the search for alternative surface engineering solutions enabling elimination of iterations or trial-and-error methods in the development and modernization of surface technologies. This is one of the fastest growing trends in surface engineering, of great innovative potential.

A complex energetic model is presented in the paper, encompassing a combination of artificial intelligence methods with a data base.

The model enables performing the following tasks:

- searching analogies and contrasts between processes of surface treatment (data mining methods),
- concluding on the physical, chemical and operational features of surface layers in computer-designed surface treatment (an expert system),
- prediction of the chosen layers' properties (artificial neural networks) and
- calculation of selected parameters of the environment of thermo-diffusional processes (evolutionary algorithms).

Transport and Optical Properties of New Polysulfone–Polydimethylsiloxane Block Copolymers in Thin Films

G. I. Rusu[1], A. Airinei[2], M. Rusu[1], V. Hamciuc[2], A. P. Râmbu[1], M. Diciu[3], P. Prepelita[1]

[1] *Faculty of Physics, Al. I. Cuza University, 11 Carol I Blvd., Iași, 700506, Romania*

[2] *P. Poni Institute of Macromolecular Chemistry, Aleea Grigore Ghica Voda, 41A, 700487, Iași, Romania*

[3] *Traian Tehnical College, 203 Traian Blvd., 800186, Galați, Romania*

In recent years, there has been growing interest in block polymers mainly due to their unique properties, different from those of the component polymers.

In the solid state, polysulfone (PSF)-polydimethylsiloxane (PDMS) block copolymers have a continuous phase formed by PSF blocks in which PDMS blocks are dispersed.

Such copolymers, of various compositions (Tab. 1), were prepared by condensing chloro-terminated polysulfone oligomers with α, ω-dihydrogensilyl-polydimethylsiloxane in a refluxing chlorobenzene solution in the presence of urea as hydrogen chloride acceptor. The resulting copolymers had alternating blocks of PSF and PDMS of the $(AB)_n$ type. Their electrical and optical properties were investigated in thin film samples (d = 300–2600 nm) deposited onto glass substrates from an N,N-dimethylformamide solution by the spin coating deposition method.

The films' electrical conductivity was measured using surface-type cells. The Seebeck coefficient was determined by the thermal probes method. The temperature dependences of electrical conductivity and the Seebeck coefficient were studied in the ΔT = 300–475 K temperature range. It was established experimentally that the samples with a stable solid-state structure can be obtained by being subjected to a heat treatment consisting of several successive heating and cooling phases within a certain temperature range, ΔT, characteristic for each copolymer (Tab. 1).

Copolymer	Cs [%]	d [nm]	η [%]	σ_c [Ω^{-1} cm^{-1}]	ΔT [K]	σ_T [Ω^{-1} cm^{-1}]	T_c [K]	ΔE [eV]
AH.P1	6.23	1150	0.33	$7.25\text{x}10^{-8}$	300-475	$5.16\text{x}10^{-8}$	350	1.60
AH.P2	10.53	1100	0.37	$6.24\text{x}10^{-8}$	300-430	$1.25\text{x}10^{-7}$	330	1.44
AH.P3	18.32	980	0.18	$2.66\text{x}10^{-9}$	300-476	$1.10\text{x}10^{-8}$	360	1.50
AH.P4	28.44	950	0.19	$2.15\text{x}10^{-8}$	300-465	$2.25\text{x}10^{-8}$	340	1.40
AH.P5	38.03	1050	0.12	$1.06\text{x}10^{-7}$	300-475	$3.04\text{x}10^{-7}$	355	1.66

Table 1: Cs – siloxane content [%]; η – reduced viscosity (0.2 g/dL solution in dichloroethane at 25°C); d – film thickness; σ_c – electrical conductivity at room temperature before heat treatment; ΔT – temperature range in which the heat treatment of sample was performed; σ_T – electrical conductivity at room temperature after the heat treatment; T_c – the characteristic temperature for respective samples; ΔE – the energy band gap

An exponential increase in electrical conductivity with temperature has been observed for the studied copolymers throughout the ΔT temperature range. Thus, the polymers have shown semiconducting characteristics determined by their specific macromolecular structure, which affords extended conjugation of electrons along the copolymer chain.

It has been found that the intrinsic conduction domain begins at a certain temperature, T_c, characteristic for each sample (Tab. 1). For $T < T_c$ the polymers exhibit extrinsic conduction.

For the studied copolymers, the expression

$$\ln \sigma_0 = \beta + \Delta E, \tag{1}$$

describing the compensation effect, has been verified by our experimental results. In Eq. (1), σ_0 is an pre-exponential factor in the standard semiconduction equation

$$\sigma = \sigma_0 . \exp\left(-\frac{\Delta E}{2kT}\right), \tag{2}$$

where ΔE is the thermal activation energy of electrical conduction, while β and γ are characteristic parameters. (For the investigated class of polymers, $\beta = -14.52$ and $\gamma = 15.58$ eV^{-1}).

The Seebeck coefficient, S, is positive in the intrinsic domain and decreases with increasing temperature. The values of carriers' mobility, b, ($b = \mu_e/\mu_h$, where μ_e is the electron mobility and μ_h is the hole mobility) has been estimated from $S = f(1/T)$ dependences. The obtained values, $b = 0.85$–0.95, are interpreted by supposing that the conduction band has a complex structure.

The transmission spectra have a sharp edge at the wavelength corresponding to the forbidden energy gap of the respective polymer. The optical band gap has been estimated by supposing that forbidden direct band-to-band transitions are predominant. The obtained values ($E_g = 1.50$–1.70 eV) are in good agreement with those determined from the temperature dependence of electrical conductivity.

Structural and Optical Properties of ZnO Thin Films Deposited onto ITO/Glass Substrates

M. Rusu, G. G. Rusu, M. Girtan

Al. I. Cuza University, Faculty of Physics,
Carol I Blvd. No 11, 700506 Iași, Romania

1. Introduction

Zinc oxide (ZnO) thin films have recently enjoyed considerable attention due to their applications as an active semiconductor compound in transparent electronic devices. Several methods have been used to grow ZnO thin films such as chemical vapor deposition, electro-deposition, the sol-gel technique, metal-organic chemical vapor deposition, spray pyrolysis, r.f. magnetron sputtering, pulsed laser deposition, etc. [1–7]. Another technique used in preparation of oxide films is the thermal oxidation of vacuum-deposited metallic (Cd, Sn, In) films [8]. In this paper, ZnO thin films obtained by thermal oxidation of Zn films evaporated in vacuum onto ITO/glass substrates are studied. Structural and optical properties of so obtained ZnO films have been investigated.

2. Experimental

Metallic zinc was evaporated in standard vacuum equipment (10^{-5} Torr) onto unheated commercial ITO/glass substrates, using the quasi-closed volume technique [9]. The temperature of the evaporation source was maintained at 723 K during film deposition. After preparation, the as-deposited Zn films (d = 100–160 nm) were oxidized by heating under ambient conditions at the rate of 12 K/min from room temperature to 550 K. The crystalline structure of the studied films was investigated by X-ray diffraction (XRD) analysis using Cu-K α radiation (λ = 1.5418 Å) in the range of 2θ = 20–80°. The films' transmittance was measured using a UV-VIS spectrometer in the 350–1400 nm wavelength range.

3. Results and discussion

3.1. Structural characteristics

XRD patterns representative for as-deposited (Fig. 1b) and heat-treated (Fig. 1c) Zn films are shown in Fig. 1. The XRD pattern of the ITO/glass substrate used for deposition of the studied films is also shown in Fig. 1a. As follows from Fig. 1b, the as-deposited Zn films are polycrystalline and have a hexagonal structure. The intense (002) reflection at 2θ = 36.3° indicates that, in respective films, Zn microcrystallites grow predominantly with their (002) plane parallel to the substrate's surface. Heating up to the temperature of 550 K determines the oxidation of Zn films and the films' transparence. The well-defined (002) and (101) diffraction peaks shown in Fig. 1c, characteristic for the polycrystalline hexagonal structure of bulk ZnO, indicate the formation of the respective compound, with preferred (002) orientation of microcrystallites. Comparing the patterns from Figs. 1a and 1c one can conclude that the annealing process does not affect the crystalline structure of the ITO substrate.

3.2. Optical properties

The reflection and transmission spectra of the sample shown in Fig. 1c are plotted in Fig. 2. Apparently, heat-treatment determines an important increase in the film's transmittance. The absorption coefficient was calculated from the transmission spectra. Assuming allowed direct transitions, the $(\alpha h\nu)^2$ vs. $h\nu$ dependence has been plotted in Fig. 3. By extrapolating the linear portion of the plot to $(\alpha h\nu)^2 = 0$,

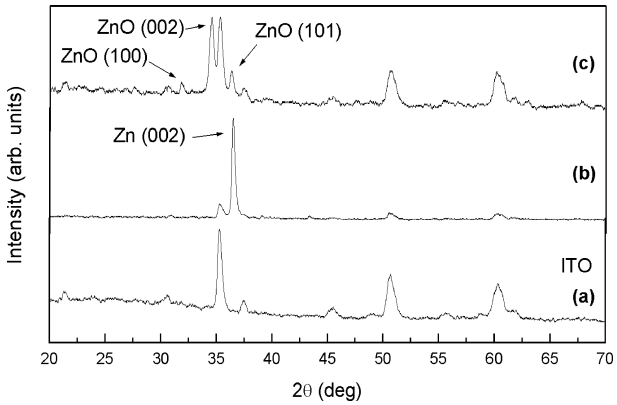

Figure 1: XRD patterns typical for the studied films: (a) ITO substrates; (b) as-deposited; and (c) heat-treated samples (the non-indexed peaks are of the ITO substrate)

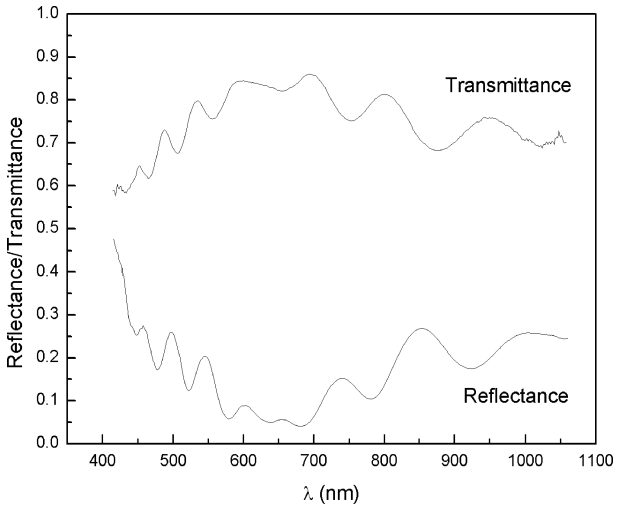

Figure 2: Reflexion (bottom) and transmission (top) spectra for ZnO/ITO samples

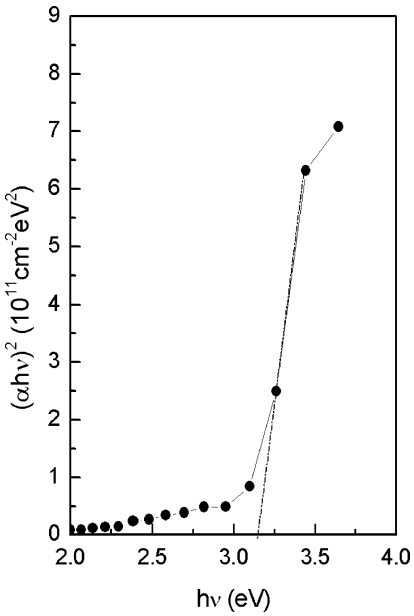

Figure 3: $(\alpha h\nu)^2$ vs. $h\nu$ plot for ZnO/ITO samples

the value of the optical band gap energy, E_g, has been calculated. The value of 3.16 eV obtained for the optical band gap is relatively lower than those of ZnO single crystals (3.37 eV). This lower value of E_g may be due to the greater density of donor states near the conduction band determined by the oxygen vacancies.

4. Conclusions

ZnO films were obtained by post-deposition heating of Zn films evaporated onto ITO substrates. They have a polycrystalline hexagonal (002)-oriented structure, an optical transmittance in excess of 80% and a value of 3.16 eV for the optical band gap.

5. References

1. P. Wu, J. Zhon, N. W. Emanetoglu, S. Muthukumar, Y. Lu, J. Electron. Mater., 33 (6) (2004) 596
2. S. Kumar, V. Gupta, K. Sreenivas, Nanotechnology, 16 (2005) 1167
3. Z. L. Wang, J. Phys.-Condens. Mat., 16 (2004), R829
4. M. N. Kamalasanan, S. Chandra, Thin Solid Films, 288 (1996) 112
5. F. Xiu, Z. Yang, D. Zhao, J. Liu, K. A. Alim, A. A. Baladin, M. E. Itkis, R. C. Haddon, J. Cryst. Growth, 286 (2006) 61
6. K. Ramamoorthy, C. Sanjeeviraja, K. Sankaranarayanan, P. Misra, L. M. Kukreja, Curr. Appl. Phys., 6 (2006) 103
7. Y. J. Kim, Y. T. Kim, H. K. Yang, J. C. Park, J. I. Han, Y. E. Lee, H. J. Kim, J. Vac. Sci. Technol. A, 15(3) (1997) 1103
8. M. Girtan, G. I. Rusu, G. G. Rusu, S. Gurlui, Appl. Surf. Sci., 162–163 (2000) 492
9. M. Rusu, I. I. Nicolaescu, G. G. Rusu, Appl. P. A 70 (2000) 565

Sol-Gel Synthesis and Characterization of Nd-doped $Y_4Al_2O_9$ Nanopowders

A. Rzepka[1]*, W. Ryba-Romanowski[2], R. Diduszko[1], L. Lipińska[1], A. Pajączkowska[1]

[1] *Institute of Electronic Materials Technology, 01-919 Warsaw, Poland*

[2] *Institute of Low Temp. and Struct. Research, Polish Ac. Sc., 50-422 Wroclaw, Poland*

$Y_4Al_2O_9$ – yttrium aluminum monoclinic (YAM) crystals are known as a host matrix for solid-state lasers. YAM belongs to monoclinic structures with space group $P2_1/c$ and melts congruently at 2030°C. Difficulties have been reported in YAM crystal growth and even in sol-gel synthesis [1]. Recently, the sol-gel processes have been mainly investigated with addition of nitrates.

In the present research, nanosized powders of YAM, pure and doped with 3 at% Nd ions, were obtained by the sol-gel method. A solution with ethylene glycol as the complexing agent and acetic acid was used. No one-phased YAM was obtained from the solution without the complexing agent.

The gels were dried at 120°C for 12 h and then ground in an agate mortar until fine powder was obtained. The powder was annealed at 1100°C for 12 h in air. The samples obtained from the solution with ethylene glycol were one-phased and their crystallite sizes calculated from the Scherrer formula were about 50 nm. The morphology of powders obtained from the solutions with and without the complexing agent was different. All samples had large areas of agglomeration (several dozen μm) but those without ethylene glycol had agglomerates with understructure.

The samples' crystal structures were characterized with X-ray diffraction (XRD) using a Siemens D-500 diffractometer with CuK_α radiation at 1.548 Å. The size and morphology of nanopowders were analyzed with scanning electron microscopy (SEM) performed with a DSM-950 microscope. The nanopowders' luminescence spectra and luminescence decay curves were recorded at room temperature.

References

1. Hess N J, Maupin G D, Chick L A, Sunberg D S, McCreedy DE and Armstrong T R, 1994 Journal of Materials Science **29** 1873–1878.

*Corresponding author: Agnieszka.Rzepka@itme.edu.pl

The Equation of State of Liquid Metallic Hydrogen

V. Shvets[1], Ya. Lepikh[2], T. Shvets[1], O. Vlasenko[1]

[1] *Department of High Mathematics, Odessa State Academy of Refrigeration, Dvorianska 1/3, 65082 Odessa, Ukraine*

[2] *Department of Experimental Physics, Odessa National University, Dvorianska 2, 65082 Odessa, Ukraine*

The equation of state of liquid metallic hydrogen is explored numerically. Investigations are carried out at temperatures from 3000 to 20 000 K and densities from 0.2 to 3 mole/cm^3, corresponding to the experimental conditions under which metallic hydrogen is produced on earth and the conditions in the cores of giant planets of the solar system such as Jupiter and Saturn. It is assumed that hydrogen is in the atomic state and all its electrons are collectivized. The perturbation theory is applied in the electron-proton interaction to determine the thermodynamic potentials of metallic hydrogen. The electron subsystem is considered in the random phase approximation with regard to the exchange interaction and the correlation of electrons in the local-field approximation. The proton-proton interaction is taken into account in the hard-spheres approximation. The thermodynamic characteristics of metallic hydrogen are calculated with regard to the zero-, second-, and third- order perturbation theory terms. The third-order term proves to be essential at moderately high temperatures and densities, though it is much smaller than the second-order term. The thermodynamic potentials of metallic hydrogen are monotonically increasing functions of density and temperature. The values of pressure for the temperatures and pressures characteristic of conditions under which metallic hydrogen is produced on earth coincide with the corresponding values reported by the discoverers of metallic hydrogen to a high degree of accuracy. The temperature and density ranges in which the liquid phase of metallic hydrogen exists are found.

References

1. Shvets V T 2007 *Physics of Disordered Metals*, Maiak, 500
2. Shvets V T 2007 *JETP* **104** (4) 655

Light Intensity Dependence of the Short-circuit Current in Bilayer Organic Photovoltaic Devices

R. Signerski

Department of Physics of Electronic Phenomena,
Gdansk University of Technology,
Narutowicza 11/12, 80-952 Gdansk, Poland
ryszard@mif.pg.gda.pl

The short-circuit current density's dependence on the intensity of light, ($jsc(I_0)$), is often studied in order to analyze the influence of transport processes and charge carrier recombination on the performance of organic photovoltaic systems [1, 2]. This work concerns bilayer organic photovoltaic devices ($M_1|O_1|O_2|M_2$), consisting of two organic layers, O_1 and O_2, forming a planar heterojunction, $O_1|O_2$, and electrodes, M_1 and M_2. Photogeneration of charge carriers is a result of exciton dissociation on the $O_1|O_2$ interface. Electrons and holes are separated. Consequently, there is only electron current in one organic layer and only hole current in the other layer. This means that charge carrier recombination and photogeneration may be present only in a very thin layer, near the $O_1|O_2$ interface.

This work presents an analytical and numerical description of the $jsc(I_0)$ dependence for bilayer organic photovoltaic devices. Taking into account a constant-field approximation [3] for the two organic layers, a simple expression describing the $jsc(I_0)$ relationship has been derived. The influence of charge carrier trapping in organic layers on the $jsc(I_0)$ is analyzed numerically.

The results obtained from theoretical calculations are compared with experimental $jsc(I_0)$ characteristics.

Acknowledgements

This work has been supported by the Polish Ministry of Science and Higher Education with a grant for years 2006-2009 under Program No. 3T11B06530.

References

1. Brabec C, Dyakonov V, Parisi J and Sariciftci N S (Eds) 2003 *Organic Photovoltaics*, Springer
2. Sun S-S and Sariciftci N S (Eds) 2005 *Organic Photovoltaics*, Taylor&Francis
3. Hall K J, Bonham J S and Lyons L E 1978 *Aust. J. Chem.*, **31** 1661

P-78

Assembling Amphiphilic Multi-arm Star-branched Copolymers: a Computer Simulation Study

K. Charmuszko, D. Gront, A. Sikorski

Department of Chemistry, University of Warsaw
Pasteura 1, 02-093 Warszawa, Poland

A lattice model of branched polymer chains was designed and studied. Its chains consisted of united atoms (segments) in positions restricted to a [310] type lattice. The model macromolecules were star-branched chains consisting of two kinds of polymer segments defined as hydrophilic and hydrophobic. The applied force field consisted of the long-range contact potential between a pair of non-bonded segments and of a local stiffness. We used a variant of the Monte Carlo method referred to as the pruned-enriched Rosenbluth method (PERM) to study the static and thermodynamic properties of the model chain. The static properties and structure of model chains were studied under a wide range of solvent conditions. The influence of the number of arms on the process of their self-assembly was shown and discussed. The applicability of the PERM method was compared with other simulation techniques (Replica Exchange, Multi-histogram)

Temperature Dependence of EPR/FMR Spectra of Carbon-coated Nickel Nanoparticles and a TEMP Spin Probe Dispersed in Paraffin

M. Soboń[1*], I. E. Lipiński[2], N. Guskos[2,3], U. Narkiewicz[4], M. Podsiadły[4]

[1] *The Faculty of Management and Economics of Services of Szczecin University, Cukrowa 8, 71-004 Szczecin*

[2] *Institute of Physics, Szczecin University of Technology, Al. Piastów 17, 70-310 Szczecin*

[3] *Solid State Section, Physics Department, University of Athens, Panepistimiopolis, 15 784 Zografou, Athens, Greece*

[4] *Institute of Chemical and Environment Engineering, Szczecin University of Technology, Pułaskiego 10, 70-332 Szczecin*

Agglomerated magnetic nanoparticles of nickel coated with carbon and a low-concentration TEMP spin probe dispersed in a paraffin matrix have been studied. Temperature dependences of the EPR/FMR (ferromagnetic resonance) spectra have been recorded in a wide range of temperatures. Very intense EPR spectra of the TEMP spin probe and a broad FMR line of nickel have been recorded throughout the temperature range. The temperature dependence of the EPR line and the position of the spin probe's resonance line have been shifted towards low magnetic fields. After thermal annealing, the "soft" matrix field with low concentration of magnetic nanoparticles could provide new arrangement of dipole-dipole interaction which influence on the internal magnetic field.

*Corresponding author: marcin.sobon@wzieu.pl

The Role of Clustering in the Formation of the Gel-like Phase of N_2O Condensates.

A. A. Solodovnik*, V. V. Danchuk, M. A. Strzhemechny

B. Verkin Institute for Low Temperature Physics and Engineering of National Academy of Sciences of Ukraine, 47 Lenin ave., Kharkov 61103, Ukraine

A theoretical analysis [1] of the nucleation behavior of polar substances predicts the formation of a variety of clusters: linear chains, branched chains and ring *polymers* during the condensation process. Their particles have been found [2] to associate and form chains of dipoles aligned *head-to-tail*. According to experimental data [3] polar molecules may be sufficiently associated in supersaturated vapors. In this case, the vapor is composed of individual molecules and small, relatively stable complexes. In this system, nucleation is initiated by chainlike clusters.The system may form a *glassy* structure with percolated chains [4]. An interpenetrating network of uncollapsed dipolar chain clusters floating in a dispersion medium is the model of a gel-like phase according to [1]. A convenient model object to investigate the polar substance is solid N_2O. This molecular crystal consists of asymmetric linear molecules with dipole moment. The Pa_3 space group describes the solid nitrous oxide's structure, i.e. the molecular axes and their dipole moments are directed along the $\langle 111 \rangle$ cube diagonals. Investigations were carried out by the transmission electron diffraction technique with a special liquid-helium cryostat. Specimens were prepared directly in situ by simultaneously depositing 99.99% pure N_2O gas on the substrates consisting of two parallel strips of different materials, amorphous carbon and fine-grained polycrystalline aluminum. Condensation was realized at various temperatures. The gas was previously cooled in a condensation coil passing through a vessel containing liquid nitrogen. The condensation of cooled N_2O gas at 3.4 K led to the formation of an anomalous state of the deposits. A non-crystalline phase was observed after sample preparation. The diffraction pattern showed one bright broad halo in the position where the (111) and (200) reflections of Pa_3 phase were expected to occur. The obtained phase was stable at the helium temperature. This disordered state of the condensates was very different from that of a typical *simple* amorphous phase. Its unusual character became apparent during the annealing process. Heating the samples above 11–12 K caused a surprising transformation. Bright point reflexes and a halo appeared. The relative location and intensities of the diffraction peaks indicated that the transition resulted in the growth of hexagonal-lattice nanoparticles, coexisting with an amorphous medium. The corresponding calculation gave the following values of interplanar distances, and (hkl), respectively: 3.471 Å (100), 3.238 Å (002) and 3.072 Å (101). These peaks are important in establishing hexagonal symmetry. A new phase transition occurred which had no analog in the phase diagram of the molecular crystals formed from linear 3-atom molecules. The structure of condensates did not change at a constant temperature, but the dimension of crystallites decreased. The point reflexes were transformed into diffraction circular arcs. The temperature range in which the hexagonal phase existed was limited. On heating the samples up to 28–30 K, the patterns changed quickly: the hexagonal reflexes disappeared and a halo was observed. The new crystalline phase was stable up to 30 K, following which the crystallites collapsed. When the annealed samples were cooled to the helium temperature at the initial stage of vanishing diffraction peaks, some of these exhibited a weaker tendency to form the unusual phase. Upon warming by more than 30 K, the hexagonal phase did not reappear on the subsequent cooling to the helium temperature, the change being irreversible. The properties of phases with and without permanent molecular dipole moments were studied to investigate the role of dipolar interaction in the nucleation process. The nearest analog of the solid nitrous oxide is the solid carbon dioxide. As a molecule, CO_2 is physically very similar to N_2O, except for its dipole moment. A study was carried out for CO_2 condensates under the same conditions

*Corresponding author: solodovnik@ilt.kharkov.ua

as the N_2O samples in order to compare the results. It was established that the condensation of undercooled CO_2 gas led to the formation of an amorphous phase. The diffraction reflexes did not appear upon heating and cooling the samples. The obtained results confirmed that the presence of a dipole moment was an important factor in the formation of this *glassy* state. When the condensation temperature was increased to 10 K, the structure of as-grown samples corresponded to the disordered phase. Hexagonal reflexes, a halo and traces of unknown peaks were observed upon heating. Above 30 K all crystallites collapsed.

On the basis of the above experimental findings, we may suggest that these unexpected states of N_2O condensates are in many respects analogs of sol-gel glasses. The local structure of the obtained disordered phase is actually quite different from the usual amorphous one. N_2O aggregates were formed due to the presence of critical nuclei in the cooled vapor. We believe that N_2O nanoparticles of hexagonal structure were present in the dispersion medium. The novel temperature behavior of the structural characteristics during annealing may also be an indirect confirmation of this assumption. Although our techniques do not allow obtaining direct information about nuclear shapes, one can assume that the presence of the dipole moment is an essential factor for the formation of the gel-like state.

References

1. P R ten Wold D W Oxtoby and D Frenkel 1998 *Phys. Rev. Lett.* **81** (3695)
2. J J Weis and D Levesque 1993 *Phys. Rev. Lett.* **71** (2729)
3. D Wright R Caldwell C Moxeley and M S El-Shall 1993 *J. Chem. Phys.* **98** (3356)
4. M E van Leeuwen and B Smit 1993 *Phys. Rev. Lett.* **71** (3991)

Finite Element Analysis of Deformation of Auxetic Plates

T. Stręk[1], B. Maruszewski[1], K. W. Wojciechowski[2]

[1] *Institute of Applied Mechanics, Poznan University of Technology, ul. Piotrowo 3, 60-965 Poznan, Poland*

[2] *Institute of Molecular Physics, Polish Academy of Sciences, Smoluchowskiego 17, 60-179 Poznan, Poland*

A new field of challenge are studies of materials exhibiting negative Poisson's ratio, first manufactured in 1987 by R. S. Lakes [1] and later named auxetics by K. E. Evans [2]. Auxetic materials are those having a negative Poisson's ratio. Poisson's ratio is a negative ratio of transverse dimension change to longitudinal dimension change of a body when an infinitesimal change of a stress acting along the longitudinal direction occurs whereas the other stress components remain unchanged [3]. Thus, when stretched along one direction auxetic materials expand at least in one of perpendicular directions. Similarly, a contraction along one dimension causes a contraction along at least one of perpendicular directions. Auxetics are of interest both intellectually [4] and also from the point of view of potential applications [5].

In this work, shape deformation of auxetic thin plates is analysed using the finite element method. Two kinds of square plates, of sides parallel to the x, y axes, respectively, were studied: (i) without any fixed boundary conditions, (ii) with the 'sides' parallel to the x axis being fixed. In both cases, a uniform stress acting along the x direction was symmetrically applied to those sides of the plate which were perpendicular to the x axis. Qualitatively different deformations were observed in the two studied cases when the Poisson's ratio of the material tends to -1. In the first case the displacement vector at the sides at which the stress is applied was parallel everywhere to the direction of the applied force. In the second case, however, near to the corners of the plate, the displacement vector was *anti*parallel to the applied force!

Thus, it has been shown that even for samples of very simple geometry, one can observe local behaviours characteristic to negative stiffness materials (i.e. unstable ones) for stable systems if their Poisson's ratio tends to unity. This phenomenon can be of interest, e.g., in the context of the recent studies of composites with inclusions of negative stiffness [6].

References

[1] Lakes R 1987 *Science* **235** 1038
[2] Evans K E, Nkansah M A, Hutchinson I J, and Rogers S C 1991 *Nature* **353** 124
[3] Landau L D, Lifshits E M 1986 *Theory of elasticity*, Pergamon Press, London
[4] K. W. Wojciechowski 1989 *Phys. Lett. A* **137** 60
[5] See, e.g., Wojciechowski K W, Alderson A, Alderson K L, Maruszewski B, Scarpa F 2007 *Phys. Stat. Solidi B* **244** 813; see also papers and references in that issue.
[6] Jaglinski T, Kochmann D, Stone D, Lakes R S 2007 *Science* **315** 620

Nitridation of SiO_2–B_2O_3 Aerogels

K. Szaniawska, M. Gładkowski,
L. Wicikowski, L. Murawski

Faculty of Applied Physics and Mathematics, Gdansk University of Technology,
Narutowicza 11/12, 80-952 Gdansk, Poland

SiO_2-B_2O_3 aerogels were prepared by drying wet gels under supercritical conditions for ethanol in an autoclave. Aerogels were nitrided for 6h in flowing ammonia at the temperature of 1200°C. We have found that the amount of nitrogen incorporated in these aerogels always exceed 20 wt%. This is much more than the amount of nitrogen incorporated in the pure silica aerogel nitrided under the same conditions. The specific surface area of SiO_2–B_2O_3 aerogels was measured at 77 K by the single-point BET method an the nitrogen adsorption technique. The values of specific surface area were between 311 m^2/g and 360 m^2/g. After nitridation, some shrinkage of aerogels was observed and the surface area decreases by about 20%. Bands situated at 465, 800 and 1085 cm^{-1} were observed in the FTIR spectra of SiO_2–B_2O_3 aerogels, typical for SiO_2. However, a band at 1085 cm^{-1} was very broad and extended to 1500 cm^{-1}. The absorption band between 1200 and 1500 cm^{-1} is characteristic for three-coordinated boron. After nitridation, a shift of the 1085 cm^{-1} band towards the lower wavelenghts was observed, an indication that Si–N and B–N bonds were formed in the nitrided aerogeles.

Hyperfine Interactions in 2H13 Steel Subjected to Ball Milling

T. Szydło[1], D. Oleszak[2], E. Jartych[1], T. Pikula[1]

[1] *Department of Experimental Physics, Technical University of Lublin, Poland*

[2] *Faculty of Materials Science and Engineering, Warsaw University of Technology, Poland*

Improved physical properties of steel can be achieved through refinement of their structure down to the nanocrystalline range. Ball milling is an effective technique for obtaining nanocrystalline materials. Decreasing the crystallite size during ball milling is often accompanied by phase transformations of the material. X-ray diffraction and Mössbauer spectroscopy are complementary methods of monitoring and discerning the phases formed during ball milling.

This work is devoted to obtaining the nanocrystalline structure in 2H13 steel chips subjected to ball milling in a planetary mill. An analysis of X-ray diffraction patterns was performed using the Hall-Williamson method. It enabled determining the average crystalline sizes and the mean level of internal strains at every stage of the milling process. Mössbauer spectra revealed a broad hyperfine distribution of the magnetic field. The results obtained for nanocrystalline steel powders were compared with those obtained for a bulk steel disc using the conversion electron Mössbauer spectroscopy.

Elastic Properties of Soft Sphere Crystals

K. V. Tretiakov*, K. W. Wojciechowski

Institute of Molecular Physics, Polish Academy of Sciences,
M. Smoluchowskiego 17, 60-179 Poznan, Poland

Various physical systems and phenomena have been described using inverse power potentials of the form $u(r) = \varepsilon(\sigma/r)^n$, where r is the separation between two particles, σ is the particle diameter, ε sets the energy scale and the exponent n is a parameter determining the potential hardness (softness being $\sim 1/n$). Various physical systems can be described by changing the exponent, from one-component plasma ($n = 1$) [1], through liquid alkali metals (small n) [2], molten aluminum, molybdenum and light actinides ($n = 6$) [3], molecular liquids and solids ($n = 6$, 12) [4, 5, 6], granular materials, powders and colloids (large n) [7] to hard spheres ($n \to \infty$) [8, 9]. One of the reasons of the rapidly growing interest in systems interacting through the inverse power potential is that particles of varying softness can be used for various applications.

In this work, the influence of potential softness on the elastic properties of soft spheres has been investigated with Monte Carlo (MC) simulations. The elastic constants and Poisson's ratio of soft sphere f.c.c. crystals [10, 11] were determined using a constant pressure ensemble of variable box shape (NpT). Particle motions under high pressure have been shown to decrease the Poisson's ratio with respect to the static case, corresponding to zero temperature. It has been also shown that Poisson's ratio can nbe reduced by increasing the exponent, n, in the potential. The simulations have demonstrated clearly that, when $T > 0$, the elastic constants of hard spheres can be obtained by taking the limit $n \to \infty$ for soft spheres. When $T > 0$, the elastic constants of soft spheres tend to those of the static model for any finite n.

Acknowledgements

This work was supported by the Polish Ministry of Science and Higher Education, grant no. N20207032/1512 (2007–2010).

References

1. Stringfellow G S, DeWitt H E, and Slattery W L 1990 *Phys. Rev. A* **41** 1105
2. Ben-Amotz A and Stell G 2004 *J. Chem. Phys.* **120** 4844
3. Ross M, Yang L H, and Boehler R 2004 *Phys. Rev. B* **70** 184112
4. Hoover W G, Gray S G, and Johnson K W 1971 *J. Chem. Phys.* **55** 1128
5. Young D A and Rogers F J 1984 *J. Chem. Phys.* **81** 2789
6. Brańka A C and Heyes D M 2004 *Phys. Rev. E* **69** 021202
7. Brańka A C and Heyes D M 2005 *Mol. Phys.* **103** 2359
8. Hoover W G and Ree F H 1968 *J. Chem. Phys.* **49** 3609
9. Tretiakov K V and Wojciechowski K W 2005 *J. Chem. Phys.* **123** 074509
10. Brańka A C and Heyes D M 2005 *Mol. Simulat.* **31** 937
11. Tretiakov K V and Wojciechowski K W 2007 *Materials Science* **25**

*Corresponding author: kvt@ifmpan.poznan.pl

Theoretical Research of the Phase Stratification Process in Binary Amorphous Alloys

V. I. Lysov, T. L. Tsaregradskaya*, O. V. Turkov, G. V. Saenko, V. V. Yarysh

Kyiv Taras Shevchenko National University,
Glushkova 6, Kyiv, 03022 Ukraine

The process of phase formation of binary amorphous alloy Fe–Zr and Ni–Zr systems are considered within the framework of the modified theory of homogeneous nucleation for binary alloys. A new expression is offered to describe the concentration dependence of relative free Gibbs energy for the initial amorphous phase, which takes into account the dependence of entropy on the change of volume at alloy formation. Concentration dependences are constructed of free Gibbs energy for the initial amorphous phase, for amorphous phases occurring during phase stratification and crystal phases allocated at the further phase formations. The obtained concentration dependences of relative integrated free Gibbs energy for the initial amorphous phase are S-shaped (due to the great change of volume at alloy formation and the negative value of entropy), which manifests the tendency of the researched alloys to stratification. Volumetric parts of new phases for amorphous alloys are designed within the framework of the modified theory of homogeneous nucleation for binary alloys. The results of calculations for amorphous alloys are in accordance with the experiment: there is stratification within the limits of an amorphous condition and 2 crystal phases are formed. The proposed equations are qualitatively adequate in describing the process of phase stratification and further growth in the crystal phases, i.e. there is coordination of the results of theoretical calculations with experiment.

*Corresponding author: tsar_grd@ukr.net

The Properties of a Heterojunction Based on ITO/Poly(3,4-ethylenedioxythiophene): Poly(Styrenesulfonate)/Pentacene/Al

P. Stakhira[1], V. Cherpak[1], Z. Hotra[1,2], B. Tsizh[3], D. Volynyuk[1], I. Bordun[1]

[1] *Lviv Polytechnic National University, S. Bandery 12, 79013 Lviv, Ukraine*

[2] *Rzeszów University of Technology, W. Pola 2, 35-959 Rzeszów, Poland*

[3] *Kazimierz Wielki University, Chodkiewicza 30, 85-064 Bydgoszcz, Poland*

A system analysis of ITO/poly(3,4-ethylenedioxythiophene): poly(styrenesulfonate)/pentacene/Al heterostructures has been conducted in view of their potential applications as photosensitive devices in the visible spectral range.

The dark and photo current-voltage characteristics of a ITO/PEDOT:PSS/Pc/Al heterojunction has been investigated. This structure has been shown to be characterized by rectifying properties, with the rectification factor of 10^2 at ± 2 V voltage. However, under small bias voltage (less than ± 1 V), the current-voltage characteristic does not exhibit exponential behavior. Such behavior of the current-voltage characteristic appears with bias of more than 1 V. For direct bias under comparatively small voltage, the current-voltage characteristic can be characterized by the Schottky junction formula.

The open-circuit voltage and short-circuit current for a ITO/PEDOT:PSS/Pc/Al heterojunction under xenon lamp irradiation from the ITO side have been respectively determined as 1.2 V and μA/cm^2. Electrical impedance measurements in the frequency range between 10 Hz and 1 MHz are reported. These dependencies can be modulated by an equivalent circuit, which is typical for the Schottky junction and consists of two series of connected RC-sections characterizing the heterostructure's spatial parameters, barrier parameters and series resistance.

Parallel conferences on advanced materials
The 4th International Workshop on Functional and Nanostructured Materials
The 8th Conference on Intermolecular and Magnetic Interactions in Matter
1–6 September 2007, Gdansk, Poland

Magnetic Interactions in $CrSbVO_6$ Studied with EPR

J. Typek[1*], N. Guskos[2], E. Filipek[3]

[1] *Institute of Physics, Szczecin University of Technology, Al. Piastów 17, 70-310 Szczecin, Poland*

[2] *Solid State Physics, Department of Physics, University of Athens, Panepistimiopolis, 15 784 Zografos, Athens, Greece*

[3] *Department of Inorganic and Analytical Chemistry, Szczecin University of Technology, Al. Piastów 17, 70-310 Szczecin, Poland*

Powder samples of the $CrSbVO_6$ compound were synthesized from a mixture of the relevant oxides by the solid state reaction technique and investigated with electron paramagnetic resonance (EPR) in the 4–300 K temperature range. At room temperature, the EPR spectrum consisted of two widely different components: a narrow (∼10 mT) line centered at $g_{na} = 1.967$ and an intense, almost Lorentzian, broad (∼100 mT) line at $g_b r = 1.975$. The EPR spectral parameters (line width, g-factor, amplitude, integrated intensity) of both components have displayed a marked thermal dependence. Of particular interest was the temperature dependence of the broad component: its amplitude increased upon cooling from room temperature, reaching a maximum at 50 K and, and decreased sharply during further cooling. The narrow line in the EPR spectrum of $CrSbVO_6$ was attributed to interacting V^{4+} monomers, the broad line – to spin clusters involving Cr^{3+} and V^{4+} ions.

*Corresponding author: typjan@ps.pl

Parallel conferences on advanced materials
The 4th International Workshop on Functional and Nanostructured Materials
The 8th Conference on Intermolecular and Magnetic Interactions in Matter
1–6 September 2007, Gdansk, Poland

An FMR Study of γ-Fe_2O_3 Nanoparticles in a PMMA Polymer

J. Typek[1*], N. Guskos[1,2], D. Petridis[3]

[1] *Institute of Physics, Szczecin University of Technology, Al. Piastów 17, 70-310 Szczecin, Poland*

[2] *Solid State Physics, Department of Physics, University of Athens, Panepistimiopolis, 15 784 Zografos, Athens, Greece*

[3] *Institute of Materials Science, NCSR, Demokritos, 153 10 Aghia Paraskevi, Athens, Greece*

Samples of nanocomposites consisting of γ-Fe_2O_3 (maghemite) nanoparticles embedded in a PMMA polymer matrix in 5 wt% and 10 wt% concentrations were obtained and investigated by the electron paramagnetic resonance technique. The ferromagnetic resonance (FMR) spectra obtained in the 3.5–300 K temperature range were studied to reveal the magnetic interactions and the influence of the matrix. A single, asymmetric line observed in the FMR spectra was decomposed into two Gaussian-shape lines arising from maghemite agglomerates with magnetic easy axes parallel and perpendicular to the steady magnetic field, evidence of the system's magnetic anisotropy. An analysis of the FMR integrated intensity allowed us to determine magnetic interactions in the maghemite subsystem. A study of the FMR spectral parameters (g-factors, line widths) revealed the presence of a relaxation processes in the matrix.

*Corresponding author: typjan@ps.pl

P-89

Application of a Laser Beam to Fabricate Self-organizing Semiconductor Nanostructures

I. Virt*, M. Kuzma, G. Wisz

Institute of Physics, Rzeszów University,
Rejtana 16a, 35-310 Rzeszów, Poland

In this report, induced growth of pentacene layers by the application of PLD method is presented. A pulse laser with the wavelength of $\lambda = 1064$ nm and energy per pulse of 0.1–1.0 J was used. Al_2O_3 plates with Au microspecies on the surface were used as substrates. Pentacene nucleation was shown to begin on gold "globules", the growing islands having a pyramidal shape. Optical and scanning microscopy investigations indicate that these islands are covered by pentacene of thickness much greater than the gold globules' height. We apply the results to a new method of fabricating structures containing quantum dots.

*Corresponding author: isvirt@mail.ru

Growth and Surface Properties of Pentacene Films Obtained by Pulse Laser Deposition

G. Wisz*, I. Virt, M. Kuzma

Institute of Physics, Rzeszów University,
Rejtana 16a, 35-310 Rzeszów, Poland

Pentacene is a very promising material for organic thin film transistors (OTFT). Organic films offer the possibility of producing mechanically flexible and low-cost devices. For quality devices, it is necessary to understand the growth processes in order to to control and optimize the material's structure, which affects the devices' functional properties. From a wide variety of organic materials, researchers' interest is focused on pentacene ($C_{22}H_{14}$) [1, 2, 3]. Its the growth model on all substrates in the substrate temperature range of $25°C \leq T_S \leq 70°C$ has been found to be diffusion limited aggregation [1]. In this work we present the result of producing pentacene films through pulse laser deposition (PLD). Pentacene films were obtained using the first ($\lambda = 1064$ nm) and second ($\lambda = 532$ nm) harmonics of a YAG:Nd^{3+} laser. Layers were grown at room temperature on various types of substrates: glass/ITO and silicon with mirror-polished or chemically patterned (pyramidal and plate-like) surface. The influence of the PLD process parameters (fluency, laser wavelength and pulse duration) on the layers' quality was studied. Surface morphology was investigated by optical and scanning electron microscopy. Some self-organization modes of layers' growth were noticed. Fluency and wavelength were shown to have a fundamental influence on the layers' quality. For layers obtained using the first harmonic ($\lambda = 1064$ nm) the surface heterogeneities were observed in the form of a spheroid formation and in the particle agglomerations. Deposition with the second harmonic ($\lambda = 532$ nm) leads to a reduction in the number and size of heterogeneities and the formation of relatively uniform films.

References

1. Stadlober B, Hass U., Maresch H. and Haase A. 2006 *Phys. Rev. B* **74** 165302
2. Klauk H (Eds) 2006 *Organic Electronics*, Wiley-VCH Verlag GmbH & Co. KGaA
3. http://researchweb.watson.ibm.com/leem/pentacene.html

*Corresponding author: gwisz@univ.rzeszow.pl

Formation and Stabilization of Nanocrystalline Thin Films

B. Yatsyshyn[1], O. G. Mykolaychuk[2], H. Bajtsar[2]

[1] *Department of Physics and Chemistry of Solids, Vasyl Stefanyk Prykarpathian National University, Physical-Chemical Institute, 76000, Ivano-Frankivsk, Shevchenko str. 57, Ukraine*

[2] *Department of Metal Physics, Ivan Franko Lviv National University, 8 Kyrylo and Mefodiy str., 79005 Lviv, Ukraine*

A thermodynamic description of the kinetic formation of double-phased nanocrystalline "amorphous–crystalline" systems prepared by vacuum technologies is considered. Condensation was carried out on sital isotropic substrate at room temperature with speed from 2 up to 30 nm/s. $(La,Y,Sc)_{15}(Fe,Co)_{18}$ Ge_{67} thin films of thickness ($40 \leq h \leq 200$ nm), obtained under amorphous conditions, were heated in a pre-crystallization range of temperatures until the occurrence of crystallites. The structures' formation and dispersion was investigated with electron microscopy. The electrical and magnetic properties were investigated as well.

It was established that the temporary and temperature stabilization of the physical properties of such materials depends on the thermodynamic parameters of their reception. A film of ternary compounds ($80 \leq h \leq 150$ nm), received at a growth rate of $v_g < 10$ nm/s was characterized by structural stability of one year and more, high resistivity ($\rho \approx 10^{-5}$ Ohm·m), small value of the coercive force ($H_c \approx 2$ up to 8 Oe) and magnetoresistance ($-0.2 \leq \Delta\rho/\rho \leq -1.2 \cdot 10^{-3}$). Increasing the growth rate ($5 \leq v_g \leq 20$ nm/s) during thin films' deposition ($v_g > 10$ nm/s) reduces the stability of nanostructures such as the so-called amorphous-crystalline phase more than 4 times, though such methods of condensation promote the formation of such nanocrystalline structures as the so-called crystalline-inter crystalline boundary.

It has been established that the influence of clusters formation kinetic at process nanocrystallines formation during crystallization amorphous thin films. The connection between the initial stage of condensate formation with the kinetic formation, properties and condensate stabilization has been obtained.

Magnetic-field-tuned Superconductor–Insulator Transition in $A^{IV}B^{VI}$ Heterostructures with Superconducting Nano-scaled Interface

O. Yuzephovich[1], S. Bengus[1], M. Mikhailov[1], N. Fogel[2], E. Buchstab[2], V. Volobuev[3], A. Sipatov[3]

[1] *Institute for Low Temperature Physics & Engineering, 47 Lenin Ave., 61103 Kharkov, Ukraine*

[2] *Solid State Institute, Technion, 32100 Haifa, Israel*

[3] *Kharkov Polytechnic University, 21 Frunze Street, 61002 Kharkov, Ukraine*

We report on observations of the magnetic-field-tuned superconductor-insulator transition (FSIT) found in a new type of nano-scaled two-dimensional superconducting films. A new class of superconducting nano-structures has recently been discovered arising at the interface of epitaxially-grown semiconducting $A^{IV}B^{VI}$ heterostructures consisting of monochalcogenides of various metals with a NaCl-type cubic lattice [1, 2, 3]. The most remarkable property of these heterostructures is their superconductivity at transition temperatures high for semiconductors, $T_c \leq 6$ K. Superconductivity is inherent only to heterostructures, while individual materials that constituting them are not superconductors. It has been shown that metallic-type conductivity and superconducting transitions are exclusively connected with the thin interface layer between two semiconductors. The interfaces of such systems contain the regular grids of misfit dislocations [2, 3]. The inhomogeneous elastic stress created by dislocations gives rise to the band inversion in narrow-gap semiconductors (PbTe, PbS, PbSe) near the interface. Due to the strong periodic stresses, the conducting layer located at the interface appears to be a nano-net with a period of 3.3–40 nm (depending on the monochalcogenides used). Such nano-circuits display 2D properties [3].

We have studied the transport properties of PbTe/PbS and PbTe/YbS heterostructures in magnetic fields up to $H = 5$ T, at temperatures of $T_c = 1.8$–20 K. Resistive transitions, $R(T)$, are broadening at the increase of magnetic field perpendicular and parallel to the interface. The onset of FSIT is observed in high magnetic fields (resistance increase of about 10%). Typical features of FSIT have been observed: the fan-like set of resistance curves, $R(T)$, negative magneto-resistance and crossing at a single point of $R(H)$ curves. Importantly, manifestations of FSIT are more visible on samples with obvious defects of nano-nets. Peculiarities of $H_c(T)$ dependences and manifestation of FSIT have been found to be correlated. It seems that, in our case, FSIT is connected with a non-perfect dislocation grid and the presence of weak Josephson links. The nature of FSIT in the studied systems is most probably associated with the percolation phenomenon. The present studies will be continued in higher magnetic fields and at lower temperatures.

References

1. Fogel N Ya, Pokhila A S, Bomze Yu V, Sipatov A Yu, Feorenko A I, and Shekhter R I 2001 *Phys. Rev. Lett.* **86** 512
2. Fogel N Ya, Buchstab EI, Bomze Yu V, Yuzephovich O I, Sipatov A Yu, Pashitskii E A, Danilov A, Langer V, Shekhter R I, and Jonson M 2002 *Phys. Rev. B* **66** 174513
3. Fogel N Ya, Buchstab E I, Bomze Yu V, Yuzephovich O I, Mikhailov M Yu, Sipatov A Yu, Pashitskii E A, Shekhter R I, and Jonson M 2006 *Phys. Rev. B* **73** RC161306-1

Properties of ZnS Nanoparticle Films

A. Zdyb*, K. Cieślak, J. M. Olchowik

Institute of Physics, Technical University of Lublin,
Nadbystrzycka 38 D, 20-618 Lublin, Poland

II-VI semiconductor nanoparticles attract much attention because of their size-dependent properties and promising applications in optoelectronics. ZnS is a II-VI material of potential applications as window layers of solar cells, in data storage and transfer, coatings sensitive to UV light, etc.

In this work, ZnS nanoparticles were obtained by the wet chemical method. Nanoparticles were prepared by a co-precipitation reaction from homogenous solutions of zinc acetate and manganese acetate. Sodium sulfide was added, resulting in the formation of white precipitate of ZnS nanoparticles stabilized using sodium tripolyphosphate and sodium hexametaphosphate. In our experiment, we used equal amounts of both polyphosphates. The nanoparticles' AFM images were analyzed and their size distribution estimated. Temperature-dependent conductivity measurements of ZnS nanoparticle layers were performed. The layer of ZnS nanoparticles exhibited semiconductivity.

*Corresponding author: a.zdyb@pollub.pl

WO_3-based Electrochromic System with Hybrid Organic-inorganic Gel Electrolytes

E. Żelazowska[1]*, E. Rysiakiewicz-Pasek[2]

[1] *Institute of Glass and Ceramics, Cracow Branch, 30-702 Cracow, Lipowa 3, Poland*

[2] *Institute of Physics, Wroclaw University of Technology, Wybrzeże Wyspiańskiego 27, 50-370, Wroclaw, Poland*

Thin metal oxide films for WO_3-based electrochromic systems prepared by spray pyrolysis on SnO_2 : F-coated soda lime glass, at substrate temperatures of 670–720°C, were characterized for their morphology and electrochromic properties in the electrochemical cells of a smart window arrangement, using organic-inorganic gel hybrid electrolytes. Lithium ion-doped hybrid materials for the electrolytes were obtained by the sol-gel route from tetraethyl orthosilicate (TEOS) with ca. 30–35 wt% of organic additives and solvents. Coloration-bleaching behavior in the visible and near-infrared range of the spectrum and current-voltage characteristics were observed, using prepared hybrids as electrolytes. The hybrid materials' morphology and structure were characterized by scanning electron microscopy with energy dispersive X-ray spectroscopy (SEM/EDX) and Fourier Transform Infrared Spectroscopy (FTIR). FTIR analysis results have revealed $[SiO_4]$ poly-condensation of tetrahedrons strongly influenced by organic additives and confirmed the hybrid nature of the gels, resulting in chemical bonding between their organic and inorganic parts. Room-temperature ionic conductivities of the hybrid electrolytes were in the range of 10^{-4}–10^{-3} $\Omega^{-1}\mathrm{cm}^{-1}$.

References

1. Ch. B. Greenberg, Thin Solid Films, **251** (1994), 81
2. A. Bartolotta, G. Di Marco, M. Lanza, and G. Carini, J. Non-Cryst. Solids, **172–174** (1994), 1195
3. J. Fan, R. F. Marzke, E. Sanchez, and C. A. Angell, J. Non Cryst. Solids, **172–174** (1994), 1178
4. S. Passerini, M. Lisi, T. Momma, H. Ito, T. Shimizu, and T. Osaka, J. Electrochem. Soc., **151** (2004), A578
5. T. Bando, Y. Aihara, K. Hayamizu, and E. Akiba, J. Electrochem. Soc., **151** (2004), A898
6. H. Gunzler, H.-U. Gremlich, IR Spectroscopy – An Introduction, Wiley-VCH, Weinheim, 2002
7. A. Jitianu, A. Britchi, C. Deleanu, V. Badescu, and M. Zaharescu, J. Non-Cryst. Solids, **319** (2003), 263

*Corresponding author: phone: +48-012 423 67 77, fax: +48-012 423 58 36, e-mail: ezelazowska@isic.krakow.pl

Magnetic Interactions at High Temperatures in $M_3Fe_4V_6O_{24}$ Studied with EPR

G. Żołnierkiewicz[1*], N. Guskos[1,2], J. Typek[1], E. A. Anagnostakis[2], A. Błońska-Tabero[3]

[1] *Institute of Physics, Szczecin University of Technology, Al. Piastów 17, 70-310 Szczecin, Poland*

[2] *Solid State Physics, Department of Physics, University of Athens, Panepistimiopolis, 15 784 Zografos, Athens, Greece*

[3] *Department of Inorganic and Analytical Chemistry, Szczecin University of Technology, Al. Piastów 17, 70-310 Szczecin, Poland*

Multicomponent vanadates, $M_3Fe_4V_6O_{24}$ (M = Zn(II) and Mn(II)), were synthesized using the solid state reaction method from MO, V_2O_5, Fe_2O_3 metal oxides. The temperature dependence of the electron paramagnetic resonance (EPR) spectra was performed in the 90–290 K temperature range. Both the thermal dependence of the resonance field and the integrated intensity of the EPR line had a minimum at $\approx$ 230 K. A comparison with a similar study on the $M_3Fe_4V_6O_{24}$ (M = Mg(II) and Cu(II)) compounds has been made. The observed behavior of the EPR integrated intensity is similar to that reported for the nanoscale system of exchange coupled magnetic ions. The thermal effect of EPR parameters is more pronounced if two different magnetic ions are present in the same sub-lattice. The short-range ordered spin clusters' interaction and reorientation in the high temperature range could change the effective internal magnetic field, which in turn could change the resonance condition and shift the observed resonance line. This behavior is attributable to the inherent magnetic inhomogeneity of the system (magnetic multiphase) due to the presence of different valence states of magnetic ions.

Acknowledgements

This work partially was supported by grant PBZ-KBN-1311/T09/2005/29.

*Corresponding author: gzolnierkiewicz@ps.pl

Vanadium Paramagnetic Centers in a New Double Vanadate, $Zn_2InV_3O_{11}$, Studied with EPR

G. Żołnierkiewicz[1*], J. Typek[1], N. Guskos[1,2], M. Bosacka[3]

[1] *Institute of Physics, Szczecin University of Technology, Al. Piastów 17, 70-310 Szczecin, Poland*

[2] *Solid State Physics, Department of Physics, University of Athens, 15 784 Zografos, Athens, Greece*

[3] *Department of Inorganic and Analytical Chemistry, Szczecin University of Technology, Al. Piastów 42, 71-065 Szczecin, Poland*

A new multicomponent vanadate compound, $Zn_2InV_3O_{11}$, has been synthesized and investigated using the electron paramagnetic resonance (EPR) technique. The $Zn_2InV_3O_{11}$ compound is isostructural with $M_2FeV_3O_{11}$ (M = Mg, Zn, Co, Ni), a magnetic system studied earlier. According to the nominal stoichiometry of the $Zn_2InV_3O_{11}$ compound, all ions should be nonmagnetic, but the registered EPR spectra in the 4–300 K temperature range have revealed the presence of a rich variety of paramagnetic centers, predominantly monomeric, dimeric and clusters of V^{4+} ions. The most intense EPR component, attributable to the VO^{2+} vanadyl ions of axial symmetry, displayed a well-resolved hyperfine structure. The presence of a complicated spectrum at low magnetic fields ($g \approx 4.4$) and a broad line at $g \approx 2$ has confirmed the existence of vanadium dimers. In the 270–310 mT magnetic field range, a spectral feature attributable to vanadyl spin clusters was observed at temperatures above 80 K. The role of oxygen deficiency in the appearance of the observed magnetic centers has been discussed. A comparison with the previously studied $Mg_2InV_3O_{11-\delta}$ compound has been made and the influence of specific cations on magnetic defect centers has been considered.

Acknowledgements

This work partially supported by grant PBZ-KBN-1311/T09/2005/29.

*Corresponding author: grzegorz.zolnierkiewicz@ps.pl

LAST-MINUTE ABSTRACTS

Optical Spectra of Quantum Dots: Effects of Non-adiabaticity

J. T. Devreese

Theoretische Fysica van de Vaste Stoffen – TFVS,
Universiteit Antwerpen,
Groenenborgerlan 171, 2020 Antwerpen, Belgium
jozef.devreese@ua.ac.be

It is shown that in many cases an adequate description of optical spectra of semiconductor quantum dots requires a treatment beyond the commonly used adiabatic approximation. We have developed a theory of phonon-assisted optical transitions in semiconductor quantum dots, which takes into account non-adiabaticity of the exciton-phonon system. Effects of non-adiabaticity lead to a mixing of different exciton and phonon states that provides a key to the understanding of surprisingly high intensities of phonon satellites observed in photoluminescence spectra of quantum dots. The breakdown of the adiabatic approximation gives an explanation also for discrepancies between the serial law, observed in multi-phonon optical spectra of some quantum dots, and the Franck-Condon progression, prescribed by the adiabatic approach.

I discuss the breakdown of the adiabatic approximation in terms of Feynman's *Ordered Operator Calculus* and a connection is made with the more general phenomenon of *effectively enhanced polaron* effects in the systems under discussion.

References

1. J. T. Devreese 2007 *J. Phys.: Condens. Matter* **19** 255201
2. V. M. Fomin, V. N. Gladilin, J. T. Devreese, E. P. Pokatilov, S. N. Balaban and S. N. Klimin 1998 *Phys. Rev. B* **57** 2415
3. J. T. Devreese, V. M. Fomin, V. N. Gladilin, E. P. Pokatilov and S. N. Klimin 2002 *Nanotechnology* **13** 163

Electronic Structure of $Y_3Al_5O_{12}$: V Single Crystals – Comparison with Sintered Ceramics

M. Kruczek[1,2], E. Talik[1], H. Sakowska[2], M. Świrkowicz[2], H. Węglarz[2]

[1] *University of Silesia, August Chełkowski Institute of Physics, Department of Solid State Physics, Uniwersytecka 4, Katowice 40-007, Poland*

[2] *Institute of Electronic Materials Technology, Wólczyńska 133, 01-919 Warsaw, Poland*

$Y_3Al_5O_{12}$ (YAG) single crystals doped with vanadium ions(V^{3+}) have been obtained by the Czochralski method. The thermal system consisted of a 53 mm outer diameter, 50 mm high and 1.5 mm wall thickness iridium crucible, in passive iridium afterheater placed around the crucible top on the grog, and alumina heat shields around the afterheater. A charge material was prepared on base of high purity oxides: Y_2O_3(5.0N), Al_2O_3(5.0N) and V_2O_5(4.5N) as a dopant.

The concentration of V^{5+} ions was 0.80 at%. The growing atmosphere was pure nitrogen. The following conditions of the growth processes were applied: growth rate 0.6–1.2 mm/h; rotation rate 5–20 rpm; cooling after growth – at least 24 h. The obtained single crystal up to 20 mm in diameter and 65–70 mm in length were free of macroscopic defects and inclusions of other phases (Fig. 1).

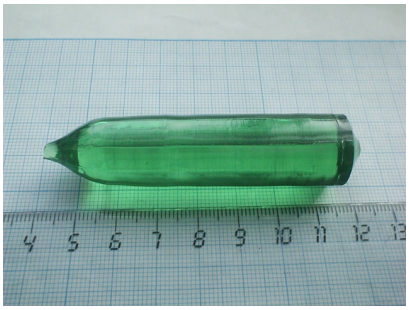

Figure 1: The YAG single crystal

The samples for measurements were taken from the crystal by slicing for a wafer ~ 1 mm thickness, and double sides polishing. A part of this wafers were annealed in reduction atmospheres:

1. in hydrogen at 1200°C for 10 min,
2. in vacuum at 1750°C for 5 hour,
3. first in hydrogen at 1200°C for 10 min and next in vacuum at 1750°C for 5 hour.

After annealing the wafers were slowly cooled down to room temperature.

Recently the YAG ceramics were synthesized to replace the YAG single crystals. These ceramics, which are characterized with similar to the YAG single crystals optical properties, were obtained to increase the doping range, simplify technological process and lower costs. Moreover, there is possible obtaining of ceramics shapes with bigger size than single crystals grown by the Czochralski method.

X-ray photoelectron spectroscopy was used to study the chemical composition and electronic structure of the YAG : V single crystals. For comparison the ceramics were investigated.

Mechanical Properties of Concrete with Low Concentration of Magnetic Nanoparticles

J. Błyszko[1], W. Kiernożycki[1], N. Guskos[2,3], G. Żołnierkiewicz[3]*, J. Typek[3], U. Narkiewicz[4], M. Podsiadły[4]

[1] *The Faculty Concrete Contractures and Technology of Concrete, Civil Engineering and Architecture Department, Szczecin University of Technology, Al. Piastów 50, 70-311 Szczecin, Poland*

[2] *Solid State Section, Department of Physics, University of Athens, Panepistimiopolis, 15 784 Zografou, Athens, Greece*

[3] *Institute of Physics, Szczecin University of Technology, Al. Piastów 17, 70-310 Szczecin, Poland*

[4] *Institute of Chemical and Environment Engineering, Szczecin University of Technology, Pułaskiego 10, 70-322 Szczecin, Poland*

Concrete samples containing low concentration (0.6 wt%) of agglomerated magnetic nanoparticles of cobalt (Co/C) or iron carbide (Fe_3C/C) coated with carbon have been synthesized. The durability of samples with and without magnetic nanoparticles on griping, bending and cramping have been investigated. Twelve different samples have been prepared and tested during 30 days to detect variation in griping, bending and cramping properties. The durability processes of bending for concrete without and with nanoparticles have showed measurable differences. During the initial stage samples with nanoparticles were more resistant to bending except samples with cobalt nanoparticles which displayed a decrease of about 7%. Samples with iron carbide agglomerates have shown an increasing of resistance to bending in comparison to undoped concrete after one week. 30 days later in both cases the bending slowly decreased for samples with magnetic nanoparticles. The durability for griping after 30 days has decreased of about 7% for samples with cobalt and 10% with iron carbide. The cramp has increased about 30% for sample with cobalt ions why no change was observed for samples with iron carbide. The FMR investigation has shown that the resonance line is shifted more intensely for samples with cobalt and it was suggested that this process could be connected with cramp caused by decreasing temperature after the freezing [1]. This kind of study could be very important for magnetic shielding effects and the selection of optimal conditions for building materials with magnetic nanoparticles could be useful for new technological solutions increasing functionality of these materials.

References

1. N. Guskos, G. Żołnierkiewicz, A. Guskos, J. Typek, J. Błyszko, W. Kiernożycki, U. Narkiewicz, and M. Podsiadły (submitted for publication)

*Corresponding author: gzolnierkiewicz@ps.pl

INDEX OF AUTHORS

(the names of conference participants are given in boldface)